RPP-RPT-60892
Revision 0

FY2017 ILAW Glass SPFT Testing for Disposal at IDF: Glass IDF21-EC14

Prepared by

Authors
Elvie Brown
Washington River Protection Solutions, LLC

Charles Viragh, Howard Abramowitz, Isabelle S. Muller, Adonia E. Papathanassiu, and Ian L. Pegg
Vitreous State Laboratory, The Catholic University of America, Washington, DC

Date Published
06/13/2018

Prepared for the U.S. Department of Energy
Office of River Protection

Contract No. DE-AC27-08RV14800

VSL-17R4320-2

Final Report

FY2017 ILAW Glass SPFT Testing for Disposal at IDF: Glass IDF21-EC14

prepared by

Charles Viragh, Howard Abramowitz, Isabelle S. Muller, Adonia E. Papathanassiu, and Ian L. Pegg

Vitreous State Laboratory
The Catholic University of America
Washington, DC 20064

for

Atkins Energy Federal EPC, Inc.
Columbia, MD 21046

and

Washington River Protection *Solutions*, LLC
Richland, WA

August 31, 2017

Rev. 0, 6/13/18

Completeness of Testing:

This report describes the results of work and testing specified by WRPS. The work and any associated testing followed established quality assurance requirements. The descriptions provided in this test report are an accurate account of both the conduct of the work and the data collected. Results required by the test program are reported. Also reported are any unusual or anomalous occurrences that are different from the starting hypotheses. The test results and this report have been reviewed and verified.

I. L. Pegg: I. Pegg **Date:** 6/13/18
VSL Program Director/Principal Investigator

I. Joseph: Innocent Joseph **Date:** 6/13/18
Atkins Sub-Contract ~~Manager~~

TABLE OF CONTENTS

List of Tables

List of Figures

List of Abbreviations

ANL-LRM	Argonne National Laboratory – Low-Activity Waste Reference Material
ASME	American Society of Mechanical Engineers
ASTM	American Society for Testing and Materials
CCC	Canister Centerline Cooling
CUA	The Catholic University of America
DCP-AES	Direct Current Plasma-Atomic Emission Spectroscopy
DOE	Department of Energy
DWPF-EA	Savannah River Laboratory-Environmental Assessment Glass
EDS	Energy Dispersive X-Ray Spectroscopy
FEP	Fluorinated Ethylene Propylene Co-polymer
HDPE	High-Density Polyethylene
HLW	High Level Waste
ICP-AES	Inductively Coupled Plasma-Atomic Emission Spectroscopy
ICP-MS	Inductively Coupled Plasma-Mass Spectroscopy
IDF	Integrated Disposal Facility
ILAW	Immobilized Low Activity Waste
IHLW	Immobilized High Level Waste
LAW	Low Activity Waste
LFRG	Low-Level Waste Disposal Facility Federal Review Group
NDR	Normalized Boron Dissolution Rate
NIST	National Institute of Standards and Technology
NQA	Nuclear Quality Assurance
ORP	Office of River Protection
PA	Performance Assessment
PEEK	Polyetheretherketone
PFA	Perfluoroalkoxy Polymer
PP	Polypropylene
QARD	Quality Assurance Requirements and Description
S/V	Glass Surface Area to Solution Volume
SEM	Scanning Electron Microscopy
SPFT	Single-Pass Flow-Through
Tris	Tri(hydroxymethyl) aminomethane
TST	Transition State Theory
VSL	Vitreous State Laboratory
WRPS	Washington River Protection *Solutions*, LLC
WTP	Hanford Tank Waste Treatment and Immobilization Plant
XRD	X-Ray Diffraction
XRF	X-Ray Fluorescence

SECTION 1.0 INTRODUCTION

1.1 Background

About 50 million gallons of high-level mixed waste is currently stored in underground tanks at The United States Department of Energy's (DOE's) Hanford site in the State of Washington. The Hanford Tank Waste Treatment and Immobilization Plant (WTP) will provide DOE's Office of River Protection (ORP) with a means of treating this waste by vitrification for subsequent disposal. The tank waste will be separated into low- and high-activity waste fractions, which will then be vitrified respectively into Immobilized Low Activity Waste (ILAW) and Immobilized High Level Waste (IHLW) products. The ILAW product will be disposed in an engineered facility – the Integrated Disposal Facility (IDF) – on the Hanford site, while the IHLW product is designed for deep geological disposal in a national facility for high-level nuclear waste. The ILAW and IHLW products must meet a variety of requirements with respect to protection of the environment before they can be accepted for disposal. The objective of the work described in this report is to perform testing, data collection, and analyses for the ILAW glass product for subsequent use in the performance assessment (PA) of the IDF to assess potential environmental risks associated with long-term storage.

The technical approach used to predict long-term release from ILAW glass for the IDF PA has been developed, refined, and updated over the past two decades. The approach and the supporting test data for ILAW glasses have been extensively documented [1-6]. The approach has gained acceptance from the Low-Level Waste Disposal Facility Federal Review Group (LFRG) and the international community evaluating the long-term corrosion of waste glass. It has also been peer reviewed and approved by a panel of independent experts during development of the 1998 IDF PA. The underlying premise of the IDF PA is that the source term for radionuclide release is controlled by the long-term weathering of the glass matrix. This engineering-based approach has been used in previous PAs to provide the defense-in-depth required to support the above premise and demonstrate through computer simulations that the proposed glass waste form will meet the regulatory requirements. The key component of this engineering-based approach is the estimation of the model parameters and chemical reaction network needed to provide a robust simulation of glass weathering and the corresponding release of radionuclides over the period of performance (~10,000 years).

The present work is part of an ongoing program to conduct the necessary testing to permit the estimation of the model parameters for representative low activity waste (LAW) glasses. These parameters are used to populate a kinetic rate law that describes the release from the glass waste form. The overall model incorporates the effects of chemical affinity and ion exchange. The model parameters $\vec{k}_0, \eta, E_a$, and K_g are used to populate a chemical affinity-based kinetic rate law that is based upon Transition State Theory (TST) [7]:

$$r = \vec{k}_0 10^{\eta pH} exp\left(\frac{-E_a}{RT}\right)\left[1-\left(\frac{Q}{K_g}\right)\right]^{\sigma} \quad (1.1)$$

where r is the dissolution rate [g/(m^2 d)], $\vec{k}_o$ is the forward rate constant [g /(m^2 d)], pH is the negative of the logarithm to base 10 of the hydrogen ion activity, η is the power law coefficient, E_a is the apparent activation energy (kJ/mol), R is the gas constant [kJ/(mo1 K)], T is the temperature (K), Q is the ion activity product (unitless), K_g is the pseudo-equilibrium constant for the rate controlling phase or phases (unitless), and σ is the Temkin coefficient which has been theoretically shown to equal one. Equation (1) relates the effect of: (1) pH, (2) temperature, (3) saturation state of the system, and (4) the activities of species that affect the rate of glass dissolution via Q. Equation 1.1 is based on the kinetic rate equation developed by Åagaard and Helgeson [8], as applied to glass by Grambow [9] wherein orthosilicic acid is the only rate controlling species in Q.

In addition to the TST rate equation, a further term has been added to the IDF PA calculations to predict the ion-exchange rate (r_{IEX}) as the glass-water reaction proceeds. In general, the ion exchange rate is a function of temperature, glass composition, and reaction progress (stage of the glass-water reaction). The potential importance of the contribution from ion exchange in the long-term corrosion mechanism had been emphasized previously by Feng and Pegg [10-12]. In previous glass testing work in support of the IDF PA, the standard approach to estimate this parameter has been that of McGrail et al. [3] and Pierce et al. [6] whereby r_{IEX} is obtained by subtraction of the boron dissolution rate from the sodium dissolution rate; measurement of its temperature dependence also permits estimation of the activation energy of the Na ion exchange reaction E_{IEX}. More recently, various issues with this approach have been identified including: (i) the reliability of this subtraction approach in view of the apparent diffusive release of boron [13, 14, 15]; (ii) an error in the calculation of r_{IEX} that has been propagated through previous work [16]; and (iii) the use of an r_{IEX} that is independent of time and solution composition [15, 16]. In view of these issues, WRPS has commissioned studies of potential alternative approaches for incorporation of ion exchange into the rate law [15, 16] that may be implemented in the future.

The use of Equation 1.1 with the ion exchange contribution and suitably estimated parameters allows for the source-term to be estimated within a reactive chemical transport modeling framework that takes into account the coupled effects of fluid flow and glass-water reactions on the chemistry of fluids percolating through the disposal facility. Coupling the fluid chemistry with a kinetic rate equation allows the simulations to describe the response of the glass corrosion rate to changes in fluid composition as a function of time and space.

In the early work supporting the IDF PAs, three or four prototypic glasses that spanned the range of glass compositions expected to be produced by the WTP were selected based upon specific processing constraints and composition projections that were current at the time. However, subsequent work has expanded the range of glass compositions that may be produced at the WTP and this type of composition range expansion is likely to continue through the life of the project. Thus, while the basic technical approach is well developed, there is a need to expand the range of glasses tested in order to span the composition range expected to be disposed of in the IDF and to develop an understanding of the dependence of the underlying model parameters and reaction network on the ILAW glass composition. Washington River Protection *Solutions*, LLC (WRPS) is leading the work to address this need and contracted with Atkins and the Vitreous State Laboratory (VSL) of The Catholic University of America (CUA) to provide scientific and technical support. The present report describes results from testing performed according to a Test Plan [17] that is responsive to the corresponding WRPS scope of work [18]. The scope of the present work was to determine the kinetic parameters $\bar{k}_o$, η, E_a, K_g, and r_{IEX} for a selected high waste loading ILAW glass (IDF21-EC14) through analysis of data obtained from glass dissolution using the single-pass flow-through (SPFT) test.

1.2 Test Overview

In the present work a full suite of SPFT tests was performed on a single high waste loading LAW glass (IDF21-EC14) in order to determine kinetic law parameters for that glass. The work included:

- Glass dissolution under dilute conditions[1] at pH(23°C) values of 7, 8, 9, 10, 11, and 12 and temperatures of 23, 40, 70, and 90°C.
- Glass dissolution under increasingly saturating conditions[2] at pH(23°C) 9 and temperatures of 23, 40, 70, and 90°C.
- Data analysis to determine the values of the kinetic parameters k_0, η, E_a, K_g, and r_{IEX} of Equation 1.1.

1.3 Report Outline

The test matrix for the present work is described in Section 2. Section 3 describes the selection and preparation of the IDF21-EC14 glass. The testing and data analysis are described in Section 4. The results are presented and discussed in Section 5, while Section 6 provides the summary and conclusions.

[1] Flow rate /surface ratio or $F/S \sim 10^{-8}$ m/s
[2] Increasing concentrations of orthosilicic acid in the influent solutions

SECTION 2.0
TEST MATRIX

The test matrix used in this work, shown in Tables 2a-d, was modeled after similar studies performed previously [6, 13]. Each table indicates all of the tests performed at a single temperature (23, 40, 70, or 90°C) and includes glass dissolution experiments under dilute conditions (variable pH and with zero influent Si concentration ($[Si]_{in}=0$); six tests per temperature) and under saturating conditions (pH=9 and $[Si]_{in}\neq0$; six tests per temperature). Each segment of Tables 2.1a-d pertains to a unique set of experimental conditions starting with the specific test temperature (col. *1*) at which all 12 specimen trains (col. *2*) were run (12 trains per temperature). Other columns in these tables provide:

- Overall test duration (col. *3*)
- Intended analytical sampling interval, Dt_{sam} (col. *4*)
- Total intended number of samples to be analyzed per specimen, *N* (col. *5*)
- Initial elemental silicon concentration in leaching (influent) solution, $[Si]_{in}$ (col. *6*)
- Leachant flow rate, *F* (col. *7*)
- Leaching solution pH (col. *8*) and
- Mass of the glass specimen, m_g (col. *9*).

Within a given run (temperature), all analytical samples (*S*) were indexed according to train number (index $1<i<12$) and order of collection (index $1<j<N$).

The duration of testing in Tables 2.1a-d was based on previous SPFT experimentation [13], which indicated that steady state was reached within 15 days for tests performed at 40, 70, and 90°C, and within 30 days for tests performed at 23°C. Typically, a minimum of 20 samples were collected from the tests performed at 40, 70, and 90°C and a minimum of 10 samples were analyzed per test. A minimum of 10 samples per test were collected and analyzed from the tests performed at 23°C. The selected influent Si concentrations, $[Si]_{in}$, were based on the results obtained from SPFT testing of LAW glass IDF1-B2 [13]. Similarly, flow rates and glass masses were selected in order to provide a sufficiently large flow rate/surface area ratio, which ensures that, for tests to be performed under dilute conditions, glass dissolution takes place in sufficiently undersaturated solutions. A number of previously published studies indicate that the *F*/*S* ratio of $\geq10^{-8}$ m/s that was selected for the present work is sufficiently large to ensure dilute conditions for trains #1-6 [6, 19]. Consequently, in the present work, testing with systematically varied F/S ratios to further confirm this was not performed. This assumption is supported by the test results discussed in subsequent section, which show that, while some deviations from the classic understanding of glass dissolution were observed, the kinetic rate law parameters could be determined and those parameter values were within the expected range for other LAW glasses.

For tests with Si in the influent solutions, the glass mass was increased progressively with increasing $[Si]_{in}$ in order to offset the effects of the associated decrease in reaction rate in an effort to ensure that the measured concentrations were above their detection limits. In the case of tests at 23ºC, with the lowest reaction rates, a high glass sample mass was used for all $[Si]_{in}$ values.

SECTION 3.0
SAMPLE PREPARATION

3.1 Glass Selection

The composition of the glass (IDF21-EC14) selected for SPFT testing is shown in Table 3.1. A description of the selection process has been provided previously [20]. Briefly, the glass shown in Table 3.1 is part of a larger on-going initiative aimed at optimizing the LAW and high level waste (HLW) glass formulations and processing parameters in order to minimize the volume of glass produced at WTP and to shorten the plant operating time. An important objective of this initiative is to determine the likely limits of LAW loading across the full range of expected LAW compositions. LAW glass formulations developed for the WTP fall into two groups: (i) LAW formulations developed by VSL to support the Bechtel WTP baseline; and (ii) LAW formulations developed by VSL for ORP to support enhancements to the original WTP baseline. Compared to the WTP baseline LAW glasses, the ORP LAW glasses have higher waste loadings. Since the major waste loading limiting constituents in Hanford LAW are sodium and sulfur, glass formulation optimization for ORP has been focused on maximizing the incorporation of these components in the glass. Thus, the ORP LAW glasses contain higher sodium and sulfur concentrations as compared to the WTP LAW glasses. Higher sodium (or alkali) loadings were achieved by modifying the glass former additives through changes such as increasing the concentration of ZrO_2 and introduction of SnO_2 as a new additive. Similarly, higher sulfur loadings were achieved by increasing the concentrations of glass former additives such as CaO and Li_2O and introducing V_2O_5 as a new additive.

An overview of the Na_2O and SO_3 loadings for the baseline WTP glasses and the ORP glasses is given in Figure 3.1. As is evident from Figure 3.1, the ORP glasses provide considerable increases in waste loadings over the WTP baseline glasses and therefore considerable potential for reductions in cost and schedule. It is recognized that it will be possible to perform SPFT testing on only a relatively small number of additional glasses to support the IDF PA. Accordingly, glasses are being selected to provide reasonable coverage of the range of likely LAW compositions. Figure 3.1 also shows glasses that have previously been subjected to SPFT testing.

The IDF21-EC14 glass, which is the subject of the present report, is representative of the high-alkali, moderate-sulfur (24 wt% Na_2O and 0.60 wt% SO_3) high waste loading formulations. Further details on the rationale for the selection of this glass are provided in reference [20] and summarized briefly below.

Recently, over 50 glasses spanning the range of alkali and sulfur concentrations in Hanford LAW were formulated and characterized to support the development of an Enhanced LAW Glass Correlation for ORP [20-23]. The strategy for the development of this Enhanced

LAW Glass Correlation for the higher waste loading LAW glasses follows a strategy similar to the one used in the development of the WTP Baseline LAW Glass Correlation [24]. As with the WTP Baseline LAW Glass Correlation, in the development of the Enhanced LAW Glass Correlation, emphasis was given to glass compositions that have already been used in melter testing to confirm acceptable processing characteristics. Similar to the Baseline Correlation, it is intended that this Enhanced LAW Glass Correlation will ultimately be developed to the point that it can be used to formulate high waste loading glasses for LAW processing at the WTP. These new glasses are designed to cover the range of alkali and sulfate concentrations in Hanford LAW. From these, thirteen glass compositions have been selected for DM100 melter testing to confirm the processability of glasses designed by the Enhanced LAW Glass Correlation; these thirteen glasses ("ORLEC" glasses) are shown in Figure 3.2, together with the 20 Phase 1 and Phase 2 IDF glasses previously selected for long-term PCT and SPFT testing. The ORLEC glasses have the advantage of incorporating more recent glass formulation and correlation development information and were therefore preferred over the Phase 1 and Phase 2 IDF glasses as the basis for the selection of glasses for FY 2017 testing to support the IDF PA. The four ORLEC glasses selected for SPFT testing in FY 2017 are also shown in Figure 3.2. All four of these glass compositions have been tested for processing characteristics in the DM100 melter system. As is evident from Figure 3.2, the ORLEC glasses recommended for SPFT testing serve to address gaps in the Na_2O-SO_3 composition space for glasses with SPFT test data. The present report addresses testing of the ORLEC14 glass formulation, which, as fabricated for the present work, is referred to as IDF21-EC14.

3.2 Glass Preparation

The IDF21-EC14 glass was prepared from reagent grade or higher purity chemicals according to VSL standard operating procedures. Briefly, an appropriate combination of well-mixed chemicals was melted at 1200ºC for 75 minutes in a platinum-gold crucible. Mixing of the melt was accomplished with a platinum stirrer beginning 15 minutes after the start of melting and continuing for the next 60 minutes, until the end of melting. The melt batch included a rhenium spike targeted at 0.1 wt% Re_2O_7, if all of it were retained in the glass. Since rhenium is subject to significant volatile loss from the glass during melting, excess Re_2O_7 was added to compensate, assuming an average retention of 53.5% based on extensive past testing [13, 14]. This results in the addition of 0.93 g, instead of 0.50 g of Re_2O_7, to each batch targeting 500 g of glass.

The procedure yielded an approximately 500 g-batch of a clear emerald colored glass with no visible sulfate layer (Figure 3.3). A portion (60 g) of the batch of as-melted glass was set aside and the reminder was subjected to canister centerline cooling (CCC) heat treatment according to the WTP LAW container cooling profile [25]. After CCC heat treatment, the sample (435.5 g) was about 11 cm in diameter at the surface and 2 cm thick (Figure 3.3). The glass was translucent dark green, except for a layer approximately 1 mm thick near the platinum crucible wall that appeared to be partially crystallized. This lighter colored crystallized section near the crucible wall was easily separated from the rest of the glass allowing quantitative evaluation of the two sections, as described in Section 3.3.

3.3 Glass Compositional Analysis

The primary method used for glass composition analysis was X-ray fluorescence spectroscopy (XRF) on powdered glass samples. A PANalytical Axios^{mAX}-Advanced XRF spectrometer was used for this purpose. The XRF was calibrated over a range of glass compositions using standard reference materials traceable to the National Institute of Standards and Technology (NIST), as well as waste glasses such as the Argonne National Laboratory – Low-Activity Waste Reference Material (ANL-LRM) [26] and the Defense Waste Processing Facility – Environmental Assessment Glass (DWPF-EA) [27]. Since boron and lithium are not determined by this procedure, it is supplemented by acid digestion followed by solution analysis, as described below.

Glass samples for analysis by direct current plasma atomic emission spectroscopy (DCP-AES) are first subjected to microwave-assisted total acid dissolution in Teflon vessels according to VSL standard operating procedures. Twenty milliliters of a 1:5 mixture of concentrated $HF:HNO_3$ is diluted to 50 ml and used for the dissolution. This procedure is similar to the American Society for Testing and Materials (ASTM) Test Method C1412-99 that has subsequently been incorporated into ASTM C1463-13, which also employs a mixture of concentrated HF and HNO_3 in microwave digestion of pulverized glass samples; supplemental use of HCl/H_3BO_3 is not included in the VSL procedure since boron is normally one of the analytes. The solutions resulting from the acid digestion are analyzed by DCP-AES.

The glass composition analysis was performed on multiple samples. The as-melted glass IDF21-EC14 and the two sections of the sample subjected to CCC (IDF21-EC14CCC) were analyzed separately for composition by XRF and DCP-AES after total acid digestion. Glass subjected to CCC heat treatment was sampled from the center of the crucible and analyzed in triplicate. Samples are typically rejected when major oxides, with target concentrations of 1 wt% or more, show relative deviations from the target composition of greater than 10% (or 0.2 wt% absolute for SO_3). The results provided in Table 3.2 show that the glass is on target for all of the major glass constituents. SO_3 is found to be about ~0.05 wt% below target, with little difference between the as-melted glass and the samples subjected to CCC. No significant differences are observed between the as-melted glass and the two sections of the sample subjected to CCC, except for small deficits in SnO_2 and ZrO_2 concentrations in the crystallized sample from near the crucible wall.

Glass ground from segments of the center area of the CCC heat treated sample was used for SPFT testing. Consequently, all of the SPFT data presented here were obtained exclusively from sample IDF21-EC14CCC-center and all references to glass IDF21-EC14 from here forward refer to IDF21-EC14CCC-center. Prior to its use in the SPFT tests, the glass was crushed and sieved to a 100-200 mesh (75-149 μm) specification. The ground glass was water-washed and air-dried to remove fines, which tend to dissolve faster than glass grains during alteration experiments and, thus, interfere with test results.

Further evaluation of the IDF21-EC14 glass included scanning electron microscopy (SEM) imaging of cross-sectioned, carbon-coated and polished grains, and X-ray diffraction (XRD) analysis. These methods were used to identify the crystalline phases observed in the layer of glass near the crucible wall and to verify that the glass in the center of the crucible was free of secondary phases (Figure 3.4). The glass sample from near the crucible wall (Figure 3.5) contained sodalite (a sodium sulfate aluminosilicate phase, probably lazurite) estimated at 8.7 vol% by SEM in the first millimeter of glass sample from the crucible wall. A small patch with a few µm-sized Sn-oxide crystals was also observed in SEM, explaining the small decrease in SnO_2 content noted by XRF in the crystallized glass sample from near the crucible wall. The main crystalline phase was identified by XRD as a sodalite ($Na_8Al_6Si_6O_{24}S_{2.5}(H_2O)_{0.6}$ or $Na_8Al_6Si_6O_{24}(B(OH_4)_2)$) based on the match of a single line in the XRD pattern (Figure 3.6) and estimated at 0.4 wt% by quantitative XRD (QXRD). In the upper section of the sample, the sodalite-bearing zone is relatively uniform in thickness and clustered within the first 0.2 mm from the crucible wall; it becomes gradually thicker towards the bottom of the sample, reaching up to 0.8 mm in thickness. The crystals are elongated, mostly 1-3 µm and clustered into dendritic skeletal crystal texture. The crystallized glass sample collected from near the crucible wall and ground for SEM and XRD analysis was 9.38 g out of the 435.50 g CCC sample, making the overall crystallized fraction by XRD about 0.01 wt%. The glass composition analysis by energy dispersive X-ray spectroscopy (EDS) of glass from the center of the crucible showed results consistent with the XRF analysis and the target glass composition, but analysis of glass from the crystallized layer near the crucible wall showed no sulfur, presumably due to partitioning of sulfur to the crystalline phase. XRD also confirmed the absence of crystals in the glass from the center of the crucible (Figure 3.6).

SECTION 4.0
SPFT TESTING AND DATA ANALYSIS

4.1 Description of the Experimental Set-up

The SPFT apparatus used in the present work follows recommendations provided in the corresponding ASTM standard practice [28] and is functionally equivalent to one previously employed for other LAW glass SPFT testing [6, 13]. Figure 4.1 shows a single specimen test train marked by an index "*i*" along the diagram. There were several such trains running simultaneously at the same constant temperature for the duration of the given test set (see the test matrix in Section 2.0). The only wetted materials throughout the system were plastics. These include high-density polyethylene (HDPE), polypropylene (PP), polyetheretherketone (PEEK), perfluoroalkoxy polymer (PFA), and fluorinated ethylene propylene co-polymer (FEP). These materials are known not to leach out any components that are relevant to the glass leaching process. However, since leaching solutions have elevated pH values and all tests have long durations, protection from ingress of atmospheric CO_2 is an issue, as all plastics are somewhat permeable to carbon dioxide. To address this, all reservoirs and enclosures were continuously purged with CO_2-free air (<1 ppm CO_2 from a dedicated Balston model 75-52NA "zero" gas generator). Reservoir bottles were outfitted with filters so influent solutions were filtered constantly to ensure that no silica crystals were present. A short length of interconnecting PEEK tubing (less than 1 m of 1.59 mm OD x 0.51 mm ID) was exposed to ambient atmosphere – an insignificant exposure considering PEEK's low carbon dioxide permeability [29] of $6.1 \cdot 10^{-9}$ $cm^3_{(STP)} \cdot cm/cm^2 \cdot s \cdot atm$ at 25 °C, which is an order of magnitude lower than those for commonly used FEP and PFA materials[3] ($7.0 \cdot 10^{-8}$ and $9.4 \cdot 10^{-8}$ $cm^3_{(STP)} \cdot cm/cm^2 \cdot s \cdot atm$ at 25 °C, respectively).

The leaching solution was prepared ahead of time in a quantity sufficient for the entire test duration. The solution was contained in a continuously purged reservoir *R* from which it is drawn into a pump *P* and discharged through the reaction cell (LC). The pump operation was computer-controlled. Two pumps were used each of which controlled six trains. Upon entering the constant temperature oven the leaching solution passed through a 50 cm long thermal equilibration coil (TEC) before reaching the reaction cell. The solution left the reactor and analytical samples were dispensed downstream via a robotic arm into a series of vials. The robotic arm was computer-controlled. Samples were collected periodically throughout the tests at predetermined times.

[3] Data from IDX Health and Science (formerly Upchurch Scientific) 2009-2010 Catalogue, p. 75.

4.2 Solution Preparation

Glass leaching experiments at a pH_{RT}[4] range from 7 to 10 were performed in 0.05 M tri(hydroxymethyl)aminomethane (Tris) solutions buffered to the target pH using concentrated HNO_3 or 1 M LiOH as described by Pierce et al. [6]. Glass leaching experiments at pH_{RT} 11 and 12 were performed in solutions of 0.001 M LiOH and 0.01 M LiOH, respectively, together with 0.01M LiCl for consistency with previous tests [6]. The pH_T[5] values of the buffer solutions, heated to the test temperature, were measured using a temperature-compensated pH meter. Determination of pH_T was necessary for the calculation of dissolution rates using Equation 1.1. Table 4.1 shows the pH values obtained at various temperatures.

Leaching solutions containing varying amounts of Si were formulated by dissolving analytical grade silicic acid powder ($SiO_2.H_2O$) in 0.05 M Tris. Due to the low solubility of amorphous silica in aqueous solutions, stock solutions containing at least 140 ppm [Si] were prepared, heated at 90°C for a period of time, decanted carefully into fresh bottles to avoid transfer of precipitated solids, and analyzed by ICP-AES or DCP in order to determine the concentration of Si. As necessary, the stock solutions were diluted to the target [Si] and buffered to pH_{RT} 9 as previously described.

4.3 Sample Analysis

Collected samples, designated for solution analysis, were acidified with a small amount of concentrated HNO_3 and analyzed by inductively coupled plasma-atomic emission spectroscopy (ICP-AES) for the presence of B, Al, Si, and Na. Samples from selected tests were additionally analyzed for Re by inductively coupled plasma-mass spectroscopy (ICP-MS). Rhenium is added into the formulation of LAW glasses as a non-radioactive surrogate for Tc and its dissolution behavior therefore provides information regarding the long-term immobilization of Tc in LAW glasses. Results from the additional analyses are presented in Table A5 of Appendix A. Each test also included a collection of samples that were designated for pH measurements in order to ensure that solution pH was maintained constant throughout a specific test.

A total of 54 tests were performed and >700 individual samples were analyzed for solution chemistry. A sample was accepted for analysis only if its flow rate deviated from the average flow rate of its specific train by ≤5%. The average flow rate for all tests was within 10% of the corresponding target flow rate. At the end of the experiment, the altered glasses were collected, water-washed gently, and air dried. Altered glass samples were archived.

[4] Subscript indicates pH values obtained from measurements at room temperature (RT).
[5] Subscript indicates pH values measured at the test temperature *T*.

4.4 Data Analysis

Calculation of Dissolution Rates. The data analysis follows the guidelines outlined in the ASTM Standard C 1662-10, which specifies that, if a glass specimen of a known surface area is contacted by a solution that flows continuously at a known flow rate and at a constant temperature, the concentration of the *i*-th soluble glass component in the effluent solution exiting the reactor vessel can be used to calculate the amount of glass that has been dissolved. The dissolution rate of the glass is then calculated as:

$$(rate) = \frac{\left[C_i - C_i^o\right] \cdot \left(\frac{F}{S^o}\right)}{f_i} \qquad (4.1)$$

where: C_i - is the steady-state concentration of component *i* measured in the effluent solution
$C_i°$ - is the background concentration of component *i* in the influent solution as measured in a blank test
F - is the solution flow rate
$S°$ - is the initial surface area of the glass sample that is exposed to solution, and
f_i - is the mass fraction of component *i* in the glass.

In Equation 4.1, the surface area (S^o) is calculated as the product of the specific surface area and the initial sample mass (m_o) used in the test. The specific surface area is approximated based on the mesh size of the fraction used in the test and the density of the glass. The particles of glass are presumed to be spherical with diameter (d) equal to the arithmetic average of the openings of the sieves used to prepare the material. The specific surface area (S_p) of a glass having a density ρ is:

$$S_p = {}^{6}\!/_{\rho \cdot d} \qquad (4.2)$$

thus,

$$S^o = S_p \cdot m_o \qquad (4.3)$$

During glass dissolution, the mass and surface area of the glass sample are expected to change over time as material is dissolved. The surface area S_j at time j during a SPFT test is calculated from the following expression [28]:

$$S_j = \frac{3}{\rho r_o} m_0^{1/3} m_j^{2/3} \qquad (4.4)$$

where r_o is the radius of the glass particle and m_j is the sample mass at time j. The parameter m_j is estimated by the equation [30]:

$$m_i = m_o - \frac{1}{f_i}\left[\sum_{n=1}^{j-1} F_n C_{n,i} \Delta t_n + F_j C_{j,i} \frac{\Delta t_j}{2}\right], \text{j} \geq 1 \tag{4.5}$$

where i is an element representative of glass dissolution such as B, which was used as the element to index glass mass loss with time. Here it should be noted that Equation 4.5 inherently assumes uniform dissolution during SPFT testing and the absence of any surface alterations such as cracking.

The volumetric flow rate (F) is calculated by dividing the mass of solution that is collected by the time for its collection and its density (which can be assumed to be 1 g/cm^3 in most cases in view of the dilute solutions involved).

Determination of Steady State. To determine the steady-state concentration (C_i), the measured concentration of the i-th component is plotted versus time in order to visually identify the data to be used. Data that precede the attainment of steady-state conditions, essentially constant concentration of the analytes, are excluded before calculating the mean and standard deviation of the subsequent data points. The relative standard deviation (the standard deviation divided by the mean) of the calculated steady state concentration must be less than 0.15 for the test results to be valid [28]. In the results described in Section 5.0, the relative standard deviations for boron were all below the 0.15 requirement, and were generally below 0.1 for all monitored components. Soluble components monitored in this fashion include silicon, aluminum, sodium, and boron. Parameters of Equation 1.1 are estimated using normalized boron dissolution rates (NDR). However, differences in rates calculated using different elements may provide added insight into the dissolution mechanism. For example, the rate of sodium ion exchange (r_{IEX}) at steady state is typically determined by a method that involves subtracting the boron from the sodium dissolution rate [3]. This value has been used to provide an estimate of the contribution of ion exchange to the overall leaching of sodium from the glass [3, 6].

Estimation of K_g. K_g is estimated from the NDR values obtained at steady state when the glass is leached in the presence of increasing influent concentrations of Si and at specific pH and T. To determine the parameter K_g at a given T, NDR values are plotted as a function of the activity of orthosilicic acid ($a[H_4SiO_4]$) dissolved in the effluent solutions at steady state (Equation 1.1) and a linear regression on the data is performed. Values of $a[H_4SiO_4]$ are determined from the corresponding solution chemistry using the geochemical code PHREEQC. According to Equation 1.1, K_g is given by the value of $a[H_4SiO_4]$ at NDR=0 [6]. To determine the K_g value at the presumed repository temperature of 15°C, the natural logarithm of the measured K_g values is plotted against the reciprocal of the absolute temperature and a linear regression is performed on the data [6].

Calculation of Parameters η, E_a, and k_0. To determine the dependence of glass dissolution rate on pH (the parameter η in Equation 1.1), log NDR is plotted as a function of pH_T at a specific temperature and linear regression of the data is performed for pH_T >7 or 8. Because the parameter η is assumed to be independent of temperature, the power law coefficient for a particular glass is considered to be the average value obtained at various temperatures. Once the parameter η is determined in this way, the activation energy E_a and rate constant k_0 of the glass are determined by performing a nonlinear regression on all data obtained under dilute conditions ($[Si]_{in}$=0)) using Equation 1.1 [6].

Estimation of r_{IEX} and E_{IEX}. The ion exchange rate, r_{IEX}, of the glass at a specific temperature was obtained from the data collected from the tests performed under saturating conditions at that temperature. Following the convention of McGrail et al. [3] and Pierce et al. [6], r_{IEX} values were estimated by subtracting B dissolution rates from the Na dissolution rates. Because B is assumed to be released only through glass dissolution, while Na is released through a combination of glass dissolution and ion exchange, the results of the subtraction is assumed to represent only the ion exchange term. The results are expressed in mol m^{-2} s^{-1}; note that "mol" refers to moles of sodium. However, as noted above, there are a number of issues with this approach including the reliability of this subtraction method in view of the diffusive release of boron [13, 14] and an error in the calculation of r_{IEX} that has been propagated through previous work [16]. The latter relates to the confusion between rates on a glass basis versus on a sodium basis, as described elsewhere [16]. This results in a correction factor between the two bases that accounts for the fraction of sodium in the given glass composition. Following McGrail et al. [3] and Pierce et al. [6], r_{IEX}, in previous work has been calculated on the glass basis but reported as being on a sodium basis; the correction factor depends on the sodium content of the glass but is typically of the order of a factor of ~7 [16]. For ease of comparison to previous work, in the present work we refer to r_{IEX} values as being "uncorrected" or "corrected."

The activation energy of the Na ion exchange reaction, E_{IEX}, and the rate of ion exchange at 15ºC, are calculated by plotting the natural logarithm of r_{IEX} as a function of the reciprocal of the absolute temperature (Arrhenius equation) and performing a linear regression on the data.

SECTION 5.0
RESULTS AND DISCUSSION

The data obtained from elemental analysis of collected effluent samples are listed in Appendix A along with the corresponding normalized[6] dissolution rates for each analyzed element as calculated from Equation 4.1; these transient rates then converge to the steady state dissolution rates once steady state is reached. Thus, the normalized dissolution rates for each element (NDR_i) were plotted against time and steady state was determined for each analyzed element for each set of experimental conditions. Samples used to determine steady state for a specific set of experimental conditions are shown in bold in Tables A1- A4 in Appendix A. Steady state B dissolution rates (mean±SD) are further highlighted in Table A6 of Appendix A along with the coefficient of variance. Table A6 features rates as determined from the highlighted samples of Tables A1-A4. Plots of the data from all tests are provided in Appendix B, where they are organized by test temperature and for dilute or saturating conditions. The *y*-axes of the graphs in Appendix B show NDR_i, where *i* is one of the following elements: B, Al, Na, Si, or Re. In the text below, when the term "dissolution rate" is used, it refers to normalized values. It should be noted that the majority of the graphs shown in the sections below (main report) are constructed from steady-state dissolution rates, which are also referred to as NDR_i; the only exceptions are for plots of NDR_i vs. time, which, obviously, also show non-steady state dissolutions rates. The glass dissolution rate is denoted as *NDR*; since boron is used as the preferred indicator of glass dissolution, this term refers to the dissolution rate of B (NDR_B) at steady state.

5.1 Dynamic Dissolution of IDF21-EC14 Under Dilute Conditions

5.1.1 Congruency of Dissolution and Mechanistic Considerations

Plots of the data for dissolution of IDF21-EC14 at various pH and temperature values under dilute conditions are shown in Appendix B, pages B2, B4, B6, and B8. Several general trends are evident in the data. At low pH at all temperatures the release rate of Na and B far exceed those of Si and Al. In some cases, B dissolution tracks that of Na, presumably through hydronium-driven hydrolysis of B-O bonds, which are more easily broken than many other M-O bonds [31-35]. As the pH increases, Na release rates move ahead of those for B, indicative of a significant ion exchange contribution. At pH_{RT} of 7 and 8 very little Si or Al release is observed. However, the Si and Al release rates increase significantly at pH_{RT} of 9 and above at all temperature and, in fact, at pH_{RT} of 9 and 10, the release rate of Si, and often Al, are close to those for Na and B. Thus, in slightly alkaline environments, where solid state inter-diffusion is expected to diminish, and silicate network depolymerization reactions are expected to begin to

[6] Normalized with respect to the content of the element *i* in the glass composition.

dominate, glass constituents dissolve congruently. At higher pH, Na shows increased dissolution when the solution buffering system is LiOH-based (pH_{RT} 11 or 12). In those instances, the inward diffusion of Li^+ and its exchange with Na^+ results in increased Na release. Because Li^+ is able to charge compensate tetrahedral B, replacement of Na^+ by Li^+ at BO_4^- sites does not lead to hydrolysis of B-O bonds. Consequently, at pH_{RT} 11 or 12, B dissolution does not track that of Na. The presence of Li is expected to suppress the diffusive nature of B dissolution and make it a better indicator for network dissolution.

Finally, a common theme throughout the graphs of Appendix B, pages B2, B4, B6, and B8, is that Al dissolution is controlled by the aqueous solubility of Al: at neutral or near-neutral pH, where Al^{3+} is scarcely soluble, the Al dissolution rate is very low, whereas, at highly alkaline pH, where Al^{3+} is soluble, Al dissolution rates that exceed those of Si or B are observed.

5.1.2 Estimation of Kinetic Parameters η, E_a, and k_0

Table 5.1 shows the measured steady-state glass dissolution rates, which correspond to the forward dissolution rate of the glass at a specific set of experimental conditions (r_0). The data were used to calculate the kinetic parameters η, E_a, and k_0.

Based on the r_0 values reported in Table 5.1, the power-law coefficient η, activation energy E_a, and rate constant k_0 were calculated as described in Section 4.4. Figure 5.1 shows the plots of log NDR vs. pH_T used to determine the η value at each temperature. Table 5.2 summarizes all of the obtained estimates from Figure 5.1. Because the parameter η is expected to be independent of temperature, its value for IDF21-EC14 is obtained by taking the mean of the values at each temperature, which gives a value of 0.48±0.04. This value is close to the values reported for glasses LAWA44 (0.49), LAWC22 (0.42), and IDF1-B2 (0.48) [6, 13, 36]. Reported values for HLW glasses are: 0.39 for the French glass R7T7, 0.43 for British Magnox glass, and 0.38-0.49 for Magnox-THORP blend glasses [19]. Chave et al. reported η values of 0.49 and 0.33 for the silicate mineral obsidian and an archeological glass, respectively [32].

A non-linear regression, performed on all data obtained for glass IDF21-EC14 at pH_T >7, gave an apparent E_a value of 76±2 kJ mol^{-1} and a kinetic rate constant of k_0=2.7 x 10^6 g m^{-2} d^{-1}; the data and regression results are plotted in Figure 5.2. The activation energy of IDF21-EC14 appears to be within the expected range for the activation energy of silicate dissolution, which varies between 50 and 90 kJ/mol [37]. This further supports the idea that the breakage of a Si-O bond is the rate-limiting step in the alteration of IDF21-EC14 under dilute conditions. For comparison purposes, the activation energies of other glasses and silicate minerals are: quartz (66-83 kJ mol^{-1}), amorphous silica (74.5 kJ mol^{-1}), basaltic glasses (72.4 kJ mol^{-}1), French glass R7T7 (71 kJ mol^{-1}), LAWA44 (60 kJ mol^{-1}), LAWB45 (53 kJ mol^{-1}), LAWC22 (64 kJ mol^{-1}), and IDF1-B2 (64 kJ mol^{-1}) [13, 36, 37]. Finally, the kinetic constant k_0 of the IDF21-EC14 dissolution is in the wide general range (~10^4 to 10^8 g m^{-2} d^{-1}) seen with other LAW glasses [13, 36, 38].

5.2 Dynamic Dissolution of IDF21-EC14 Under Saturating Conditions

5.2.1 Congruency of Dissolution and Mechanistic Considerations

Plots of the data for dissolution of IDF21-EC14 at various pH and temperature values under saturating conditions are shown in Appendix B, pages B3, B5, B7, and B9. The dissolution rate data for B, Si and Re are provided in Tables 5.3 to 5.6. Several observations can be made regarding the general trends exhibited by these data.

At 90ºC, when the influent solution was spiked with 1 ppm Si, all of the analyzed elements (B, Na, Si, Al, and Re) were leached approximately congruently at steady state (Appendix B, page B3). However, as the spiking level increased, Na and B release rate became significantly higher than those of the other elements, all of which were generally similar. Interestingly, the Re rates fell increasingly below those of B and Na with increasing spiking levels. Very little Al dissolution is observed when $[Si]_{in} \geq 80$ ppm. At all spiking levels, B, Na, and Re release rates start at high initial values and decline over the course of the test towards their steady state values. As discussed previously, [16], one explanation is that this behavior arises from an initial large release of the glass constituent (due to dissolution of fines and/or rough surfaces upon first contact with water) followed by the gradual replacement of the effluent solution without the concomitant dissolution of the constituent or with dissolution at a lower rate than the initial rate. Plots of steady state NDR_i vs. $\alpha[H_4SiO_4]$ at 90°C, shown in Figure 5.3, show increases for B and Na with increasing $\alpha[H_4SiO_4]$, contrary to expectations based on Equation (1.1). The rates for Re, however, do show a general decline.

At 70°C, the dissolution profiles of various elements in solutions with varying degrees of saturation (Appendix B, page B5) showed many of the same features as the corresponding dissolution profiles at 90°C. Plots of steady state NDR_i vs. $\alpha[H_4SiO_4]$, shown in Figure 5.4, show minima for B and Na with increasing $\alpha[H_4SiO_4]$, again, contrary to expectations based on Equation (1.1). The rates for Re, however, do show a general decline. Nevertheless, it is clear that these observations are at odds with the classical understanding of glass dissolution, which anticipates decreased glass dissolution rates with increasing solution saturation under all experimental conditions.

At 40ºC, when the influent solution was spiked with 1 ppm Si, Na rates decreased with time while B, Al, and Si increased (Appendix B, page B7), which is markedly different from that observed at 90ºC. This behavior is still evidently in the test spiked with 5 ppm Si but not at higher concentrations. Plots of steady state NDR_i vs. $\alpha[H_4SiO_4]$, shown in Figure 5.5, show minima for B and Na, though more shallow than those for tests at 70ºC.

Finally, at 23ºC, generally similar time dependences were observed at all Si spiking levels, with Na, and to a lesser extent B and Re, starting from high initial values and declining over time. Plots of steady state NDR_i vs. $\alpha[H_4SiO_4]$, shown in Figure 5.6, show steady declines for B, Al, and Re, with more scattered behavior for Na and Si.

5.2.2 Estimation of Parameters K_g and r_{IEX} at 15°C

Data from tests at various H_4SiO_4 concentrations are plotted in Figures 5.3 – 5.6. These data were used to determine the steady-state NDR values for each temperature. As described in Section 4.4, the K_g value of the glass at a specific temperature was calculated by performing a linear regression on the data points of the linear portion of the steady-state NDR vs. $\alpha[H_4SiO_4]$ plot. The linear regressions performed at each temperature and the resulting K_g values are shown in the plots of Figure 5.7 for all temperatures. At 90°C, no linear portion with negative slope could be identified and therefore no K_g value could be determined at 90°C. At 23, 40, and 70°C, a reasonable linear portion could be defined by three data points in each case, as shown in Figure 5.7. As previously stated and shown in Figure 5.7, at 40°C and even more so at 70°C after an initial decrease, NDR actually increased as $\alpha[H_4SiO_4]$ increased, which is contrary to the rate law. This effect is so strong at 90°C that only the increasing portion is evident in the data.

To estimate the value of K_g for IDF21-EC14 at the presumed repository temperature of 15°C, ln K_g values obtained at 23, 40, and 70°C as described above were plotted as a function of 1/T (K^{-1}) and a linear regression was performed on the data (Figure 5.8). The K_g value at 15°C was estimated to be 6.75×10^{-4} mol L^{-1}. This value is in the range of the corresponding values determined previously for other LAW glasses [13, 36, 38] (see also Section 5.3).

Ion exchange rates for all of the tests performed (under dilute as well as under saturating conditions) were estimated following the McGrail convention, as corrected, (see Section 4.4) and shown here in Tables 5.7-5.10. For this glass, it was possible to determine ion exchanges rates for the majority of the tests. According to the classical understanding of glass dissolution and as previously discussed, ion exchange is expected to dominate at the initial stages of alteration (especially at low temperature and acidic to neutral pH environments) and, again, when the glass dissolves near saturation at its residual rate. Consequently, the ion exchange rate of a glass at a specific temperature is obtained from tests at saturating or near saturation conditions.

As noted previously, the McGrail convention very likely underestimates ion exchange rates. Considering that: a) tetrahedral B undergoes dissolution when the Na cation responsible for charge compensating the BO_4^- site undergoes exchange with a proton and b) Na cations associated with $^{IV}B\text{-}O\text{-}B^{IV}$ clusters are exchanged before network terminal NBOs, it is possible that the difference between Na and B dissolution rates merely reflects the number of terminal NBOs sites involved in inter-diffusion.

The ion exchange rates obtained from tests at saturating or near saturation conditions at each temperature were plotted as a function of 1/T (K^{-1}) and a linear regression was performed on the data (Figure 5.9) to determine the activation energy (E_{IEX}) of the ion exchange reaction and to estimate the r_{IEX} value at the presumed repository temperature (15°C). The results give an E_{IEX} value of 41.7±4.1 kJ mol^{-1}. This value is similar to but somewhat lower than the values reported for LAWA44 [6] and IDF-B2 [13] of 65 and 58 kJ mol^{-1}, respectively.

5.3 Summary of Kinetic Parameters for IDF21-EC14

A summary of the kinetic parameters of LAW glass IDF21-EC14 determined in the present study is shown in Table 5.11. It is apparent that the glass exhibits kinetic parameters that are within the expected range for dissolution of silicate minerals and very close to values reported for other LAW Glasses (Table 5.11). The kinetic parameters of Equation 1.1 (k_0, η, E_a, and r_{IEX}) are considered to be intrinsic to a specific formulation and, thus, some dependence on glass composition is expected. The value of η for IDF21-EC14 is consistent with the trend defined by glasses LAWA44, LAWB45, LAWC22, and IDF1-B2, which suggests that this parameter increases with alkali content; however, other glasses do not follow this trend, as noted previously [14], suggesting a more complex composition dependence. In terms of r_{IEX}, the IDF21-EC14 uncorrected value of 4.2 x 10^{-10} mol m^{-2} s^{-1} (7.4 x 10^{-11} mol m^{-2} s^{-1} when corrected) is well within the range of previously reported uncorrected values exhibited by glasses with elevated Na_2O content.

Finally, the rate constant k_0 is also thought to be an intrinsic property of the glass. The results in Table 5.11 show that the measured values of this parameter vary from about 10^4 – 10^8 g m^{-2} d^{-1}. The value for IDF21-EC14 falls near the middle of that range.

SECTION 6.0
SUMMARY AND CONCLUSIONS

A complete suite of SPFT tests was performed on the high waste loading LAW glass IDF21-EC14. The results allowed for the determination of the kinetic parameters in the chemical affinity-based kinetic rate law of Equation 1.1 that is used to model LAW glass dissolution in the Hanford IDF. All of the kinetic parameter estimates for IDF21-EC14 were found to be within the expected range for dissolution of glasses and silicate phases. These results further confirm results from the first tests conducted on high waste loading LAW glasses [13], which indicated that the rate law parameters for those glasses are comparable to those for the baseline WTP glasses. The results from the present work for the high waste loading glass IDF21-EC14 are consistent with that finding. Despite that consistency, some significant deviations from the glass dissolution behavior expected based on the kinetic rate law of Equation 1.1 were evident in the data for IDF21-EC14, as summarized below.

An examination of the solution chemistry of the collected SPFT effluent samples revealed that alteration of IDF21-EC14 far from saturation followed closely the classical theory of glass dissolution (based on solid state inter-diffusion coupled with silicate network hydrolysis and the formation of a hydrated glass layer that may become passivating over time). In contrast, alteration of IDF21-EC14 in environments of increasing saturation exhibited deviations from the classical theory of glass dissolution, which requires that the rate of glass dissolution drop as the bulk solution becomes progressively more saturated with respect to a simple silicate phase, at least for elevated temperatures (90 and 70°C). Such behavior challenges the kinetic rate law as written in Equation 1.1. One of the most striking deviations from the kinetic rate law of Equation 1.1 is the failure of the rate to decrease with increasing [Si] (which should result in decreasing reaction affinity) and, indeed, the observation that the rate can even *increase* with increasing [Si]. For example, the dissolution of IDF21- EC14 under increasingly saturated conditions and 90°C showed a glass dissolution rate, as indicated by the B release rate, that continued to increase with increasing orthosilicic concentrations in the effluent solutions and reached values that exceeded the forward rate at the specific pH and temperature. In stark contrast, Re dissolution sharply decreased and eventually assumed a rate that was <10% of the corresponding glass dissolution rate. Deviations from the kinetic rate law were also observed previously for LAW glasses IDF1-B2 [13], IDF7-E12 [14], and ORPLG8 [38]; in the case of ORPLG9 it was noted that phase separation may have contributed to the observed behavior [38].

The above observations collectively highlight the importance of improved understanding of the mechanisms of LAW glass dissolution and the limitations of the present kinetic rate law. The rate law appears to be overly simplistic with respect to other more complex alteration mechanics that have been reported in the literature. From a pragmatic perspective, it is important to understand whether the present rate law, despite its limitations, is sufficiently accurate for supporting the IDF PA. However, since measurements on IDF21-EC14 have showed that the dissolution rate can increase with [Si], whereas the rate law would predict a decrease, it is difficult to argue that use of the rate law is necessarily conservative.

A further question relates to relevance of the dissolution behavior at elevated temperatures to the behavior at temperatures pertinent to the repository. The rate law in Equation 1.1 assumes that glass dissolution at elevated temperatures follows the same mechanism as at lower temperatures. It is possible, however, that different mechanisms may dominate at different temperatures. For example Stage III resumption of dissolution has been observed only at elevated temperatures and there is an ongoing debate as to the relevance of the phenomenon to typical repository temperatures. Consequently, in terms of determining the kinetic parameters for LAW glasses, it may be worth considering substituting the 90°C testing for testing at an intermediate temperature between 40 and 70°C. This substitution would focus the testing closer to the range of interest and would be more likely to allow for the inclusion of four points in the estimation of the K_g value at 15°C. In view of the very different behavior observed for boron and rhenium, it is also recommended that Re_2O_7 be included in the compositions of all LAW glasses selected for SPFT testing and that effluent solutions are subjected to Re analysis, at least for tests performed under saturating conditions.

Finally, it is clear that the McGrail convention for estimating ion exchange has limitations and needs to be revised since studies have suggested that B dissolution appears to be under the control of Na^+/H^+ exchange processes at many instances. Thus, simple subtraction of the boron rate from the sodium rate is likely to underestimate the ion exchange rate. WRPS has already commissioned studies of potential alternative approaches for incorporation of ion exchange into the rate law [15, 16] that may be implemented in the future.

SECTION 7.0
QUALITY ASSURANCE

This work was conducted under a quality assurance (QA) program compliant with the applicable criteria of 10 CFR 830.120; the American Society of Mechanical Engineers (ASME) Nuclear Quality Assurance (NQA)-1-2008 including NQA-1a-2009 addenda; and DOE Order 414.1D, Quality Assurance. These QA requirements are implemented through a Quality Assurance Project Plan for WRPS work [39] that is conducted at VSL. Test and procedure requirements by which the testing activities are planned and controlled are also defined in this plan. The program is supported by VSL standard operating procedures that were used for this work [40]. This is LAW work and is not subject to the requirements of DOE/RW-0333P, Office of Civilian Waste Management Quality Assurance Requirements and Description (QARD).

SECTION 8.0
REFERENCES

[1] "Experimentally Determined Dissolution Kinetics of Na-rich Borosilicate Glasses at Far-From-Equilibrium Conditions: Implications for Transition State Theory," J.P. Icenhower, B.P. McGrail, W.J. Shaw, E.M. Pierce, P. Nachimuthu, D.K. Shuh, E.A. Rodriguez, and J.L. Steele, *Geochimica Cosmochimica Acta* **72**, 2767-2788 (2008).

[2] "Measurement of Kinetic Rate Law Parameters on a Na-Ca-Al Borosilicate Glass for Low-Activity Waste," B.P. McGrail, W.L. Ebert, A.J. Bakel, and D.K. Peeler, *J. Nucl. Mater.* **249**, 175-189 (1997).

[3] "Low-Activity Waste Glass Studies: FY2000 Summary Report," B.P. McGrail, J.P. Icenhower, P.F. Martin, D.R. Rector, H.T. Schaef, E.A. Rodriguez, and J.L. Steele, PNNL-13381, Pacific Northwest National Laboratory, Richland, WA (2000).

[4] "Waste Form Release Data Package for the 2001 Immobilized Low-Activity Waste Performance Assessment," B.P. McGrail, J.P. Icenhower, P.F. Martin, H.T. Schaef, M.J. O'Hara, E.A. Rodriguez, and J.L. Steele, PNNL-13043, Rev. 2, Pacific Northwest National Laboratory, Richland, WA (2001).

[5] "Laboratory Testing of Bulk Vitrified Low-Activity Waste Forms to Support the 2005 Integrated Disposal Facility Performance Assessment," E.M. Pierce, B.P. McGrail, L.M. Bagaasen, E.A. Rodriguez, D.M. Wellman, K.N. Geiszler, S.R. Baum, L.R. Reed, J.V. Crum, and H.T. Schaef, PNNL-15126, Rev. 2, Pacific Northwest National Laboratory, Richland, WA (2005).

[6] "Waste Form Release Data Package for the 2005 Integrated Disposal Facility Performance Assessment," E.M. Pierce, B.P. McGrail, E.A. Rodriguez, H.T. Schaef, K.P. Saripalli, R.J. Serne, K.M. Krupka, P.F. Martin, S.R. Baum, K.N. Geiszler, L.R. Reed, and W.J. Shaw, PNNL-14805, Pacific Northwest National Laboratory, Richland, WA (2004).

[7] "The Activated Complex in Chemical Reactions," H. Eyring, *J. Chem. Phys.* **3**, 107-114 (1935).

[8] "Thermodynamic and Kinetic Constraints on Reaction Rates among Minerals and Aqueous Solutions. I. Theoretical Considerations," P. Åagaard and H.C. Helgeson, *Am. J. Sci.* **282**, 237-285 (1982).

[9] "A General Rate Equation for Nuclear Waste Glass Corrosion," B. Grambow, *Material Research Symposium Proceedings* **44**, 15-27 (1985).

[10] "Kinetic Ion Exchange Salt Effects on Glass Leaching," X. Feng and I.L. Pegg, *Energy, Environment and Information Management*, Eds. H. Wang, S. Chang, and H. Lee, Argonne, IL, p. 7-9, (1992).

[11] "Effects of Salt Solutions on Glass Dissolution," X. Feng and I.L. Pegg, *Phys. Chem. Glasses*, **35**, 1 (1994).

[12] "A Glass Dissolution Model for the Effects of S/V on Leachate pH," X. Feng and I.L. Pegg, *J. Non-Cryst. Solids*, **175**, 281 (1994).

[13] "ILAW Glass Testing for Disposal at IDF: Phase 1 Testing," A. Papathanassiu, I.S. Muller, M. Brandys, K. Gilbo, A. Barkatt, I. Joseph, and I.L. Pegg, Final Report, VSL-11R2270-1, Rev. 0, Vitreous State Laboratory, The Catholic University of America, Washington DC, 6/6/11.

[14] "FY2016 ILAW Glass SPFT Testing for Disposal at IDF," A.E. Papathanassiu, C. Viragh, I.S. Muller, and I.L. Pegg, Final Report, VSL-17R3860-1, Rev. 0, Vitreous State Laboratory, The Catholic University of America, Washington DC, 7/12/17.

[15] "Survey of Literature on the Role of Ion Exchange in Glass Corrosion," A.E. Papathanassiu, W. Gong, W. Lutze, and I.L. Pegg, Final Report, VSL-17L4320-1, Rev. 0, Vitreous State Laboratory, The Catholic University of America, Washington DC, 8/2/17.

[16] "A Critical Review of Ion Exchange in Nuclear Waste Glasses to Support the Immobilized Low-Activity Waste Integrated Disposal Facility Rate Model," C.E. Lonergan, RPT-IGTP-018, Rev A.0, Pacific Northwest Laboratory, Richland, WA, August 2017.

[17] "FY2017 ILAW Glass SPFT Testing for Disposal at IDF," A.E. Papathanassiu, I.S. Muller, and I.L. Pegg, Test Plan, VSL-16T4320-1, Rev. 0, Vitreous State Laboratory, The Catholic University of America, Washington DC, 1/25/17.

[18] Request for Off-Site Services (Technical) Statement of Work, "ILAW Glass Durability Testing to Support IDF PA Maintenance," Rev. 0, Requisition #292409, Washington River Protection Solutions, LLC (WRPS), 8/9/16.

[19] "The Initial Dissolution Rates of Simulated UK Magnox–THORP Blend Nuclear Waste Glass as a Function of pH, Temperature and Waste Loading," N. Cassingham, C.L. Corkhill, D.J. Backhouse, R.J. Hand, J.V. Ryan, J.D. Vienna, and N.C. Hyatt, *Mineralogical Magazine* **79(6)**, 1529–1542 (2015).

[20] "Selection of LAW Glasses for FY 2017 SPFT Testing," I.S. Muller and I.L. Pegg, Final Report, VSL-16L4320-1, Rev. 0, Vitreous State Laboratory, The Catholic University of America, Washington DC, 2/7/17.

[21] "Enhanced LAW Glass Correlation – Phase 1," I.S. Muller, K.S. Matlack, I.L. Pegg and I. Joseph," Final Report, VSL-16R4000-1, Rev. 0, Vitreous State Laboratory, The Catholic University of America, Washington, DC, 12/1/16.

[22] "Enhanced LAW Glass Correlation – Phase 2," I.S. Muller, K.S. Matlack, I.L. Pegg and I. Joseph," Final Report, VSL-16R4140-1, Rev. 0, Vitreous State Laboratory, The Catholic University of America, Washington, DC, 6/30/17.

[23] "Enhanced LAW Glass Correlation – Phase 3," I.S. Muller, K. Matlack, I.L. Pegg and I. Joseph," Test Plan, VSL-16T3930-1, Rev. 0, Vitreous State Laboratory, The Catholic University of America, Washington, DC, 6/13/16.

[24] "Proposed Approach for Development of LAW Glass Formulation Correlation," I.S. Muller, G. Diener, I. Joseph, and I.L Pegg, Letter Report, VSL-04L4460-1, Rev. 2, Vitreous State Laboratory, The Catholic University of America, Washington, DC, October 29, 2004.

[25] "LAW Container Centerline Cooling Data" RPP-WTP Memorandum, L. Petkus to CC. Musick, CCN# 074181, 10/16/03.

[26] "Round Robin Testing of a Reference Glass for Low-Activity Waste Forms," W.L. Ebert and S.F. Wolf, Department of Energy Report ANL-99/22, Argonne National Laboratory, Argonne, IL (1999).

[27] "Characterization of the Defense Waste Processing Facility (DWPF) Environmental Assessment (EA) Glass Standard Reference Material," C.M. Jantzen, N.E. Bibler, D.C. Beam, C.L. Crawford, and M.A. Pickett, WSRC-TR-92-346, Westinghouse Savannah River Company, Aiken, SC, June, 1993.

[28] "Standard Practice for Measurement of the Glass Dissolution Rate Using the Single-Pass Flow-Through Test Method," ASTM Standard C 1662-10.

[29] "Permeability of PEEK to Carbon Dioxide," *Journal of Applied Polymer Science,* F. De Candia and V. Vittoria, 51, 2103 (1994).

[30] "Evaluation of the Single-Pass Flow Through Test to Support a Low-Activity Waste Specification," B.P. McGrail and D.K. Peeler, Final Report, PNNL-10746, Pacific Northwest Laboratory, Richland, WA, 1995.

[31] "The Controversial Role of Inter-Diffusion in Glass Alteration," S. Gin, L. Neill, M. Fournier, P. Frugier, T. Ducasse, M. Tribet, A. Abdelouas, B. Parruzot, J. Neeway, and N. Wall, *Chem. Geol.* **440**, 115–123 (2016).

[32] "Solid State Diffusion During Nuclear Glass Residual Alteration in Solution," T. Chave, P. Fugier, A. Ayral, and S. Gin, *J. Nucl. Mater.* **362(2-3)**, 466-473 (2007).

[33] "Hydrogen–Sodium Interdiffusion in Borosilicate Glasses Investigated from First Principles," G. Geneste, F. Bouyer, and S. Gin, *J. Non-Cryst. Solids* **352**, 3147–3152 (2006).

[34] "Origin and Consequences of Silicate Glass Passivation by Surface Layers," S. Gin, P. Jollivet, M. Fournier, F. Angeli, P. Frugier, and T. Charpentier, *Nat. Commun.* **6**, 6380 (2015).

[35] "Contribution of Atom-Probe Tomography to a Better Understanding of Glass Alteration Mechanisms: Application to a Nuclear Glass Specimen Altered 25 years in a Granitic Environment," S. Gin, J.V. Ryan, D.K. Schreiber, J. Neeway , M. Cabié, *Chem. Geol.* **349–350** 99–109 (2013).

[36] "Immobilized Low-Activity Waste Glass Release Data Package for the Integrated Disposal Facility Performance Assessment," V.L. Freedman, J.V. Ryan, and D.H. Bacon, Final Report, PNNL-24615, Pacific Northwest Laboratory, Richland, WA, September 2015.

[37] "Silicate Glass and Mineral Dissolution: Calculated Reaction Paths and Activation Energies for Hydrolysis of a Q^3 Si by H_3O^+ Using Ab Initio Methods," L.J. Criscenti, J.D. Kubicki, and S.L. Brantley, *J. Phys. Chem*. A *110 (1), 198–206 (2006).*

[38] "FY2016 ILAW Glass Corrosion Testing with the Single-Pass Flow-Through Method," J.J. Neeway, B.D. Williams, R.M. Asmussen, I.I. Leavy, B.P. Parruzot, J.R. Stephenson, E.A. Cordova, E.M. Mcelroy, Final Report, PNNL-26169, RPT-IGTP-013, Rev. 0.0, Pacific Northwest Laboratory, Richland, WA, April 2017.

[39] "Quality Assurance Project Plan for WRPS Support Activities Conducted by VSL," VSL-QAPP-WRPS, Rev. 4, Vitreous State Laboratory, The Catholic University of America, Washington, DC, 9/14/16.

[40] "Master List of Controlled VSL Manuals and Standard Operating Procedures in Use," QA-MLCP, Rev. 157, Vitreous State Laboratory, The Catholic University of America, Washington, DC, 12/15/17.

Table 2.1a. Baseline Matrix for SPFT Testing at 23°C.

Temp [°C]	Train # "*i*"	Duration [*d*]	Dt_{samp} [*d*]	# Samples "*N*"	$[Si]_{in}$ [*ppm*]	F [*µl/min*]	pH	m_g [*g*]
1	*2*	*3*	*4*	*5*	*6*	*7*	*8*	*9*
23	1	30	3.0	10	0	7.0	7	1.00
	2	30	3.0	10	0	7.0	8	1.00
	3	30	3.0	10	0	7.0	9	1.00
	4	30	3.0	10	0	7.0	10	0.50
	5	30	3.0	10	0	7.0	11	0.50
	6	30	3.0	10	0	7.0	12	0.50
	7	30	3.0	10	1.0	7.0	9	4.00
	8	30	3.0	10	15	7.0	9	4.00
	9	30	3.0	10	22.5	7.0	9	4.00
	10	30	3.0	10	30	7.0	9	4.00
	11	30	3.0	10	45	7.0	9	4.00
	12	30	3.0	10	52.5	7.0	9	4.00

Table 2.1b. Baseline Matrix for SPFT Testing at 40°C.

Temp [°C]	Train # "*i*"	Duration [*d*]	Dt_{samp} [*d*]	# Samples "*N*"	$[Si]_{in}$ [*ppm*]	F [*µl/min*]	pH	m_g [*g*]
1	*2*	*3*	*4*	*5*	*6*	*7*	*8*	*9*
40	1	20	2.0	10	0	28.0	7	1.00
	2	20	2.0	10	0	28.0	8	1.00
	3	20	2.0	10	0	28.0	9	1.00
	4	20	2.0	10	0	28.0	10	0.50
	5	20	2.0	10	0	28.0	11	0.50
	6	20	2.0	10	0	28.0	12	0.50
	7	20	2.0	10	1.0	7.0	9	0.50
	8	20	2.0	10	5	7.0	9	0.50
	9	20	2.0	10	15	7.0	9	1.00
	10	20	2.0	10	30	7.0	9	1.00
	11	20	2.0	10	45	7.0	9	2.00
	12	20	2.0	10	60	7.0	9	2.00

Table 2.1c. Baseline Matrix for SPFT Testing at 70°C.

Temp [°C]	Train # "*i*"	Duration [*d*]	Dt_{samp} [*d*]	# Samples "*N*"	$[Si]_{in}$ [*ppm*]	F [*μl/min*]	pH	m_g [*g*]
1	*2*	*3*	*4*	*5*	*6*	*7*	*8*	*9*
70	1	10	1	10	0	35	7	1.00
	2	10	1	10	0	35	8	1.00
	3	10	1	10	0	35	9	1.00
	4	10	1	10	0	35	10	0.50
	5	10	1	10	0	35	11	0.50
	6	10	1	10	0	35	12	0.50
	7	10	1	10	1	45	9	0.50
	8	10	1	10	5	45	9	1.00
	9	10	1	10	10	45	9	1.00
	10	10	1	10	20	45	9	1.00
	11	10	1	10	40	45	9	2.00
	12	10	1	10	80	45	9	2.00

Table 2.1d. Baseline Matrix for SPFT Testing at 90°C.

Temp [°C]	Train # "*i*"	Duration [*d*]	Dt_{samp} [*d*]	# Samples "*N*"	$[Si]_{in}$ [*ppm*]	F [*µl/min*]	pH	m_g [*g*]
1	*2*	*3*	*4*	*5*	*6*	*7*	*8*	*10*
90	1	10	1	10	0	35	7	0.75
	2	10	1	10	0	35	8	0.75
	3	10	1	10	0	35	9	0.50
	4	10	1	10	0	35	10	0.50
	5	10	1	10	0	35	11	0.50
	6	10	1	10	0	35	12	0.50
	7	10	1	10	1.0	50	9	0.50
	8	10	1	10	5	50	9	1.00
	9	10	1	10	10	50	9	1.00
	10	10	1	10	20	50	9	1.00
	11	10	1	10	80	50	9	2.00
	12	10	1	10	120	50	9	2.00

Table 3.1. Target Composition (wt%) of Glass IDF21-EC14 (ORLEC14) Selected for SPFT Testing.

Component	IDF21-EC14
Al_2O_3	10.00
B_2O_3	10.00
CaO	1.95
Cr_2O_3	0.34
Fe_2O_3	0.34
K_2O	0.50
MgO	1.00
Na_2O	24.00
NiO	0.01
PbO	0.01
SiO_2	38.71
SnO_2	2.33
TiO_2	0.34
V_2O_5	0.35
ZnO	3.00
ZrO_2	6.03
Cl	0.20
F	0.08
P_2O_5	0.12
SO_3	0.60
Re_2O_7	0.10
Total	100.0

Table 3.2. Target and Analyzed Compositions (wt%) of IDF21-EC14 Glasses.

Component	IDF21-EC14	IDF21-EC14 As-melted	IDF21-EC14CCC glass from center of crucible			IDF21-EC14CCC layer near crucible wall
	Target	Analyzed*	Analyzed*			Analyzed*
Al_2O_3	10.00	10.03	10.03	9.98	10.04	10.17
B_2O_3	10.00	9.63	9.61			9.57
CaO	1.95	2.07	1.94	1.97	2.00	1.88
Cr_2O_3	0.34	0.35	0.33	0.34	0.36	0.33
Fe_2O_3	0.34	0.35	0.37	0.36	0.35	0.33
K_2O	0.50	0.52	0.49	0.46	0.48	0.46
MgO	1.00	1.04	0.94	0.97	0.93	0.91
Na_2O	24.00	23.39	24.77	24.60	24.50	24.86
NiO	0.01	0.01	0.01	0.02	0.01	0.01
PbO	0.01	0.01	0.01	0.01	0.02	0.01
SiO_2	38.71	39.20	38.58	38.63	38.80	39.33
SnO_2	2.33	2.13	2.11	2.19	2.12	1.94
TiO_2	0.34	0.38	0.40	0.41	0.40	0.35
V_2O_5	0.35	0.37	0.34	0.38	0.36	0.33
ZnO	3.00	3.03	2.88	2.87	2.87	2.69
ZrO_2	6.03	5.96	5.69	5.74	5.69	5.30
Cl	0.20	0.16	0.16	0.15	0.15	0.15
F	0.08	0.08$	0.08$	0.08$	0.08$	0.08$
P_2O_5	0.12	0.14	0.14	0.13	0.14	0.14
SO_3	0.60	0.57	0.56	0.53	0.53	0.55
Re_2O_7	0.10	0.15	0.14	0.12	0.13	0.10
SUM	100.0	99.6	99.6	99.6	99.6	99.5

*Analyzed by XRF except for boron and lithium, which were measured by DCP-AES
$ Target concentration

Table 4.1. Measured in Situ pH (pH_T) of Influent Solutions.

$pH_{23°C}$	$pH_{40°C}$	$pH_{70°C}$	$pH_{90°C}$
7.0	6.6	6.0	5.6
8.0	7.6	6.9	6.6
9.0	8.6	8.0	7.6
10.0	9.6	9.0	8.6
11.0	10.7	10.0	9.6
12.0	11.6	10.9	10.5

Table 5.1. Measured Steady-State Glass Dissolution Rates for Glass Alteration Under Dilute Conditions.

Target pH_{RT}	**T (°C)**	**r_0, measured ($g\ m^{-2}\ d^{-1}$)**
7	90	0.7282
8	90	0.4294
9	**90**	**0.1512**
10	90	0.2357
11	90	1.0585
12	90	2.8921
7	70	0.3299
8	70	0.1728
9	**70**	**0.0446**
10	70	0.1239
11	70	0.3732
12	70	1.0357
7	40	0.0173
8	40	0.0048
9	**40**	**0.0077**
10	40	0.0264
11	40	0.0753
12	40	0.1588
7	23	1.6450-03
8	23	4.174E-04
9	**23**	**1.303E-03**
10	23	6.678E-03
11	23	1.972E-02
12	23	4.5890E-02

In bold: Forward dissolution rates at pH_{RT} 9.

Table 5.2. Estimation of the Average Value of the Kinetic Parameter η for Glass IDF21-EC14.

Temperature (°C)	η
23	0.4723
40	0.4754
70	0.4407
90	0.5262
Average	0.4787
Standard Deviation	0.035

Table 5.3. Dissolution Rates of B, Si, and Re from Tests with Increasing $[Si]_{in}$ at 90°C.

Line	Target [Si]	NDR_B, g m^{-2} d^{-1}	NDR_{Si}, g m^{-2} d^{-1}	NDR_{Re}, g m^{-2} d^{-1}
SP20-C	0	0.1512±0.0028	0.1444±0.0034	-
SP20-G	1 ppm	0.1015±0.0054	0.1432±0.0043	0.1259±0.0077
SP20-H	5 ppm	0.1271±0.014	0.0926±0.002	0.0288±0.0045
SP20-I	10 ppm	0.1959±0.0102	0.0874±0.0042	0.0903±0.0061
SP20-J	20 ppm	0.2156±0.0093	0.096±0.0055	0.0779±0.0066
SP20-K	80 ppm	0.229±0.0096	0.0701±0.0086	0.0085±0.0012
SP20-L	120 ppm	0.222±0.0087	0.0692±0.0078	0.0064±0.0009

Table 5.4. Dissolution Rates of B and Si from Tests with Increasing $[Si]_{in}$ at 70°C.

Line	Target [Si]	NDR_B, g m^{-2} d^{-1}	NDR_{Si}, g m^{-2} d^{-1}	NDR_{Re}, g m^{-2} d^{-1}
SP21-C	0	0.0446±0.0014	0.0459±0.0014	-
SP21-G	1 ppm	0.0782±0.0008	0.0822±0.0008	0.1078±0.001
SP21-H	5 ppm	0.0667±0.004	0.0701±0.0032	0.0925±0.008
SP21-I	10 ppm	0.0331±0.0003	0.0297±0.001	0.0333±0.0043
SP21-J	20 ppm	0.0322±0.004	0.0343±0.0041	0.0325±0.0008
SP21-K	40 ppm	0.0649±0.0026	0.039±0.0007	0.0264±0.0021
SP21-L	80 ppm	0.0864±0.0047	0.0486±0.0023	0.0118±0.0001

Table 5.5. Dissolution Rates of B, Si, and Re from Tests with Increasing $[Si]_{in}$ at 40°C.

Line	Target [Si]	NDR_B, g m^{-2} d^{-1}	NDR_{Si}, g m^{-2} d^{-1}	NDR_{Re}, g m^{-2} d^{-1}
SP22-C	0	0.0077±0.0001	0.0085±0.0002	-
SP22-G	1 ppm	0.0126±0.0002	0.0134±0.0004	0.0022±0.0001
SP22-H	5 ppm	0.0116±0.0001	0.0135±0.0011	0.0018±0.0001
SP22-I	15 ppm	0.005±0.0001	0.0081±0.0013	0.0008±0.0001
SP22-J	30 ppm	0.0033±0.0003	0.0158±0.0013	0.00036±0.00003
SP22-K	45 ppm	0.0042±0.0002	0.0153±0.0007	0.00023±0.00002
SP22-L	60 ppm	0.0051±0.0002	0.0219±0.0012	0.00020±0.00003

Table 5.6. Dissolution Rates of B, Si, and Re from Tests with Increasing $[Si]_{in}$ at 23°C.

Line	Target [Si]	NDR_B, g m^{-2} d^{-1}	NDR_{Si}, g m^{-2} d^{-1}	NDR_{Re}, g m^{-2} d^{-1}
SP23-C	0	0.001303±0.000004	0.001724±0.000037	-
SP23-G	1 ppm	0.000594±0.000011	0.00073±0.00003	0.001184±0.000036
SP23-H	15 ppm	0.00034±0.000031	0.001687±0.000064	0.000464±0.000034
SP23-I	22.5 ppm	0.000463±0.000037	0.000843±0.00013	0.000626±0.00006
SP23-J	30 ppm	0.000385±0.000033	0.001858±0.000234	0.00056±0.00004
SP23-K	45 ppm	0.000357±0.00003	0.000954±0.0001	0.00008±0.0000002
SP23-L	52.5 ppm	0.000351±0.000023	0.001854±0.000222	0.00048±0.00005

Table 5.7. Ion Exchange Rates ("Corrected" Values) for all Tests Performed at 23°C.

23°C				
pH(in situ)	**pH_{RT}**	**$[Si]_{in}$, ppm**	**NDR, $g\ m^{-2}\ d^{-1}$**	**$r_{IEX} \times 10^8$ $mol\ m^{-2}\ s^{-1}$**
7	7	0	1.6499E-03	0.00839±0.00129
8	8	0	4.1742E-04	0.01258±0.00072
9	9	0	1.3031E-03	0.00614±0.00061
10	10	0	6.6783E-03	-
11	11	0	1.9717E-02	0.2051±0.02427
12	12	0	4.5897E-02	0.45244±0.05693
9	9	1	5.9367E-04	0.00605±0.0007
9	9	15	3.4001E-04	0.00858±0.00107
9	9	22.5	4.6338E-04	0.01252±0.00148
9	9	30	3.8452E-04	0.0131±0.00147
9	9	45	3.5659E-04	0.00992±0.00082
9	9	52.5	3.5131E-04	0.00919±0.00114

[a]Highlighted rows indicate ion exchange with Li due to the use of LiOH buffers.

Table 5.8. Ion Exchange Rates ("Corrected" Values) for all Tests Performed at 40°C.

40°C				
pH(in situ)	**pH_{RT}**	**$[Si]_{in}$, ppm**	**NDR, $g\ m^{-2}\ d^{-1}$**	**$r_{IEX} \times 10^8$, $mol\ m^{-2}\ s^{-1}$**
6.63	7	0	0.0173	0.0213
7.61	8	0	0.0048	0.0296±0.0017
8.63	9	0	0.0077	0.0011
9.63	10	0	0.0264	-
10.67	11	0	0.0753	0.6734±0.0561
11.62	12	0	0.1588	1.4273±0.0608
8.67	9	1	0.0126	0.0471±0.0041
8.67	9	5	0.0116	0.0339±0.0068
8.67	9	15	0.0050	0.0539±0.0064
8.67	9	30	0.0033	0.0699±0.0059
8.67	9	45	0.0042	0.0661±0.0078
8.67	9	60	0.0051	0.0643±0.0065

[a]Highlighted rows indicate ion exchange with Li due to the use of LiOH buffers.

Table 5.9. Ion Exchange Rates ("Corrected" Values) for all Tests Performed at 70°C.

70°C				
pH(in situ)	**pH_{RT}**	**$[Si]_{in}$, ppm**	**NDR, $g\ m^{-2}\ d^{-1}$**	**r_{IEX} x 10^8, $mol\ m^{-2}\ s^{-1}$**
5.96	7	0	0.3299	0.0974
6.91	8	0	0.1728	0.0955±0.0164
7.98	9	0	0.0446	0.0723
8.98	10	0	0.1239	-
9.96	11	0	0.3732	2.367±0.0468
10.86	12	0	1.0357	5.1692±0.3741
7.99	9	1	0.0782	0.0739±0.0112
7.99	9	5	0.0667	0.0937
7.99	9	10	0.0331	0.1098±0.0175
7.99	9	20	0.0322	0.2508±0.0113
7.99	9	40	0.0649	0.0869±0.0109
7.99	9	80	0.0864	0.0256

[a]Highlighted rows indicate ion exchange with Li due to the use of LiOH buffers.

Table 5.10. Ion Exchange Rates ("Corrected" Values) for all Tests Performed at 90°C.

90°C				
pH(in situ)	**pH_{RT}**	**$[Si]_{in}$, ppm**	**NDR, $g\ m^{-2}\ d^{-1}$**	**$r_{IEX} \times 10^8$, $mol\ m^{-2}\ s^{-1}$**
5.6	7	0	0.7282	-
6.6	8	0	0.4294	0.8328±0.0668
7.6	9	0	0.1512	0.153
8.6	10	0	0.2357	0.0453
9.6	11	0	1.0585	3.9469±0.3735
10.5	12	0	2.8921	10.8748±0.7011
7.6	9	1	0.1015	0.621±0.086
7.6	9	5	0.1271	0.6267±0.0666
7.6	9	10	0.1959	0.3305±0.0334
7.6	9	20	0.2156	0.3403±0.0289
7.6	9	80	0.2290	0.1243±0.1714
7.6	9	120	0.2220	0.2785±0.0553

[a]Highlighted rows indicate ion exchange with Li due to the use of LiOH buffers.

Table 5.11. Summary of Kinetic Parameters for IDF21-EC14 and Other LAW Glasses.

Glass Name	k_0 g m^{-2} d^{-1}	η	Eα kJ mol^{-1}	K_g(15°C) mol L^{-1}	r_{IEX} (15°C) * mol m^{-2} s^{-1}	Source
IDF21-EC14	**$2.7x10^6$**	**0.48±0.04**	**76±2**	**6.75×10^{-4}**	**7.4×10^{-11} ** (4.2×10^{-10})**	**This work**
IDF18-A161	$5.9x10^6$	0.28±0.06	61±6	2.3×10^{-4}	7.6×10^{-11}	[38] RPT-IGTP-013, Rev. 0
ORPLG9	$2.5x10^8$	0.36±0.07	81±7	log Kg = 100	5.3×10^{-11}	[38] RPT-IGTP-013, Rev. 0
IDF7-E12	$5.7x10^4$	0.32±0.03	55±5	$1.87x10^{-3}$	$<1x10^{-10}$	[14] VSL-17R3860-1, Rev. 0
LAWA44	$1.3x10^4$	0.49±0.08	60±7	$1.87x10^{-3}$	$5.3x10^{-11}$	[36] PNNL-24615 RPT-IGTP-005, Rev. 0
LAWB45	$1.6x10^4$	0.34±0.03	53±3	$1.79x10^{-3}$	0	[36] PNNL-24615 RPT-IGTP-005, Rev. 0
LAWC22	$1.0x10^5$	0.42±0.02	64±2	$1.80x10^{-3}$	$1.2x10^{-10}$	[36] PNNL-24615 RPT-IGTP-005, Rev. 0
IDF1-B2	$4.6x10^4$	0.49±0.05	64±4	$1.70x10^{-3}$	$3.4x10^{-10}$	[13] VSL-11R2270-1, Rev. 0
LAWABP1	$3.4x10^6$	0.35±0.03	68±3	$4.90x10^{-4}$	$3.4x10^{-11}$	[36] PNNL-24615 RPT-IGTP-005, Rev. 0

* As-reported values; uncorrected except where indicated (see Section 4.4).
** Corrected value

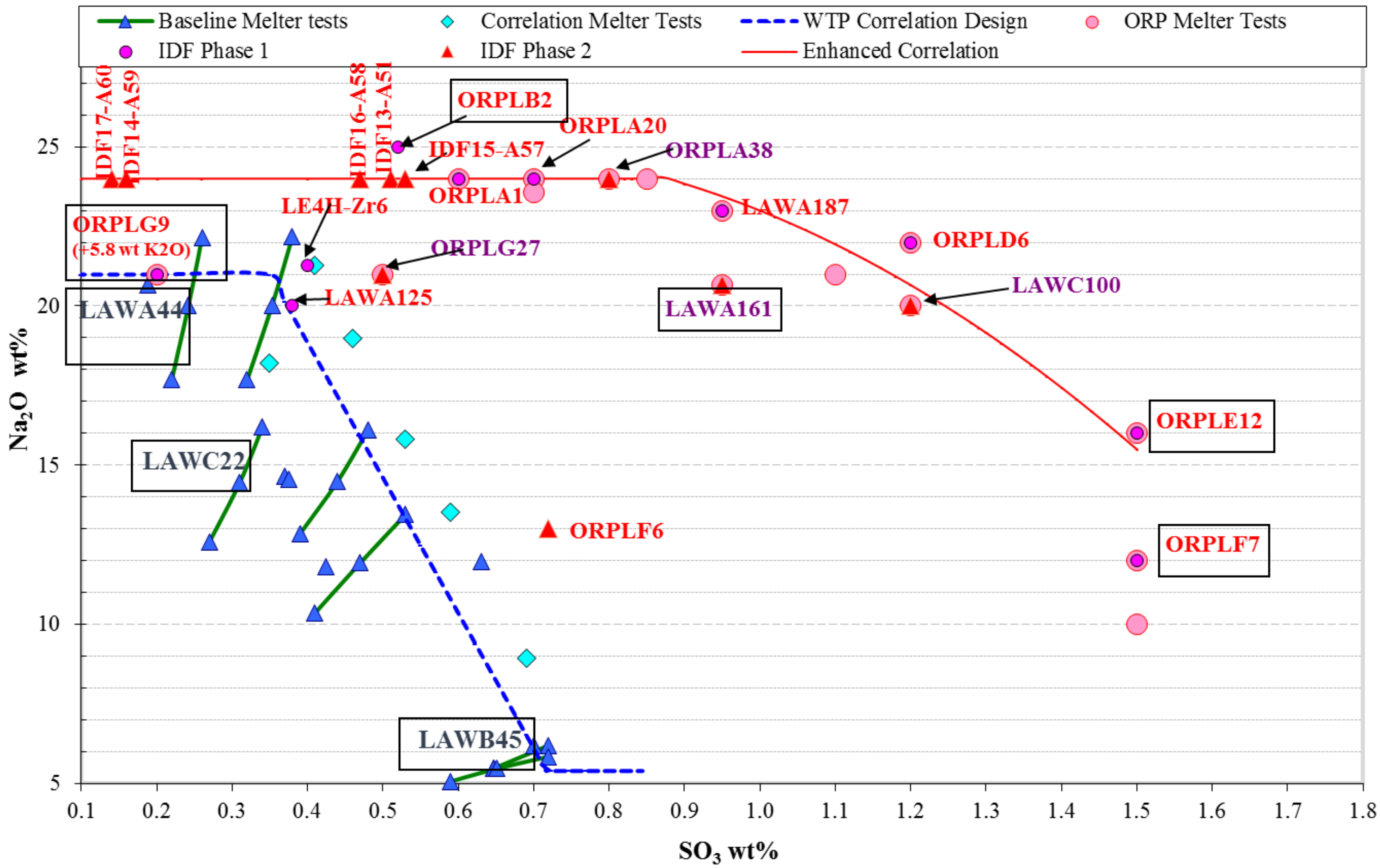

Figure 3.1. Overview of Na_2O and SO_3 loadings for WTP, ORP and IDF glasses (glasses selected earlier for SPFT testing are indicated by a box around the glass name).

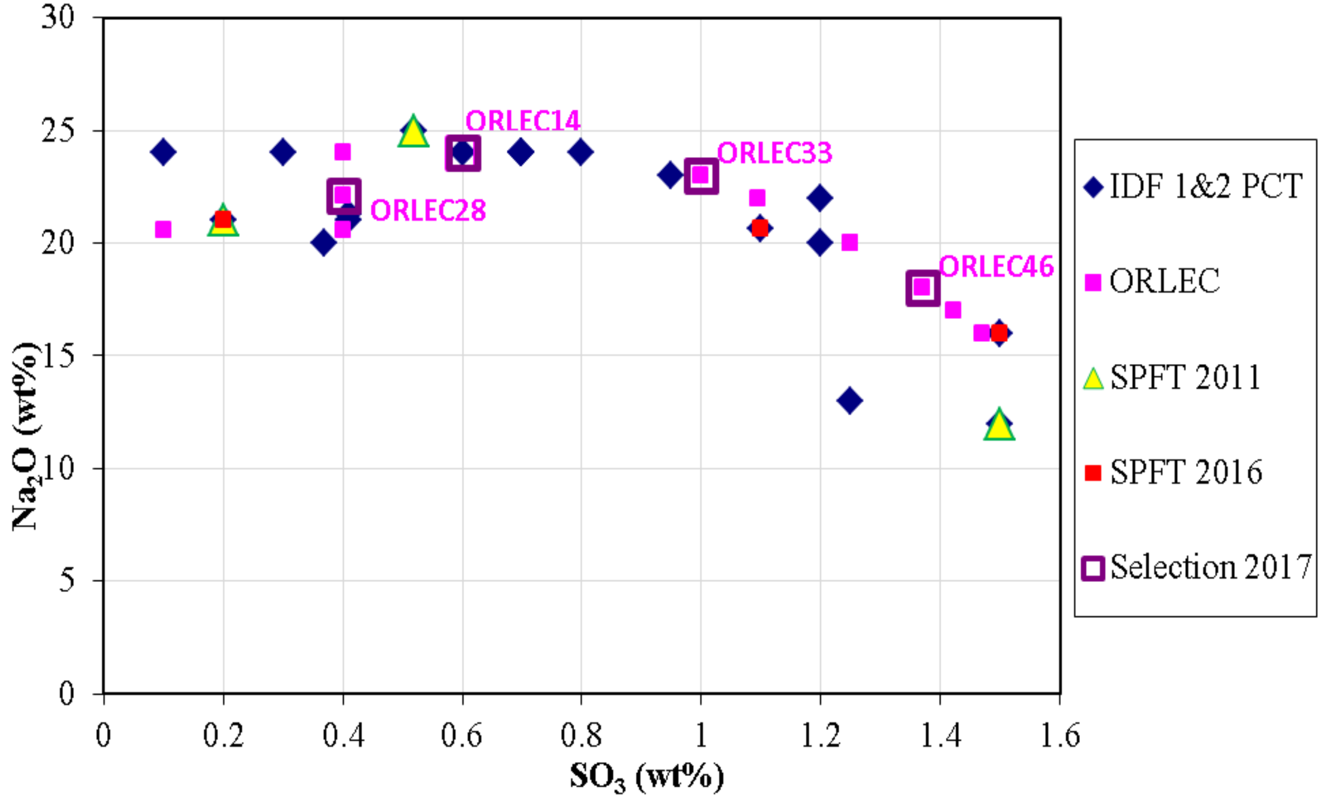

Figure 3.2. Na_2O and SO_3 concentrations for the 20 IDF glasses (blue diamonds); the three glasses SPFT tested in 2011 (green/yellow triangles); the three glasses SPFT tested in 2016 (red circles); the new Enhanced LAW Correlation glasses (pink squares) and the four ORLEC glasses selected for FY17 testing: ORLEC28, ORLEC14, ORLEC33 and ORLEC46. The present report addresses ORLEC14.

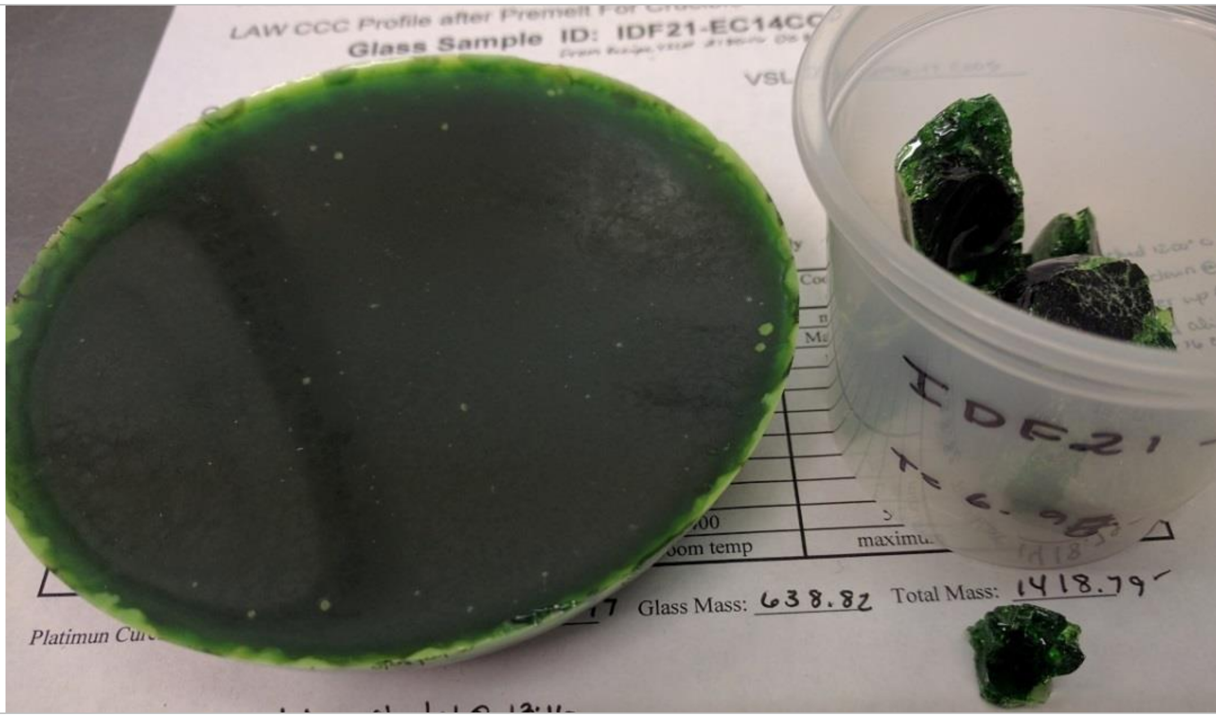

Figure 3.3. Photograph of sample IDF21-EC14CCC after CCC (left) and IDF21-EC14 as-melted (right).

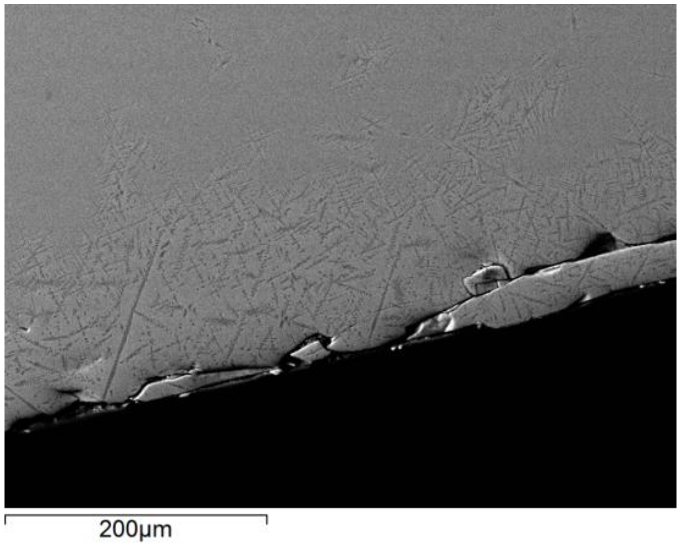

Figure 3.4. SEM micrograph of cross-section of IDF21-EC14CCC glass from the center of the crucible (top) to the crucible wall (bottom; black area at the bottom is epoxy).

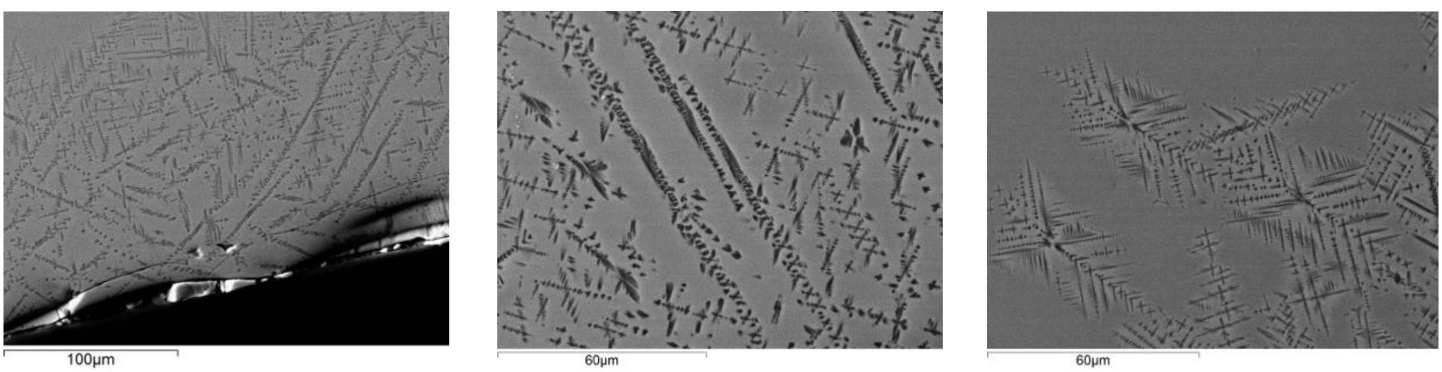

Figure 3.5. SEM micrographs of the crystallized glass layer near the crucible wall in IDF21-EC14CCC showing sodalite crystals (darker grey), probably lazurite.

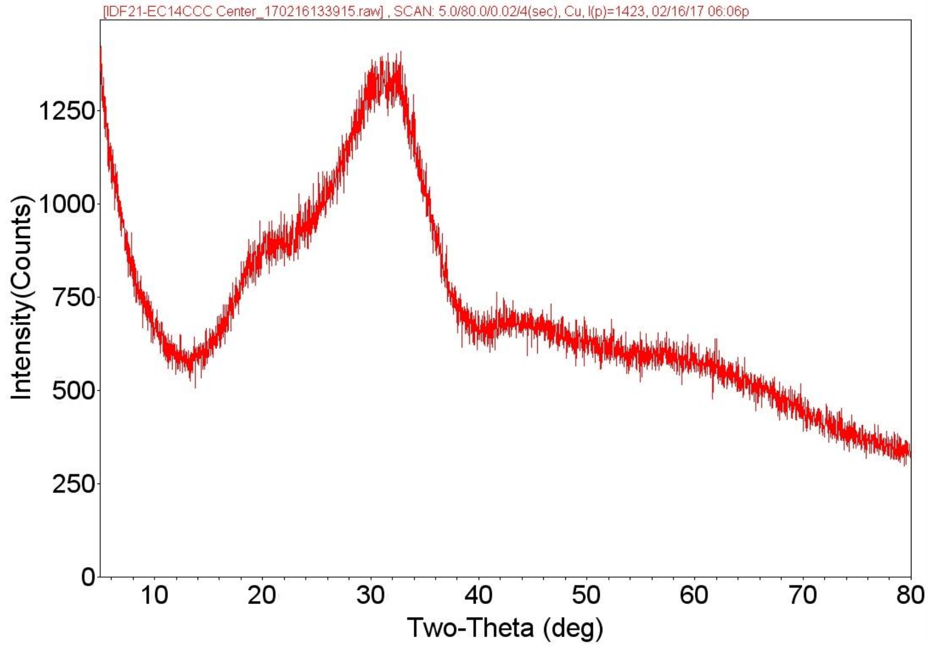

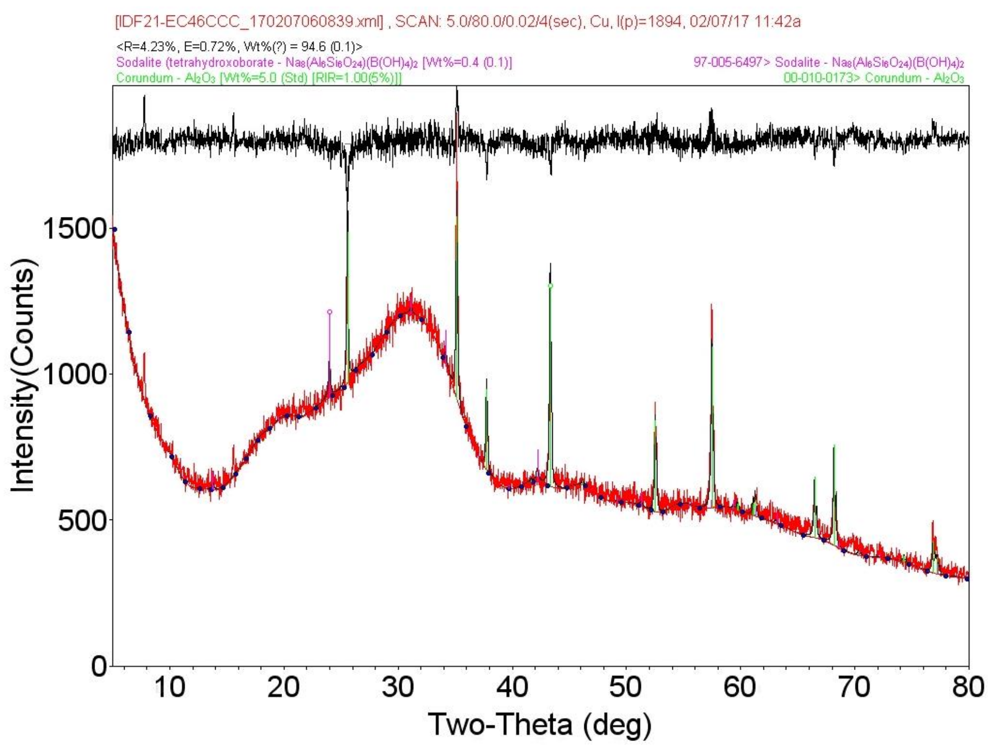

Figure 3.6. XRD powder patterns (raw data and best match) of the IDF21-E14CCC glass from the center of the crucible (top), which shows no crystals, and glass from near the crucible wall (bottom), showing trace amounts of sodalite; lines from the internal standard (corundum) are also evident (shown in green).

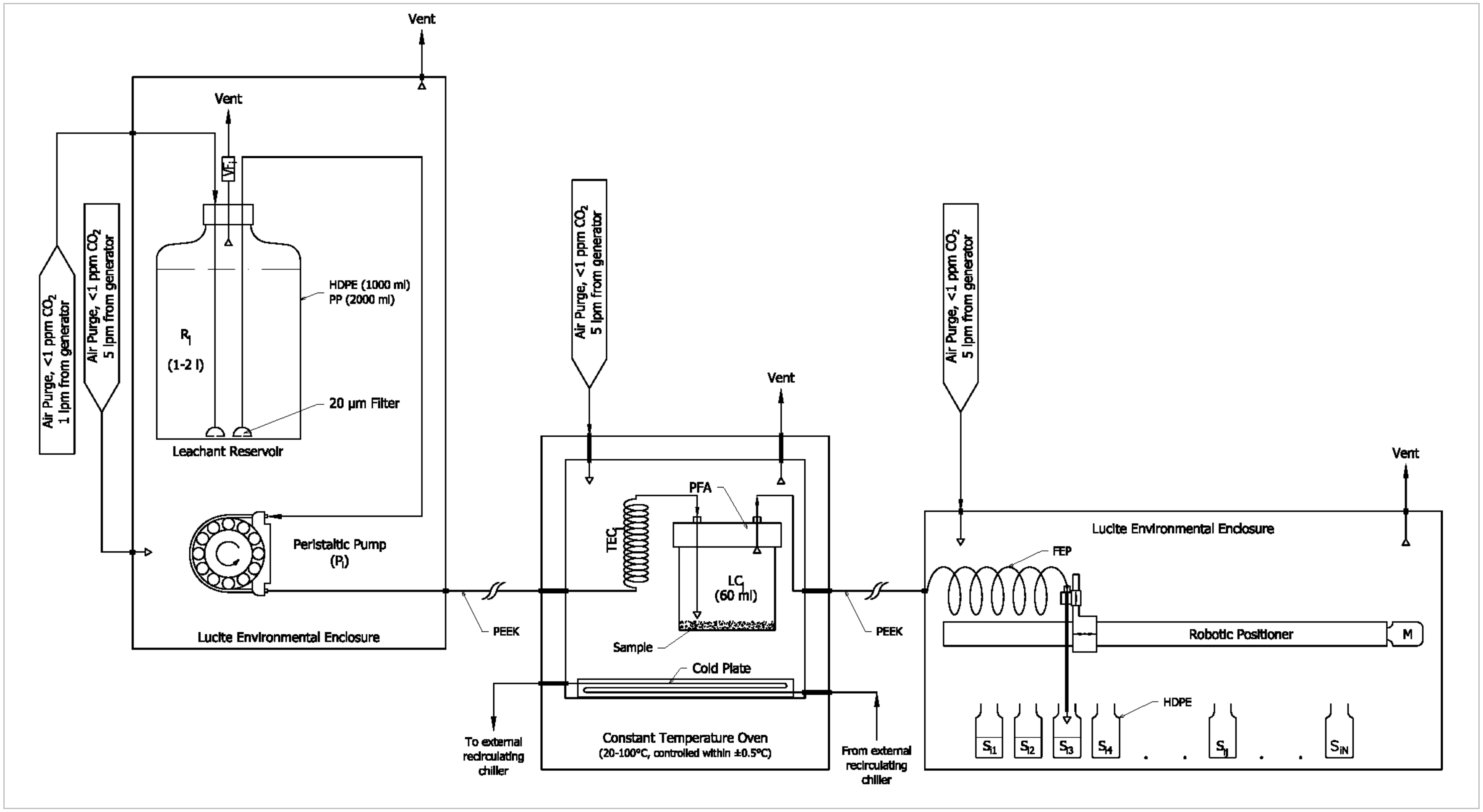

Figure 4.1. Schematic diagram of the SPFT experimental set-up showing a single train.

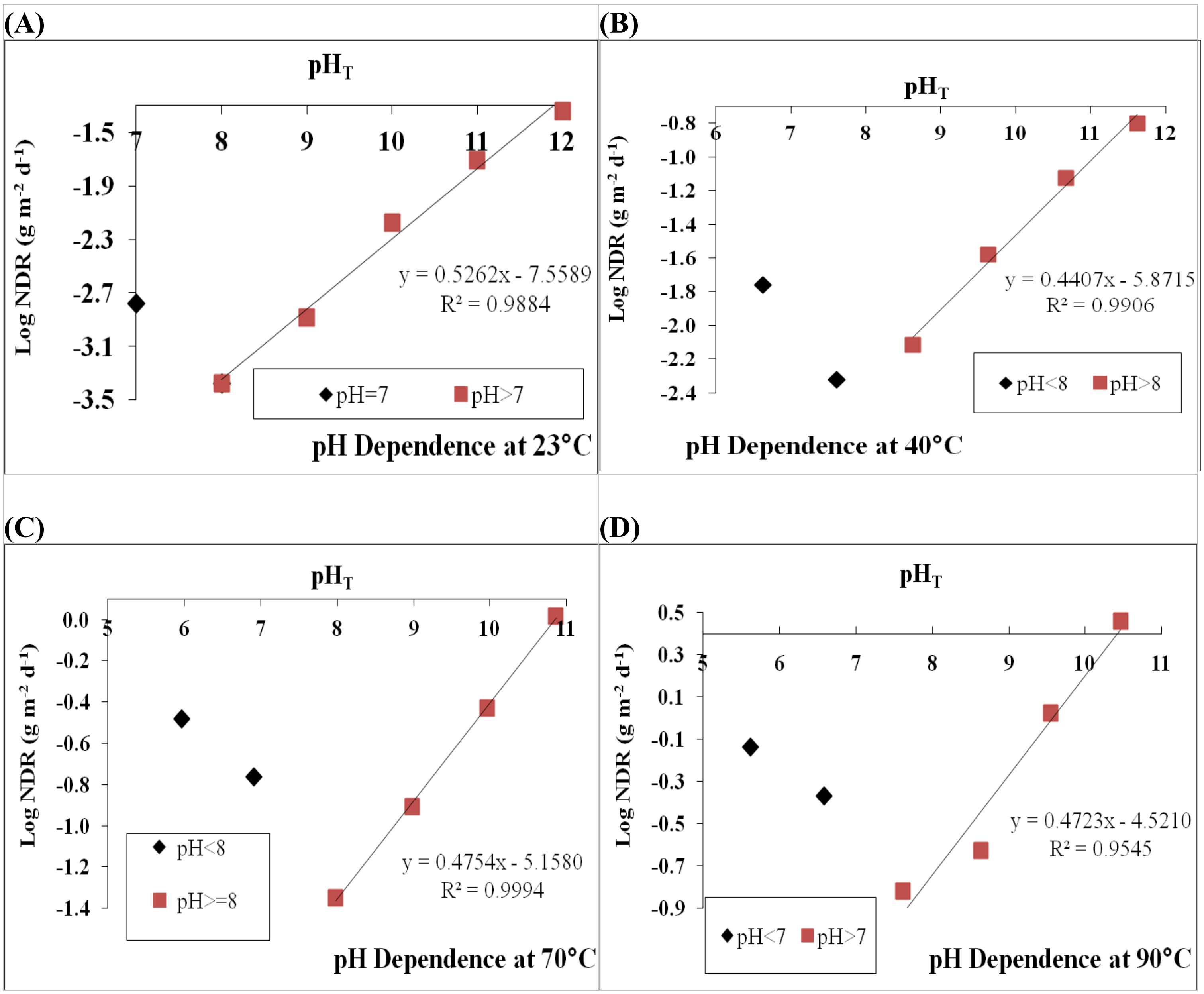

Figure 5.1. Plots of Log NDR vs. pH_T used to generate the average value of the coefficient η.

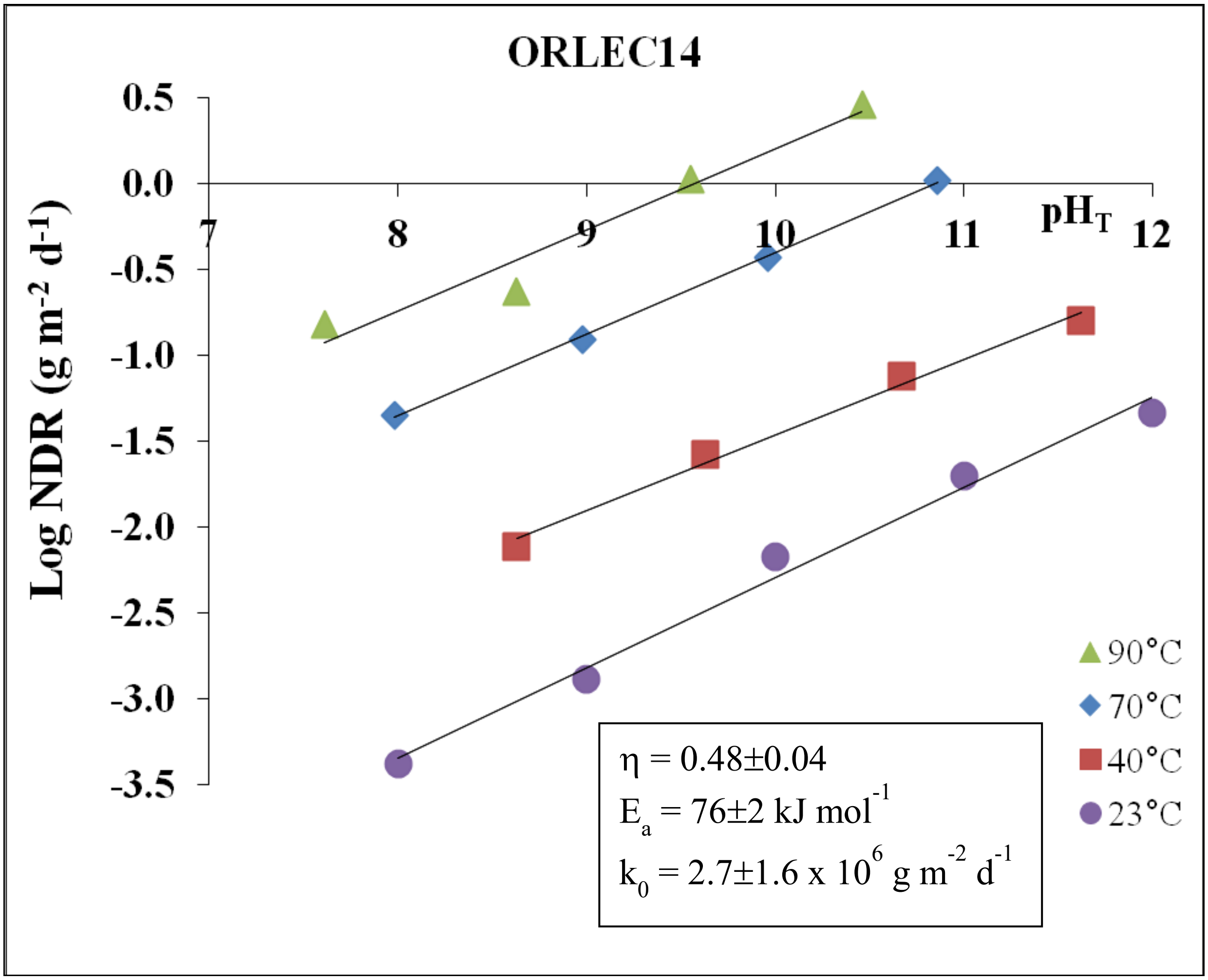

Figure 5.2. Plots of Log NDR vs. pH_T and regression results (solid lines) that determine the parameters k_0 and E_a.

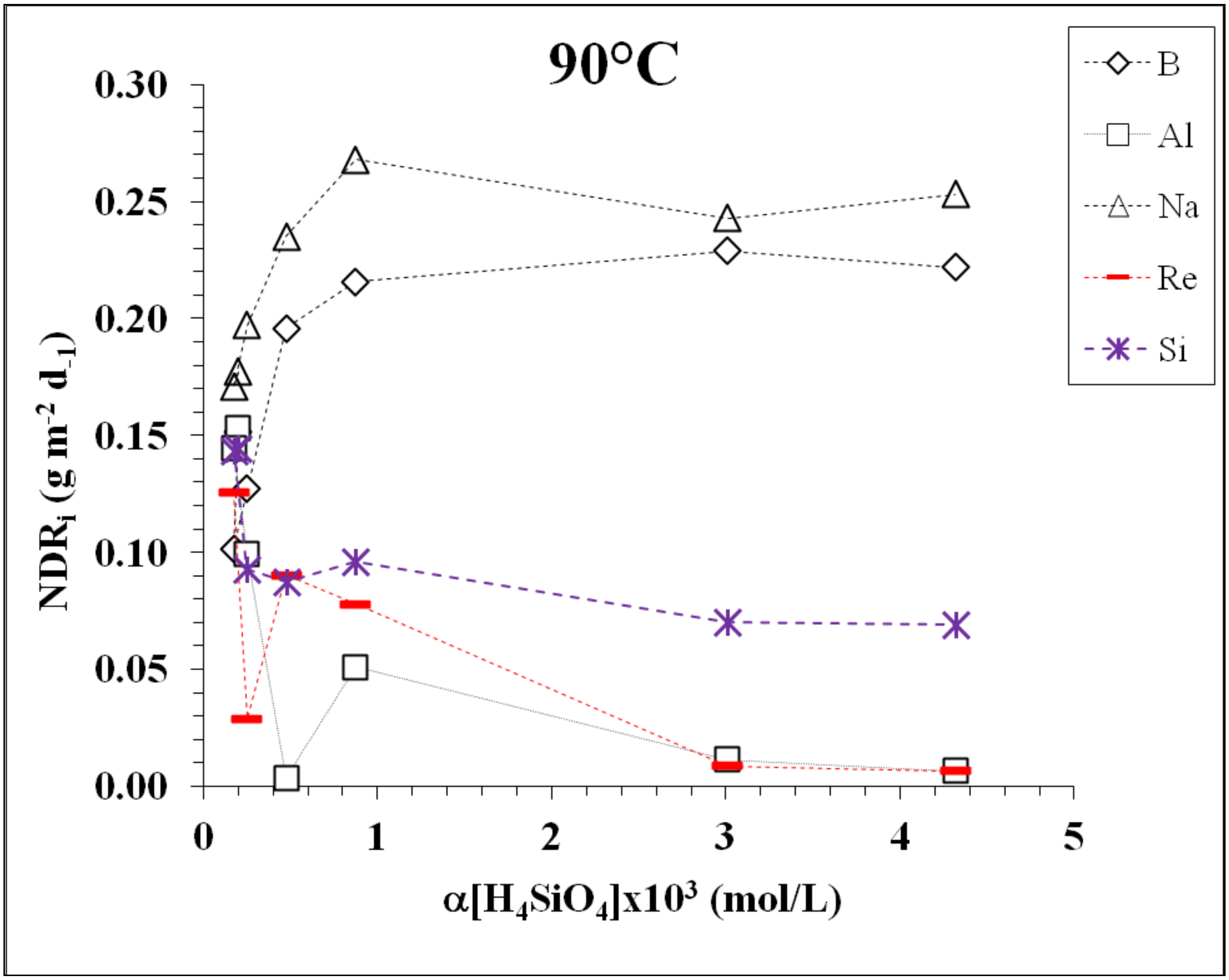

Figure 5.3. NDR$_i$ as a function of α[H_4SiO_4] at 90°C, where *i*=B, Al, Na, Si, and Re.

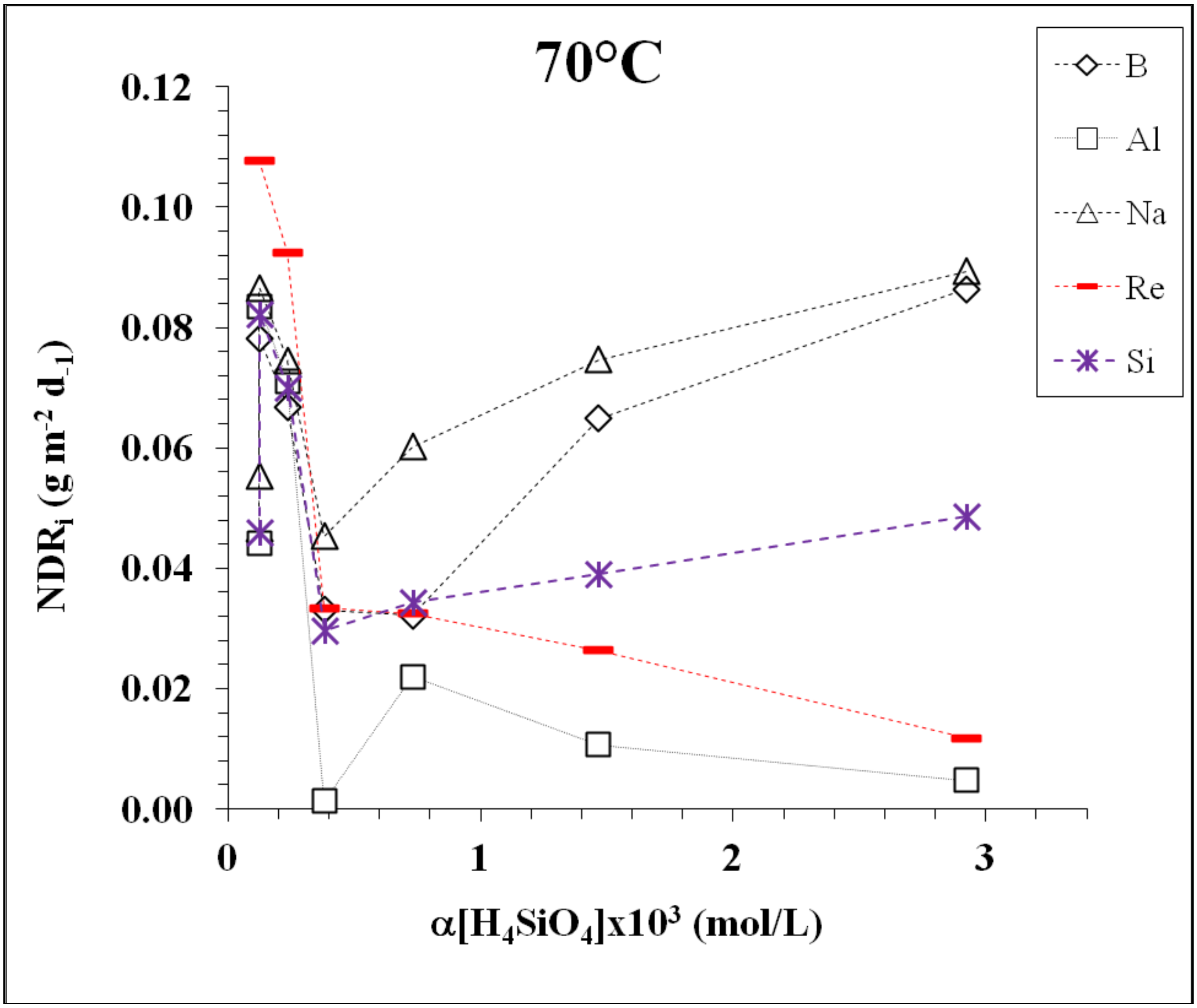

Figure 5.4. NDR$_i$ as a function of α[H_4SiO_4] at 70°C, where *i*=B, Al, Na, Si, and Re.

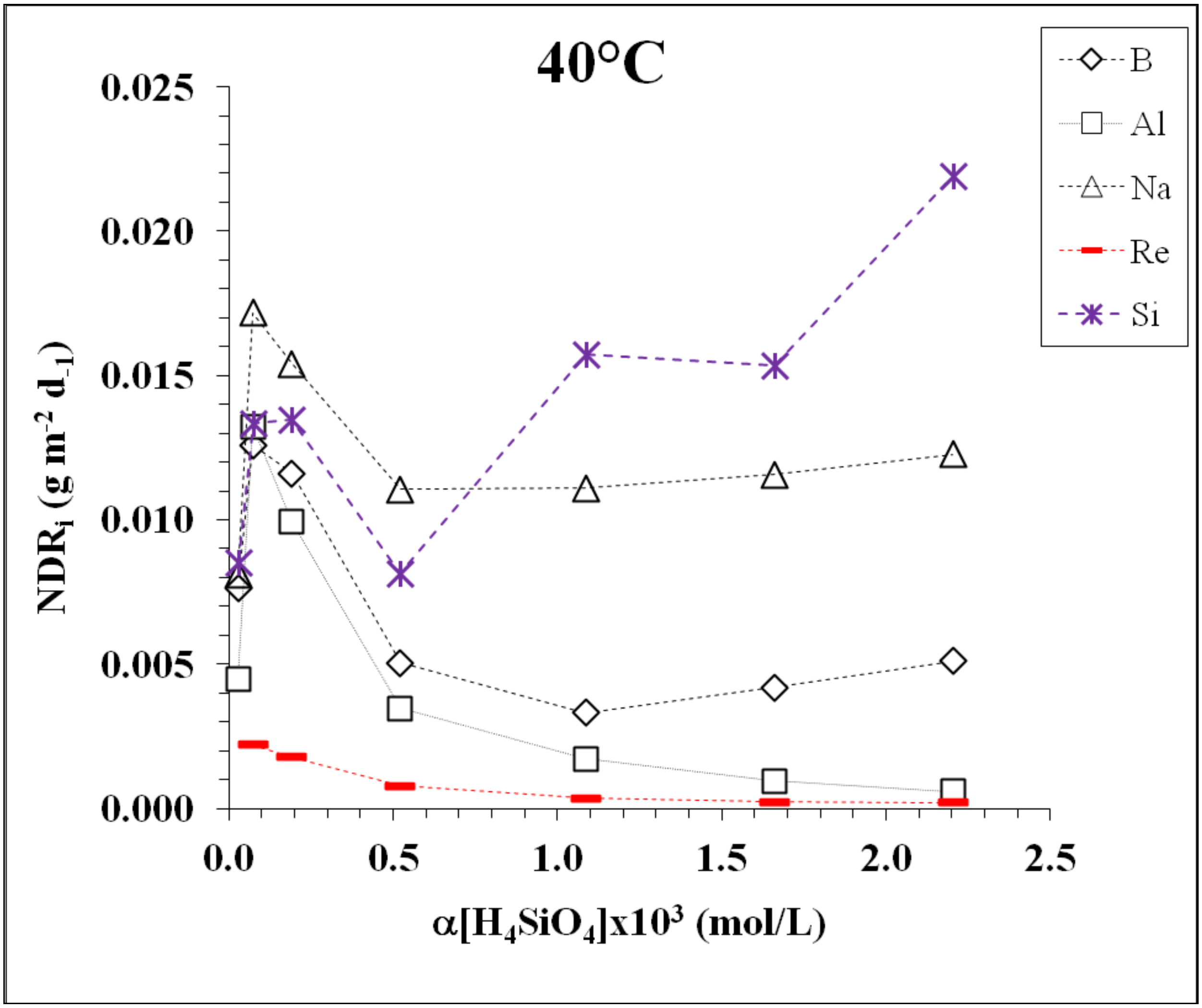

Figure 5.5. NDR$_i$ as a function of α[H_4SiO_4] at 40°C, where *i*=B, Al, Na, Si, and Re.

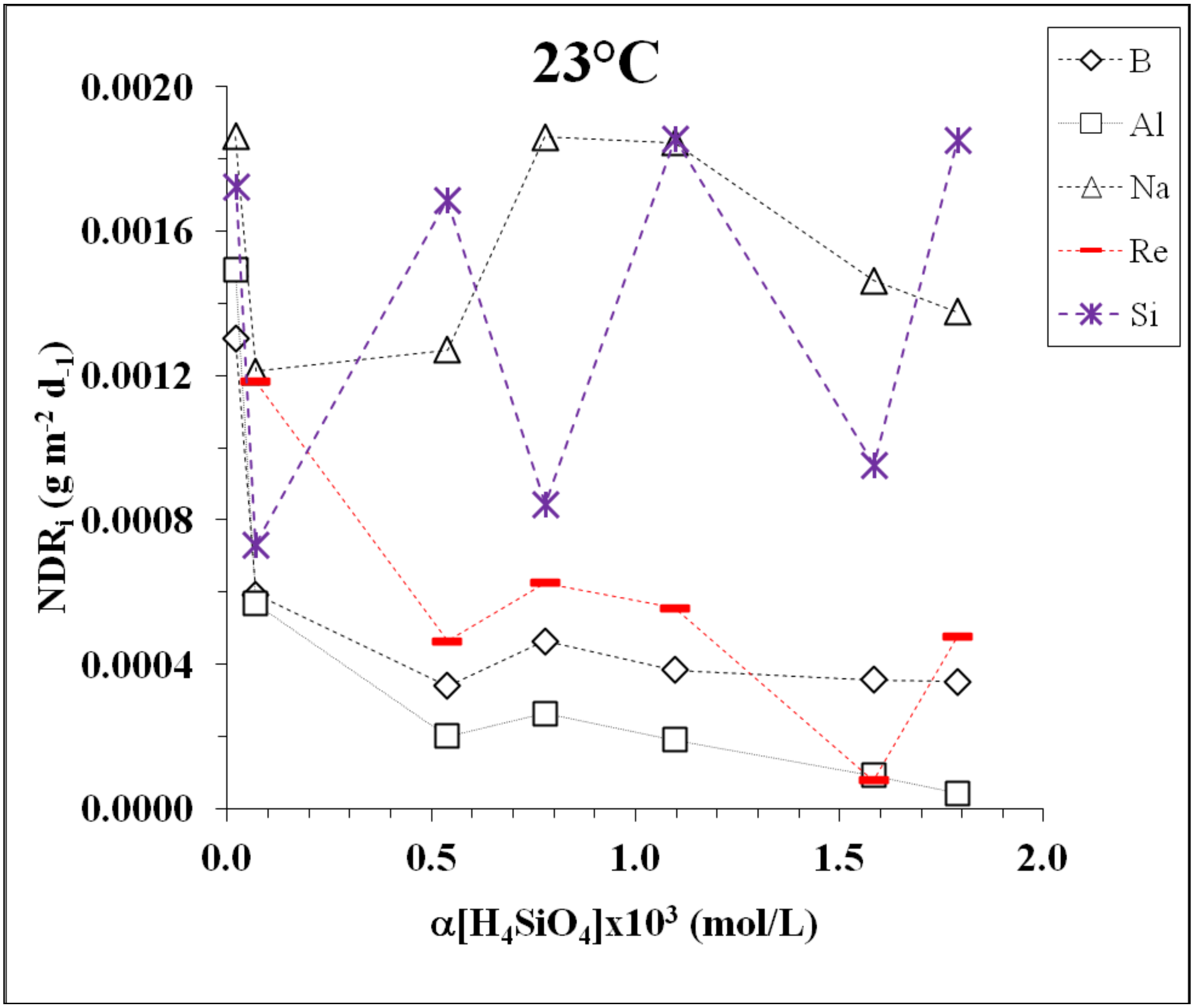

Figure 5.6. NDR$_i$ as a function of α[H_4SiO_4] at 23°C, where *i*=B, Al, Na, Si, and Re.

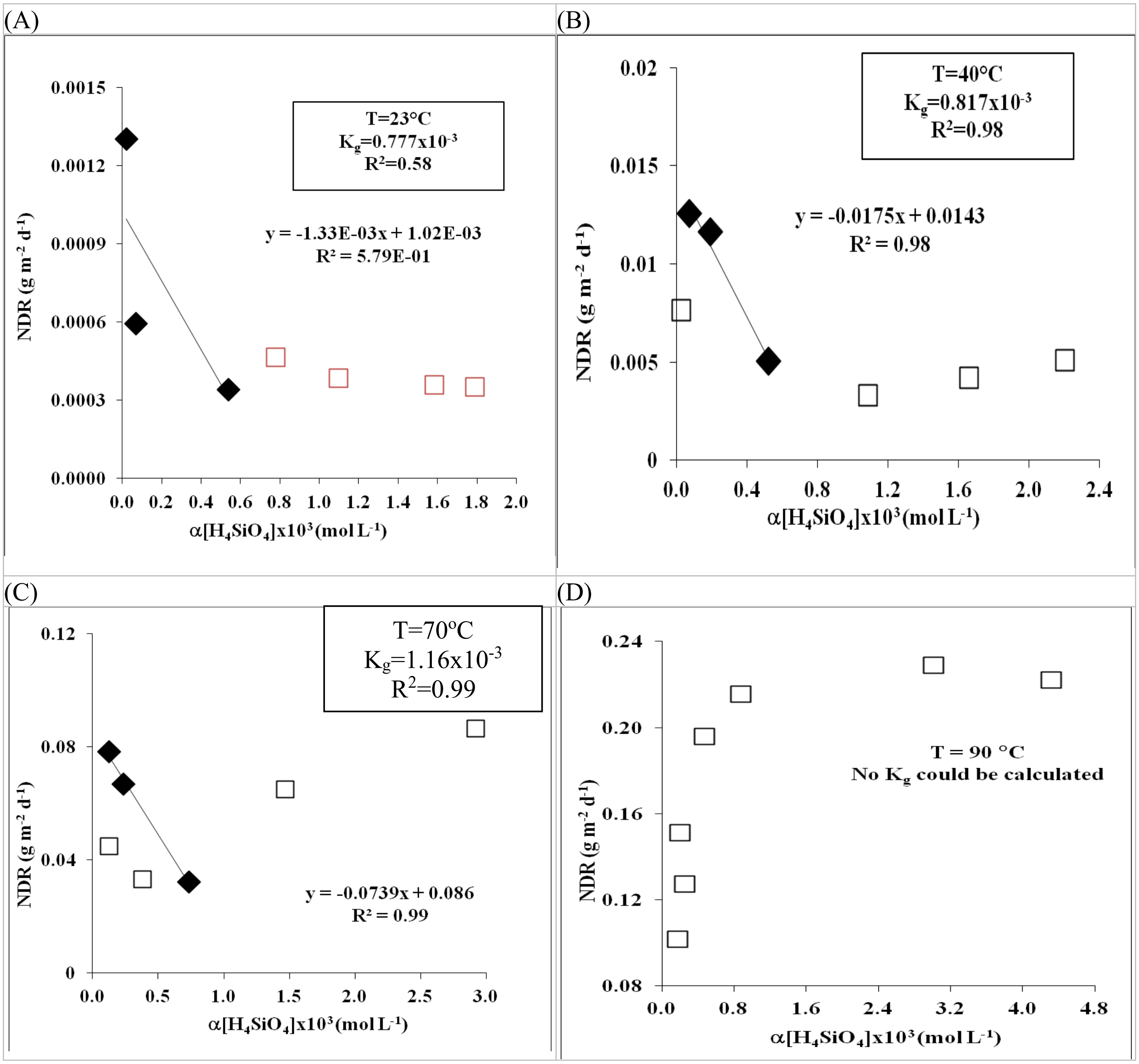

Figure 5.7. Linear regressions used to calculate the K_g value of glass IDF21-EC14 at a specific temperature. Filled diamonds: data points of the linear portion of the plots; Open squares: data points not used in the regression. Uncertainties are listed in Table A6 and are generally smaller than the size of the symbols.

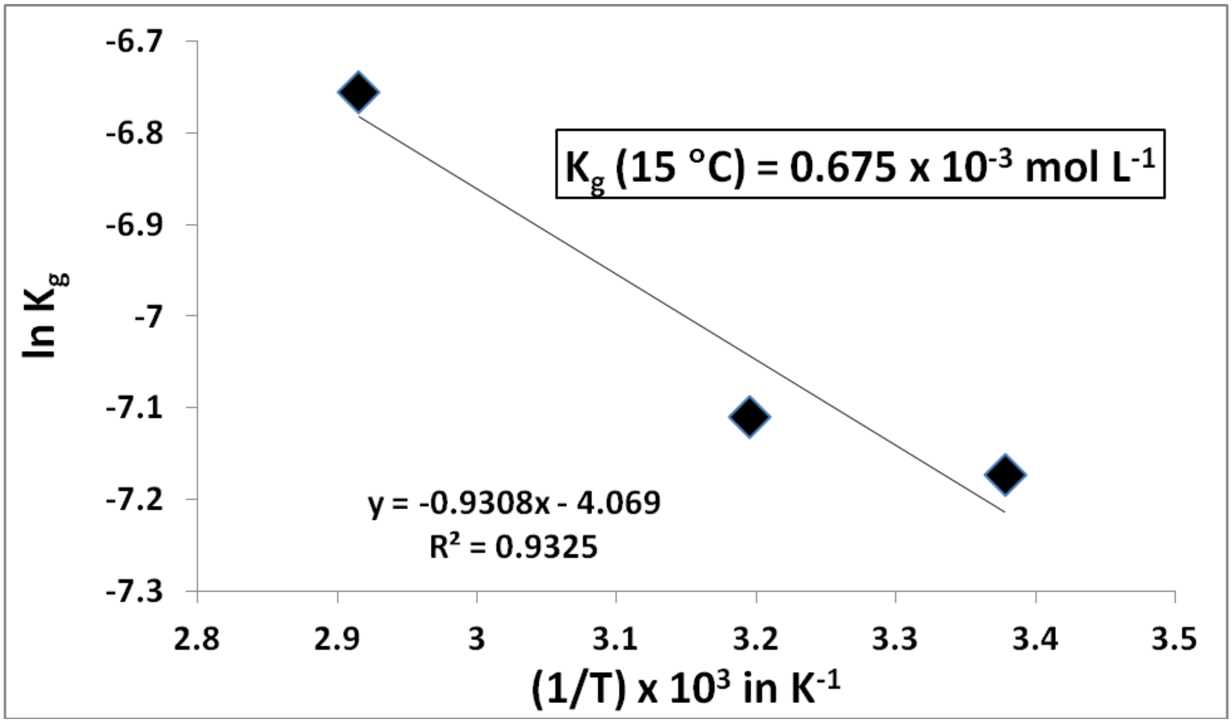

Figure 5.8. Plot of LnK_g vs. 1/T used for estimating the K_g value of IDF21-EC14 at 15°C.

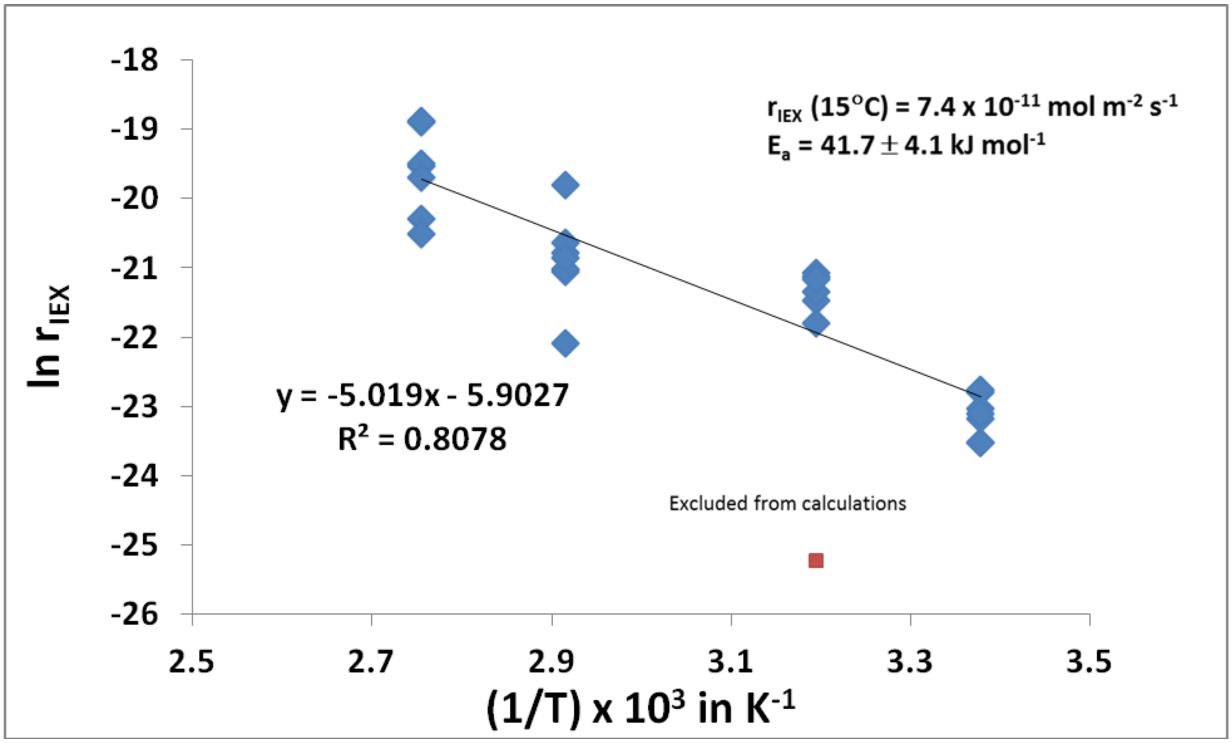

Figure 5.9. Plot of lnr_{IEX} vs. 1/T used for estimating the r_{IEX} value of IDF21-EC14 at 15°C; the r_{IEX} values are "corrected" values, as described in the text.

APPENDIX A

SPFT DATA FOR LAW GLASS IDF21-EC14

Table A1. SPFT Results from Dissolution of Glass IDF21-EC14 at 90°C.

Sample ID	Inf [Si] ppm	T °C	Flow Rate, m^3/d	Time, days	pH 23°C	Glass Mass g	SA m^2	[B] ppm	B Rate $g\ m^{-2}\ d^{-1}$	[Al] ppm	Al Rate $g\ m^{-2}\ d^{-1}$	[Na] ppm	Na Rate $g\ m^{-2}\ d^{-1}$	[Si] ppm	Si Rate $g\ m^{-2}\ d^{-1}$	r_{IEX} $mol\ m^{-2}\ s^{-1}$
Exp. 1																
SP-20-A-BLK1	0	90			7			<DL		<DL		<DL		0.0353		
SP-20-A-BLK2	0	90			7			< DL		<DL		<DL		0.0111		
SP-20-A-BLK3	0	90			7			< DL		0.0187		0.0268		0.0582		
SP-20-A-02	0	90	5.00E-05	1.00	7	0.7485	0.016	17.2954	1.6946	1.5296	0.0885	73.8719	1.2782	24.4939	0.4174	-2.10E-07
SP-20-A-04	0	90	4.93E-05	2.00	7	0.7215	0.016	16.9389	1.6793	1.2437	0.0727	78.5826	1.3758	25.1008	0.4328	-1.53E-07
SP-20-A-06	0	90	4.87E-05	3.00	7	0.6951	0.015	16.8842	1.6933	1.1891	0.0703	67.5314	1.1961	23.3145	0.4067	-2.50E-07
SP-20-A-08	0	90	5.12E-05	4.00	7	0.6706	0.015	14.0017	1.5141	1.0520	0.0670	55.7811	1.0654	19.8381	0.3731	-2.26E-07
SP-20-A-10	0	90	5.08E-05	5.00	7	0.6494	0.015	12.2144	1.3372	0.9355	0.0602	45.4978	0.8798	16.1708	0.3078	-2.30E-07
SP-20-A-12	0	90	5.21E-05	6.00	7	0.6320	0.014	9.0668	1.0366	0.8559	0.0575	43.4974	0.8788	13.5106	0.2686	-7.94E-08
SP-20-A-14	0	90	5.13E-05	7.00	7	0.6179	0.014	8.1765	0.9334	0.7904	0.0530	41.0203	0.8276	11.5685	0.2296	-5.33E-08
SP-20-A-16	0	90	5.15E-05	8.00	7	0.6052	0.014	7.3268	0.8517	0.8526	0.0583	34.0391	0.6993	9.9786	0.2016	-7.67E-08
SP-20-A-18	0	90	5.29E-05	9.00	7	0.5936	0.014	6.7020	**0.8102**	0.7980	0.0567	34.4594	0.7364	8.8955	0.1869	-3.71E-08
SP-20-A-20	0	90	5.09E-05	10.00	7	0.5833	0.014	5.8124	**0.6844**	0.7649	0.0529	31.3582	0.6529	7.8340	0.1603	-1.58E-08
SP-20-A-22	0	90	5.25E-05	11.00	7	0.5739	0.014	5.6197	**0.6898**	0.7561	0.0545	30.3868	0.6596	7.0914	0.1512	-1.52E-08
Exp. 2																
sp-20-B-BLK1	0	90			8			<DL		<DL		<DL		0.09		
sp-20-B-BLK2	0	90			8			<DL		<DL		<DL		<DL		
sp-20-B-BLK3	0	90			8			<DL		<DL		<DL		<DL		
sp-20-B-02	0	90	4.96E-05	1.00	8	0.7442	0.016	10.9121	1.0691	0.5467	0.0313	58.7214	1.0165	2.4929	0.0422	-2.65E-08
sp-20-B-04	0	90	4.92E-05	2.00	8	0.7262	0.016	12.0267	1.1885	0.6700	0.0388	66.2789	1.1571	2.6215	0.0448	-1.58E-08
sp-20-B-06	0	90	5.03E-05	3.00	8	0.7079	0.016	11.1449	1.1454	0.6646	0.0400	61.3791	1.1145	2.4630	0.0437	-1.56E-08
sp-20-B-08	0	90	5.14E-05	4.00	8	0.6917	0.015	8.9130	0.9499	0.6330	0.0395	50.1087	0.9437	2.2833	0.0420	-3.11E-09
sp-20-B-10	0	90	5.23E-05	5.00	8	0.6778	0.015	8.0149	0.8810	0.6114	0.0393	45.3721	0.8815	2.1691	0.0412	2.30E-10
sp-20-B-13	0	90	5.30E-05	6.00	8	0.6665	0.015	5.5452	0.6242	0.5538	0.0364	37.6416	0.7494	2.0571	0.0400	6.30E-08
sp-20-B-14	0	90	5.14E-05	7.00	8	0.6576	0.015	5.1982	0.5722	0.5661	0.0364	35.0686	0.6828	2.0057	0.0381	5.57E-08
sp-20-B-17	0	90	5.10E-05	8.00	8	0.6498	0.015	4.3910	0.4840	0.5474	0.0353	30.7829	0.6004	1.9506	0.0371	5.86E-08
sp-20-B-18	0	90	5.26E-05	9.00	8	0.6427	0.015	4.2142	**0.4821**	0.5486	0.0367	28.8029	0.5831	1.8998	0.0375	5.08E-08
sp-20-B-20	0	90	4.90E-05	10.00	8	0.6362	0.014	3.8356	**0.4115**	0.5446	0.0342	26.4805	0.5029	1.8729	0.0347	4.60E-08
sp-20-B-22	0	90	5.13E-05	11.00	8	0.6304	0.014	3.4956	**0.3946**	0.5258	0.0347	24.0607	0.4809	1.8278	0.0356	4.35E-08
Exp. 3																
sp-20-C-BLK1	0	90						<DL		<DL		<DL		0.0126		
sp-20-C-BLK2	0	90			9			<DL		<DL		<DL		< DL		
sp-20-C-BLK3	0	90			9			<DL		<DL		<DL		< DL		
sp-20-C-02	0	90	5.09E-05	1.00	9	0.4999	0.011	1.3199	0.1964	1.4585	0.1293	13.7902	0.3656	5.0065	0.1243	8.51E-08
sp-20-C-04	0	90	4.71E-05	2.00	9	0.4980	0.011	1.1012	0.1517	1.8343	0.1511	12.1539	0.2989	6.0238	0.1401	7.41E-08
sp-20-C-06	0	90	5.15E-05	3.00	9	0.4965	0.011	0.9855	0.1484	1.8602	0.1678	9.8433	0.2649	5.9490	0.1513	5.86E-08
sp-20-C-08	0	90	4.72E-05	4.00	9	0.4949	0.011	0.9799	0.1356	1.8389	0.1525	8.7708	0.2169	5.9720	0.1397	4.09E-08
sp-20-C-10	0	90	4.68E-05	5.00	9	0.4935	0.011	0.9869	0.1356	1.6969	0.1396	8.1973	0.2012	5.8496	0.1357	3.30E-08
sp-20-C-12	0	90	5.03E-05	6.00	9	0.4920	0.011	1.0186	0.1508	1.6996	0.1505	7.5831	0.2004	5.9435	0.1485	2.50E-08
sp-20-C-14	0	90	5.15E-05	7.00	9	0.4904	0.011	1.0202	0.1550	1.6540	0.1503	7.4380	0.2017	5.8663	0.1504	2.35E-08
sp-20-C-16	0	90	5.12E-05	8.00	9	0.4887	0.011	1.0196	0.1544	1.6416	0.1487	7.2754	0.1967	5.8128	0.1485	2.13E-08

Table A1. SPFT Results from Dissolution of Glass IDF21-EC14 at 90°C (cont.)

Sample ID	Inf [Si] ppm	T °C	Flow Rate, m^3/d	Time, days	pH 23°C	Glass Mass g	SA m^2	[B] ppm	B Rate $g\ m^{-2}\ d^{-1}$	[Al] ppm	Al Rate $g\ m^{-2}\ d^{-1}$	[Na] ppm	Na Rate $g\ m^{-2}\ d^{-1}$	[Si] ppm	Si Rate $g\ m^{-2}\ d^{-1}$	r_{IEX} $mol\ m^{-2}\ s^{-1}$
sp-20-C-18	0	90	5.12E-05	9.00	9	0.4871	0.011	1.0176	**0.1545**	1.7321	0.1574	7.1190	0.1929	5.7924	0.1483	1.93E-08
sp-20-C-20	0	90	4.95E-05	10.00	9	0.4854	0.011	1.0171	**0.1497**	1.7012	0.1498	6.5504	0.1720	5.7702	0.1432	1.13E-08
sp-20-C-22	0	90	4.97E-05	11.00	9	0.4839	0.011	1.0110	**0.1496**	1.7236	0.1527	6.3113	0.1667	5.6834	0.1418	8.59E-09
Exp. 4																
sp-20-D-BLK1	0	90						<DL		<DL		<DL		0.0249		
sp-20-D-BLK2	0	90						<DL		<DL		<DL		0.0187		
sp-20-D-BLK3	0	90			10			<DL		<DL		<DL		<DL		
sp-20-D-02	0	90	4.86E-05	1.00	10	0.5003	0.011	1.4925	0.2120	2.6281	0.2229	11.7061	0.2959	7.6599	0.1874	4.22E-08
sp-20-D-05	0	90	4.80E-05	2.00	10	0.4978	0.011	1.7123	0.2415	2.8711	0.2416	11.2975	0.2831	8.9067	0.2167	2.09E-08
sp-20-D-06	0	90	4.70E-05	3.00	10	0.4953	0.011	1.6472	0.2280	2.7827	0.2298	11.0141	0.2710	8.5270	0.2035	2.16E-08
sp-20-D-09	0	90	5.05E-05	4.00	10	0.4928	0.011	1.6309	0.2437	2.6945	0.2402	9.7933	0.2600	8.5728	0.2209	8.23E-09
sp-20-D-10	0	90	4.80E-05	5.00	10	0.4903	0.011	1.5917	0.2267	2.6830	0.2281	9.6139	0.2434	8.3669	0.2055	8.39E-09
sp-20-D-12	0	90	4.95E-05	6.00	10	0.4878	0.011	1.6184	0.2383	2.6424	0.2321	9.4950	0.2484	8.5668	0.2175	5.11E-09
sp-20-D-14	0	90	4.77E-05	7.00	10	0.4853	0.011	1.5971	0.2277	2.6329	0.2240	9.0122	0.2283	8.4507	0.2077	3.18E-10
sp-20-D-16	0	90	4.70E-05	8.00	10	0.4830	0.011	1.5876	0.2233	2.6062	0.2187	9.0079	0.2252	8.4684	0.2054	9.38E-10
sp-20-D-18	0	90	5.06E-05	9.00	10	0.4806	0.010	1.5538	**0.2363**	2.6159	0.2374	9.0828	0.2455	8.4267	0.2210	4.65E-09
sp-20-D-20	0	90	4.79E-05	10.00	10	0.4781	0.010	1.5855	**0.2292**	2.6793	0.2311	9.0266	0.2319	8.4404	0.2104	1.36E-09
sp-20-D-22	0	90	5.09E-05	11.00	10	0.4757	0.010	1.5707	**0.2417**	2.6395	0.2424	9.0221	0.2467	8.4115	0.2232	2.54E-09
Exp. 5																
sp-20-E-BLK1	0	90			11			<DL		0.00		< 0.0241		0.01		
sp-20-E-BLK2	0	90			11			<DL		0.27		< 0.0344		0.18		
sp-20-E-BLK3	0	90			11			<DL		0.26		<DL		0.20		
sp-20-E-02	0	90	4.72E-05	1.00	11	0.4981	0.011	3.0830	0.4296	5.4006	0.4338	34.6779	0.8562	15.7529	0.3805	2.15E-07
sp-20-E-05	0	90	5.08E-05	2.00	11	0.4920	0.011	3.8105	0.5758	6.2376	0.5454	38.8623	1.0397	18.4314	0.4830	2.33E-07
sp-20-E-06	0	90	5.00E-05	3.00	11	0.4863	0.011	4.2477	0.6377	6.8653	0.5978	42.2234	1.1219	20.6179	0.5370	2.44E-07
sp-20-E-09	0	90	5.04E-05	4.00	11	0.4793	0.010	4.5725	0.6985	7.5217	0.6677	44.9967	1.2162	21.9833	0.5826	2.61E-07
sp-20-E-10	0	90	4.98E-05	5.00	11	0.4719	0.010	4.7430	0.7229	7.4657	0.6611	44.5929	1.2025	22.0838	0.5839	2.41E-07
sp-20-E-12	0	90	5.07E-05	6.00	11	0.4639	0.010	5.2401	0.8233	8.0709	0.7379	44.1774	1.2277	22.6902	0.6184	2.03E-07
sp-20-E-14	0	90	5.22E-05	7.00	11	0.4552	0.010	5.4459	0.8929	8.3915	0.8013	47.0878	1.3655	24.0133	0.6831	2.38E-07
sp-20-E-16	0	90	5.21E-05	8.00	11	0.4459	0.010	5.7187	0.9473	8.7236	0.8422	47.7462	1.3987	25.0308	0.7195	2.27E-07
sp-20-E-18	0	90	5.25E-05	9.00	11	0.4362	0.010	5.9845	**1.0146**	8.8243	0.8720	49.1144	1.4724	25.6722	0.7552	2.30E-07
sp-20-E-20	0	90	5.14E-05	10.00	11	0.4260	0.010	6.3771	**1.0761**	9.0756	0.8930	51.8439	1.5468	26.6703	0.7810	2.37E-07
sp-20-E-22	0	90	4.97E-05	11.00	11	0.4157	0.010	6.5465	**1.0846**	9.2225	0.8912	50.4433	1.4775	26.6316	0.7656	1.98E-07
Exp. 6																
sp-20-F-BLK1	0	90			12			<DL		<DL		0.77		0.03		
sp-20-F-BLK2	0	90			12			<DL		0.18		0.73		0.18		
sp-20-F-BLK3	0	90			12			<DL		0.19		0.72		0.21		
sp-20-F-02	0	90	5.02E-05	1.00	12	0.4949	0.011	9.2977	1.3850	17.3454	1.5251	83.6067	2.1822	45.6028	1.1800	4.01E-07
sp-20-F-04	0	90	4.76E-05	2.00	12	0.4769	0.010	13.9654	2.0238	22.3008	1.9096	113.1430	2.8780	60.4457	1.5220	4.30E-07
sp-20-F-06	0	90	4.57E-05	3.00	12	0.4553	0.010	15.2509	2.1866	23.3053	1.9747	122.3560	3.0805	63.6503	1.5857	4.50E-07
sp-20-F-08	0	90	4.95E-05	4.00	12	0.4312	0.010	16.4467	2.6521	23.1488	2.2058	122.9260	3.4807	63.8594	1.7892	4.17E-07
sp-20-F-10	0	90	4.95E-05	5.00	12	0.4056	0.009	16.1487	2.7125	22.9871	2.2816	126.9020	3.7437	66.9264	1.9534	5.19E-07

Table A1. SPFT Results from Dissolution of Glass IDF21-EC14 at 90°C (cont.)

Sample ID	Inf [Si] ppm	T °C	Flow Rate, m^3/d	Time, days	pH 23°C	Glass Mass g	SA m^2	[B] ppm	B Rate $g\ m^{-2}\ d^{-1}$	[Al] ppm	Al Rate $g\ m^{-2}\ d^{-1}$	[Na] ppm	Na Rate $g\ m^{-2}\ d^{-1}$	[Si] ppm	Si Rate $g\ m^{-2}\ d^{-1}$	r_{IEX} $mol\ m^{-2}\ s^{-1}$
sp-20-F-12	0	90	4.85E-05	6.00	12	0.3799	0.009	16.7470	2.8782	23.3877	2.3753	121.9450	3.6798	66.3911	1.9826	4.03E-07
sp-20-F-15	0	90	4.90E-05	7.00	12	0.3550	0.009	15.4059	2.7990	21.3132	2.2872	118.2630	3.7722	61.4427	1.9395	4.90E-07
sp-20-F-16	0	90	5.14E-05	8.00	12	0.3304	0.008	15.4860	3.0956	21.6520	2.5568	112.7020	3.9540	61.9391	2.1512	4.32E-07
sp-20-F-19	0	90	4.94E-05	9.00	12	0.3065	0.008	14.1988	**2.8684**	19.9634	2.3814	113.7910	4.0351	56.7853	1.9929	5.87E-07
sp-20-F-20	0	90	4.97E-05	10.00	12	0.2849	0.007	13.3115	**2.8378**	18.6616	2.3483	107.1430	4.0081	53.6700	1.9875	5.89E-07
sp-20-F-22	0	90	5.18E-05	11.00	12	0.2639	0.007	12.6921	**2.9702**	17.9644	2.4809	104.1010	4.2741	51.8609	2.1081	6.56E-07
Exp. 7																
sp-20-G-BLK1	1	90			9			<DL		<DL		<DL		1.00		
sp-20-G-BLK2	1	90			9			<DL		<DL		<DL		1.01		
sp-20-G-BLK3	1	90			9			<DL		<DL		<DL		0.95		
sp-20-G-02	1	90	6.75E-05	1.00	9	0.5000	0.011	2.0501	0.4056	1.2446	0.1460	14.9582	0.5253	4.9284	0.1367	6.02E-08
sp-20-G-04	1	90	6.62E-05	2.00	9	0.4957	0.011	1.6073	0.3131	1.3639	0.1580	12.4528	0.4313	5.1495	0.1424	5.95E-08
sp-20-G-06	1	90	6.54E-05	3.00	9	0.4934	0.011	1.0640	0.2044	1.2865	0.1475	9.5862	0.3287	5.0109	0.1364	6.26E-08
sp-20-G-08	1	90	6.78E-05	4.00	9	0.4915	0.011	0.7059	0.1401	1.2974	0.1547	7.7515	0.2763	5.0198	0.1421	6.86E-08
sp-20-G-10	1	90	6.85E-05	5.00	9	0.4903	0.011	0.4989	0.0993	1.2328	0.1486	6.2549	0.2254	4.9993	0.1430	6.35E-08
sp-20-G-12	1	90	6.83E-05	6.00	9	0.4893	0.011	0.4353	0.0862	1.2182	0.1467	5.6157	0.2021	5.1166	0.1471	5.84E-08
sp-20-G-15	1	90	6.72E-05	7.00	9	0.4884	0.011	0.4492	0.0877	1.2515	0.1486	5.1977	0.1843	5.1291	0.1454	4.86E-08
sp-20-G-16	1	90	6.80E-05	8.00	9	0.4874	0.011	0.4629	0.0916	1.2370	0.1488	4.9778	0.1788	5.1449	0.1478	4.38E-08
sp-20-G-18	1	90	6.86E-05	9.00	9	0.4864	0.011	0.4861	**0.0973**	1.2448	0.1512	4.7997	0.1740	5.0966	0.1475	3.86E-08
sp-20-G-20	1	90	6.56E-05	10.00	9	0.4854	0.011	0.5178	**0.0995**	1.2444	0.1448	4.5481	0.1580	5.1532	0.1433	2.94E-08
sp-20-G-22	1	90	6.71E-05	11.00	9	0.4843	0.011	0.5462	**0.1077**	1.1548	0.1375	5.0694	0.1804	4.9290	0.1389	3.66E-08
Exp. 8																
sp-20-H-BLK1	5	90			9			<DL		<DL		<DL		4.73		
sp-20-H-BLK2	5	90			9			<DL		<DL		<DL		4.73		
sp-20-H-BLK3	5	90			9			<DL		<DL		<DL		4.72		
sp-20-H-02	5	90	6.92E-05	1.00	9	0.4994	0.011	2.4460	0.4975	1.0082	0.1212	16.8451	0.6076	7.6418	0.1038	5.54E-08
sp-20-H-04	5	90	7.09E-05	2.00	9	0.4942	0.011	2.3038	0.4828	1.0975	0.1361	15.5325	0.5774	7.7837	0.1122	4.76E-08
sp-20-H-06	5	90	7.06E-05	3.00	9	0.4895	0.011	1.8942	0.3973	1.0105	0.1255	12.6949	0.4728	7.6842	0.1087	3.80E-08
sp-20-H-08	5	90	6.89E-05	4.00	9	0.4857	0.011	1.5624	0.3212	1.0277	0.1253	10.1928	0.3725	7.5652	0.1025	2.58E-08
sp-20-H-10	5	90	7.04E-05	5.00	9	0.4825	0.011	1.3196	0.2779	0.8643	0.1079	9.0527	0.3394	7.5285	0.1038	3.10E-08
sp-20-H-12	5	90	7.18E-05	6.00	9	0.4798	0.010	1.1135	0.2396	0.8917	0.1141	8.0119	0.3075	7.4783	0.1044	3.42E-08
sp-20-H-14	5	90	6.81E-05	7.00	9	0.4775	0.010	0.9370	0.1913	0.8734	0.1062	7.0070	0.2556	7.3579	0.0949	3.24E-08
sp-20-H-16	5	90	6.73E-05	8.00	9	0.4757	0.010	0.7948	0.1604	0.8530	0.1028	6.0893	0.2201	7.3098	0.0923	3.01E-08
sp-20-H-18	5	90	6.78E-05	9.00	9	0.4741	0.010	0.7024	**0.1426**	0.8388	0.1020	5.7205	0.2086	7.3413	0.0943	3.32E-08
sp-20-H-20	5	90	6.86E-05	10.00	9	0.4727	0.010	0.6015	**0.1234**	0.8106	0.0998	5.1095	0.1888	7.2737	0.0931	3.29E-08
sp-20-H-22	5	90	7.13E-05	11.00	9	0.4715	0.010	0.5412	**0.1153**	0.7440	0.0953	5.0384	0.1938	7.1030	0.0905	3.95E-08
Exp. 9																
sp-20-I-BLK1	10	90			9			<DL		<DL		< -0.1146		9.19		
sp-20-I-BLK2	10	90			9			<DL		<DL		< 0.1161		9.31		
sp-20-I-BLK3	10	90			9			<DL		<DL		< -0.1173		9.21		
sp-20-I-02	10	90	6.83E-05	1.00	9	0.9976	0.022	4.4942	0.4525	0.0787	0.0041	29.2215	0.5182	14.9124	0.0998	3.31E-08
sp-20-I-04	10	90	7.10E-05	2.00	9	0.9879	0.021	4.3406	0.4573	0.0938	0.0053	27.0022	0.5008	14.9812	0.1057	2.19E-08

Table A1. SPFT Results from Dissolution of Glass IDF21-EC14 at 90°C (cont.)

Sample ID	Inf [Si] ppm	T °C	Flow Rate, m^3/d	Time, days	pH 23°C	Glass Mass g	SA m^2	[B] ppm	B Rate $g\ m^{-2}\ d^{-1}$	[Al] ppm	Al Rate $g\ m^{-2}\ d^{-1}$	[Na] ppm	Na Rate $g\ m^{-2}\ d^{-1}$	[Si] ppm	Si Rate $g\ m^{-2}\ d^{-1}$	r_{IEX} $mol\ m^{-2}\ s^{-1}$
sp-20-I-06	10	90	7.19E-05	3.00	9	0.9788	0.021	3.7107	0.3982	0.0867	0.0049	21.7598	0.4108	14.2692	0.0944	6.34E-09
sp-20-I-08	10	90	7.10E-05	4.00	9	0.9708	0.021	3.2839	0.3497	0.0859	0.0048	20.0743	0.3761	14.5969	0.0998	1.33E-08
sp-20-I-10	10	90	6.97E-05	5.00	9	0.9640	0.021	2.8375	0.2977	0.0747	0.0040	18.1324	0.3345	13.9573	0.0866	1.86E-08
sp-20-I-12	10	90	7.13E-05	6.00	9	0.9580	0.021	2.5606	0.2758	0.0766	0.0043	15.8271	0.2996	14.5263	0.0997	1.20E-08
sp-20-I-14	10	90	7.16E-05	7.00	9	0.9525	0.021	2.3161	0.2515	0.0712	0.0040	14.4747	0.2761	13.847	0.0877	1.24E-08
sp-20-I-16	10	90	7.09E-05	8.00	9	0.9475	0.021	2.1356	0.2304	0.0667	0.0036	14.3144	0.2714	13.9633	0.0893	2.06E-08
sp-20-I-18	10	90	7.06E-05	9.00	9	0.9430	0.021	1.9186	**0.2065**	0.0659	0.0036	12.7102	0.2403	14.084	0.0915	1.70E-08
sp-20-I-20	10	90	7.20E-05	10.00	9	0.9388	0.021	1.7743	**0.1951**	0.0657	0.0037	11.9574	0.2309	13.7758	0.0876	1.80E-08
sp-20-I-22	10	90	7.27E-05	11.00	9	0.9349	0.021	1.6696	**0.1860**	0.0611	0.0034	11.9386	0.2337	13.4847	0.0831	2.40E-08
Exp. 10																
sp-20-J-BLK1	20	90			9			<DL		0.01		0.06		20.15		
sp-20-J-BLK2	20	90			9			<DL		0.01		0.17		20.40		
sp-20-J-BLK3	20	90			9			<DL		0.01		0.05		20.46		
sp-20-J-02	20	90	7.35E-05	1.00	9	0.9942	0.021	4.5671	0.4970	0.8528	0.0546	28.1408	0.5403	28.2636	0.1505	2.18E-08
sp-20-J-04	20	90	7.43E-05	2.00	9	0.9835	0.021	4.4325	0.4909	1.1906	0.0778	25.8342	0.5048	28.2636	0.1532	6.97E-09
sp-20-J-06	20	90	7.64E-05	3.00	9	0.9737	0.021	3.9007	0.4467	1.0486	0.0708	23.2307	0.4694	25.7723	0.1087	1.14E-08
sp-20-J-08	20	90	7.41E-05	4.00	9	0.9650	0.021	3.3617	0.3755	1.0193	0.0672	19.8764	0.3917	25.3970	0.0987	8.13E-09
sp-20-J-10	20	90	7.19E-05	5.00	9	0.9577	0.021	2.9725	0.3235	0.8976	0.0576	18.6490	0.3581	25.1500	0.0915	1.74E-08
sp-20-J-12	20	90	6.98E-05	6.00	9	0.9513	0.021	2.6734	0.2838	0.9363	0.0586	15.8039	0.2959	24.6867	0.0807	6.09E-09
sp-20-J-14	20	90	7.25E-05	7.00	9	0.9456	0.021	2.4204	0.2676	0.9119	0.0595	14.6878	0.2865	25.0212	0.0906	9.49E-09
sp-20-J-16	20	90	7.42E-05	8.00	9	0.9403	0.021	2.1947	0.2493	0.8545	0.0573	14.1521	0.2837	24.6658	0.0861	1.73E-08
sp-20-J-18	20	90	6.97E-05	9.00	9	0.9354	0.021	2.1009	**0.2247**	0.7044	0.0444	14.0543	0.2654	25.5978	0.0985	2.04E-08
sp-20-J-20	20	90	7.15E-05	10.00	9	0.9308	0.021	1.9642	**0.2161**	0.4741	0.0305	13.1335	0.2551	25.5193	0.0999	1.96E-08
sp-20-J-22	20	90	7.44E-05	11.00	9	0.9265	0.020	1.7951	**0.2061**	0.7521	0.0509	13.9768	0.2835	24.7933	0.0897	3.90E-08
Exp. 11																
sp-20-K-BLK1	80	90			9			<DL		0.06		0.15		79.47		
sp-20-K-BLK2	80	90			9			<DL		0.06		0.27		80.44		
sp-20-K-BLK3	80	90			9			<DL		0.06		0.16		80.07		
sp-20-K-02	80	90	7.37E-05	1.00	9	1.9888	0.043	9.9037	0.5405	0.3178	0.0083	52.5580	0.5051	90.1010	0.0961	-1.78E-08
sp-20-K-04	80	90	7.17E-05	2.00	9	1.9664	0.043	9.5234	0.5091	0.4155	0.0113	47.3366	0.4455	85.9612	0.0556	-3.20E-08
sp-20-K-06	80	90	7.43E-05	3.00	9	1.9458	0.042	8.2295	0.4594	0.3938	0.0111	42.0992	0.4136	84.4182	0.0430	-2.30E-08
sp-20-K-08	80	90	7.49E-05	4.00	9	1.9272	0.042	7.4721	0.4232	0.4207	0.0121	37.5676	0.3743	87.3788	0.0729	-2.46E-08
sp-20-K-10	80	90	7.34E-05	5.00	9	1.9107	0.042	6.5550	0.3654	0.3833	0.0107	35.4457	0.3476	85.6653	0.0551	-8.96E-09
sp-20-K-12	80	90	7.57E-05	6.00	9	1.8967	0.042	5.2996	0.3064	0.3759	0.0108	30.0148	0.3051	82.0160	0.0204	-6.39E-10
sp-20-K-14	80	90	7.55E-05	7.00	9	1.8845	0.041	4.8398	0.2801	0.3872	0.0112	27.7462	0.2823	85.9382	0.0600	1.09E-09
sp-20-K-16	80	90	7.33E-05	8.00	9	1.8735	0.041	4.4366	0.2502	0.3826	0.0108	27.2337	0.2700	87.3004	0.0719	9.97E-09
sp-20-K-18	80	90	7.37E-05	9.00	9	1.8635	0.041	4.2072	**0.2392**	0.3929	0.0112	24.4533	0.2443	84.2125	0.0419	2.55E-09
sp-20-K-20	80	90	7.52E-05	10.00	9	1.8539	0.041	3.9139	**0.2277**	0.3936	0.0115	22.3589	0.2284	85.9664	0.0607	3.68E-10
sp-20-K-22	80	90	7.40E-05	11.00	9	1.8447	0.041	3.8318	**0.2201**	0.3912	0.0113	25.3428	0.2559	87.7289	0.0776	1.80E-08
Exp. 12																
sp-20-L-BLK1	120	90			9			<DL		0.0388		<DL		118.5570		
sp-20-L-BLK2	120	90			9			<DL		0.0381		<DL		117.1080		

Table A1. SPFT Results from Dissolution of Glass IDF21-EC14 at 90°C (cont.)

Sample ID	**Inf [Si]** ppm	**T °C**	**Flow Rate,** m^3/d	**Time,** days	**pH** 23°C	**Glass Mass** g	**SA** m^2	**[B]** ppm	**B Rate** $g\ m^{-2}\ d^{-1}$	**[Al]** ppm	**Al Rate** $g\ m^{-2}\ d^{-1}$	**[Na]** ppm	**Na Rate** $g\ m^{-2}\ d^{-1}$	**[Si]** ppm	**Si Rate** $g\ m^{-2}\ d^{-1}$	r_{IEX} $mol\ m^{-2}\ s^{-1}$
sp-20-L-BLK3	120	90			9			<DL		0.0369		<DL		118.5930		
sp-20-L-02	120	90	7.24E-05	1.00	9	1.9924	0.043	8.8838	0.4755	0.3105	0.0073	45.7144	0.4301	120.3010	0.0207	-2.29E-08
sp-20-L-04	120	90	7.10E-05	2.00	9	1.9717	0.043	9.2531	0.4893	0.2614	0.0057	46.5892	0.4331	122.1950	0.0379	-2.83E-08
sp-20-L-06	120	90	6.95E-05	3.00	9	1.9519	0.042	8.5439	0.4453	0.2429	0.0050	43.3755	0.3973	123.9050	0.0528	-2.42E-08
sp-20-L-08	120	90	7.20E-05	4.00	9	1.9335	0.042	7.7658	0.4219	0.2330	0.0049	40.5226	0.3868	126.9940	0.0843	-1.77E-08
sp-20-L-10	120	90	7.54E-05	5.00	9	1.9157	0.042	7.4542	0.4264	0.2399	0.0054	40.3499	0.4055	129.5710	0.1145	-1.05E-08
sp-20-L-13	120	90	7.30E-05	6.50	9	1.8983	0.042	4.9210	0.2743	0.2297	0.0050	29.6045	0.2895	117.9690	-0.0011	7.64E-09
sp-20-L-15	120	90	7.51E-05	7.50	9	1.8844	0.041	4.4377	0.2556	0.2402	0.0055	27.7155	0.2799	118.6280	0.0054	1.23E-08
sp-20-L-16	120	90	7.71E-05	8.00	9	1.8765	0.041	4.2668	0.2528	0.2410	0.0057	25.1983	0.2616	122.0720	0.0412	4.43E-09
sp-20-L-18	120	90	8.09E-05	9.00	9	1.8687	0.041	4.0291	0.2511	0.2429	0.0060	24.1386	0.2635	138.8310	0.2256	6.26E-09
sp-20-L-20	120	90	7.82E-05	10.00	9	1.8588	0.041	3.8369	**0.2320**	0.2492	0.0061	24.1673	0.2560	124.1150	0.0636	1.21E-08
sp-20-L-21	120	90	7.59E-05	10.50	9	1.8518	0.041	3.6971	**0.2176**	0.2620	0.0064	24.3617	0.2512	116.5650	-0.0156	1.69E-08
sp-20-L-22	120	90	7.55E-05	11.00	9	1.8474	0.041	3.6938	**0.2164**	0.2773	0.0069	24.5359	0.2520	125.3910	0.0747	1.79E-08

***In bold: Samples used to calculate steady state dissolution rates.**

**** The r_{IEX} values listed are calculated based on the previous conventional formula without any correction. To obtain the corrected values, the listed values have to be multiplied by the correction factor of 0.24x46/62 = 0.178.**

Table A2. SPFT Results from Dissolution of Glass IDF21-EC14 at 70°C.

Sample ID	Inf [Si] ppm	T °C	Flow Rate, m^3/d	Time, days	pH 23°C	Glass Mass g	SA m^2	[B] ppm	B Rate $g\ m^{-2}\ d^{-1}$	[Al] ppm	Al Rate $g\ m^{-2}\ d^{-1}$	[Na] ppm	Na Rate $g\ m^{-2}\ d^{-1}$	[Si] ppm	Si Rate $g\ m^{-2}\ d^{-1}$	r_{IEX} $mol\ m^{-2}\ s^{-1}$
Exp. 13																
sp-21-A-BLK1	0	70			7			<DL		<DL		<DL		<DL		
sp-21-A-BLK2	0	70			7			< DL		<DL		<DL		<DL		
sp-21-A-BLK3	0	70			7			< DL		<DL		<DL		0.0731		
sp-21-A-02	0	70	5.24E-05	1.00	7	0.9937	0.021	6.2059	0.4821	0.0831	0.0034	38.2022	0.5247	1.1439	0.0151	2.15E-08
sp-21-A-04	0	70	5.01E-05	2.00	7	0.9827	0.021	7.3722	0.5512	0.1023	0.0041	42.6698	0.5639	1.0975	0.0139	6.40E-09
sp-21-A-06	0	70	4.90E-05	3.00	7	0.9716	0.021	6.7717	0.4993	0.1102	0.0044	38.6499	0.5038	0.8943	0.0111	2.26E-09
sp-21-A-08	0	70	5.04E-05	4.00	7	0.9616	0.021	5.8520	0.4468	0.1091	0.0045	33.8129	0.4566	0.7223	0.0092	4.89E-09
sp-21-A-10	0	70	5.07E-05	5.00	7	0.9527	0.021	5.3130	0.4101	0.1069	0.0044	30.8535	0.4212	0.6135	0.0079	5.59E-09
sp-21-A-12	0	70	4.89E-05	6.00	7	0.9445	0.021	5.0229	0.3760	0.1070	0.0043	29.8515	0.3953	0.5573	0.0069	9.70E-09
sp-21-A-14	0	70	5.01E-05	7.00	7	0.9369	0.021	4.6953	0.3625	0.1056	0.0044	28.0925	0.3837	0.5174	0.0066	1.07E-08
sp-21-A-16	0	70	4.90E-05	8.00	7	0.9296	0.020	4.5624	0.3460	0.1097	0.0045	26.7099	0.3584	0.5115	0.0064	6.23E-09
sp-21-A-18	0	70	4.91E-05	9.00	7	0.9226	0.020	4.4055	**0.3366**	0.1064	0.0044	26.1352	0.3533	0.5119	0.0064	8.42E-09
sp-21-A-20	0	70	5.19E-05	10.00	7	0.9158	0.020	4.1622	**0.3375**	0.1066	0.0047	23.8167	0.3417	0.4955	0.0066	2.14E-09
sp-21-A-23	0	70	5.21E-05	11.50	7	0.9076	0.020	3.8529	**0.3158**	0.0986	0.0043	22.5163	0.3266	0.4845	0.0065	5.47E-09
Exp. 14																
sp-21-B-BLK1	0	70			8			<DL		<DL		0.04		0.03		
sp-21-B-BLK2	0	70			8			<DL		<DL		0.02		0.04		
sp-21-B-BLK3	0	70			8			<DL		<DL		<DL		0.05		
sp-21-B-02	0	70	5.34E-05	1.00	8	1.0006	0.022	2.8579	0.2240	0.2491	0.0112	19.8456	0.2755	1.1745	0.0156	2.59E-08
sp-21-B-03	0	70	4.95E-05	2.50	8	0.9942	0.021	3.3724	0.2466	0.2952	0.0124	22.4064	0.2901	1.2569	0.0156	2.19E-08
sp-21-B-06	0	70	5.10E-05	3.00	8	0.9888	0.021	3.5978	0.2720	0.3089	0.0135	21.6055	0.2891	1.2225	0.0156	8.60E-09
sp-21-B-08	0	70	4.76E-05	4.00	8	0.9849	0.021	3.2491	0.2297	0.2924	0.0119	19.6479	0.2459	1.0965	0.0131	8.16E-09
sp-21-B-09	0	70	4.94E-05	4.50	8	0.9812	0.021	3.1249	0.2297	0.2890	0.0122	18.2758	0.2379	1.0669	0.0132	4.10E-09
sp-21-B-12	0	70	5.24E-05	6.00	8	0.9765	0.021	2.7869	0.2178	0.2836	0.0128	16.2810	0.2254	1.0187	0.0134	3.81E-09
sp-21-B-13	0	70	5.23E-05	6.50	8	0.9719	0.021	2.6739	0.2092	0.2838	0.0128	15.6913	0.2175	0.9906	0.0130	4.16E-09
sp-21-B-16	0	70	5.26E-05	8.00	8	0.9677	0.021	2.4724	0.1952	0.2810	0.0128	14.8595	0.2079	0.9682	0.0128	6.39E-09
sp-21-B-18	0	70	5.20E-05	9.00	8	0.9627	0.021	2.3390	**0.1830**	0.2742	0.0123	13.8801	0.1924	0.9579	0.0126	4.77E-09
sp-21-B-20	0	70	5.23E-05	10.00	8	0.9590	0.021	2.2047	**0.1739**	0.2633	0.0119	13.1321	0.1837	0.9371	0.0124	4.90E-09
sp-21-B-23	0	70	5.41E-05	11.50	8	0.9546	0.021	1.9729	**0.1615**	0.2550	0.0120	12.0004	0.1743	0.8961	0.0123	6.42E-09
Exp. 15																
sp-21-C-BLK1	0	70						<DL		<DL		<DL		0.0126		
sp-21-C-BLK2	0	70			9			<DL		<DL		<DL		< DL		
sp-21-C-BLK3	0	70			9			<DL		<DL		<DL		< DL		
sp-21-C-02	0	70	4.58E-05	1.00	9	1.0009	0.022	0.6728	0.0445	0.6989	0.0276	9.2263	0.1098	2.4913	0.0289	3.29E-08
sp-21-C-04	0	70	4.91E-05	2.00	9	1.0000	0.022	0.6849	0.0487	1.0690	0.0456	8.9708	0.1146	3.6725	0.0459	3.32E-08
sp-21-C-06	0	70	4.87E-05	3.00	9	0.9988	0.022	0.7234	0.0511	1.1535	0.0489	7.3878	0.0937	4.1139	0.0511	2.14E-08
sp-21-C-08	0	70	4.67E-05	4.00	9	0.9978	0.022	0.7036	0.0477	1.1468	0.0467	6.3302	0.0770	4.0537	0.0483	1.48E-08
sp-21-C-10	0	70	4.93E-05	5.00	9	0.9968	0.021	0.6786	0.0485	1.2741	0.0548	5.8634	0.0753	3.9352	0.0496	1.35E-08
sp-21-C-11	0	70	4.94E-05	5.50	9	0.9960	0.021	0.6740	0.0482	1.2564	0.0541	5.6473	0.0726	3.9727	0.0501	1.23E-08
sp-21-C-14	0	70	4.99E-05	7.00	9	0.9949	0.021	0.6604	0.0478	1.0905	0.0474	5.0594	0.0658	3.8414	0.0490	9.06E-09
sp-21-C-15	0	70	4.99E-05	7.50	9	0.9939	0.021	0.6622	0.0480	1.0833	0.0472	4.9397	0.0643	3.8692	0.0494	8.22E-09

Table A2. SPFT Results from Dissolution of Glass IDF21-EC14 at 70°C (cont.)

Sample ID	Inf [Si] ppm	T °C	Flow Rate, m^3/d	Time, days	pH 23°C	Glass Mass g	SA m^2	[B] ppm	B Rate $g\ m^{-2}\ d^{-1}$	[Al] ppm	Al Rate $g\ m^{-2}\ d^{-1}$	[Na] ppm	Na Rate $g\ m^{-2}\ d^{-1}$	[Si] ppm	Si Rate $g\ m^{-2}\ d^{-1}$	r_{IEX} mol $m^{-2}\ s^{-1}$
sp-21-C-18	0	70	4.94E-05	9.00	9	0.9929	0.021	0.6458	**0.0463**	1.0845	0.0467	4.6818	0.0603	3.7582	0.0475	7.06E-09
sp-21-C-20	0	70	4.79E-05	10.00	9	0.9917	0.021	0.6278	**0.0437**	1.0258	0.0429	4.2860	0.0536	3.6722	0.0451	5.00E-09
sp-21-C-23	0	70	5.01E-05	11.50	9	0.9906	0.021	0.6029	**0.0439**	0.9807	0.0430	3.9676	0.0520	3.5199	0.0452	4.06E-09
Exp. 16																
sp-21-D-BLK1	0	70						<DL		<DL		< 0.0068		0.04		
sp-21-D-BLK2	0	70						<DL		<DL		0.03		0.03		
sp-21-D-BLK3	0	70			10			<DL		<DL		0.02		0.05		
sp-21-D-02	0	70	4.65E-05	1.00	10	0.5014	0.011	0.7101	0.0954	1.2083	0.0975	5.4714	0.1318	3.9091	0.0923	1.83E-08
sp-21-D-04	0	70	4.90E-05	2.00	10	0.5002	0.011	0.8359	0.1189	1.5560	0.1328	5.8862	0.1498	4.6582	0.1163	1.55E-08
sp-21-D-05	0	70	4.67E-05	2.50	10	0.4990	0.011	1.7123	0.2344	2.8711	0.2344	11.2975	0.2746	8.9067	0.2129	2.03E-08
sp-21-D-07	0	70	4.95E-05	3.50	10	0.4976	0.011	0.8875	0.1281	1.4771	0.1277	5.4128	0.1395	4.8571	0.1229	5.74E-09
sp-21-D-08	0	70	4.90E-05	4.00	10	0.4966	0.011	0.8840	0.1263	1.6982	0.1455	5.4507	0.1391	4.9041	0.1229	6.43E-09
sp-21-D-10	0	70	4.96E-05	5.00	10	0.4956	0.011	0.8854	0.1282	1.5840	0.1375	5.4383	0.1407	4.8501	0.1232	6.25E-09
sp-21-D-12	0	70	4.65E-05	6.00	10	0.4942	0.011	0.8968	0.1220	1.0184	0.0827	4.9391	0.1199	4.7961	0.1144	-1.05E-09
sp-21-D-14	0	70	4.96E-05	7.00	10	0.4929	0.011	0.8961	0.1303	1.5164	0.1322	4.9497	0.1285	4.9620	0.1265	-9.30E-10
sp-21-D-15	0	70	4.61E-05	7.50	10	0.4919	0.011	0.9123	**0.1236**	1.5088	0.1225	5.0642	0.1225	5.0758	0.1206	-5.89E-10
sp-21-D-18	0	70	4.61E-05	9.00	10	0.4906	0.011	0.8778	**0.1189**	1.4876	0.1208	4.8797	0.1180	4.8921	0.1162	-4.55E-10
sp-21-D-20	0	70	5.02E-05	10.00	10	0.4890	0.011	0.8726	**0.1291**	1.5123	0.1341	4.9540	0.1308	4.8263	0.1252	8.89E-10
Exp. 17																
sp-20-E-BLK1	0	70			11			<DL		<DL		0.07		<DL		
sp-20-E-BLK2	0	70			11			<DL		0.46		0.06		0.29		
sp-20-E-BLK3	0	70			11			<DL		0.49		0.06		0.32		
sp-20-E-02	0	70	5.20E-05	1.00	11	0.4996	0.011	1.8308	0.2794	3.3879	0.2800	19.1127	0.5171	8.4958	0.2218	1.20E-07
sp-20-E-04	0	70	5.16E-05	2.00	11	0.4957	0.011	2.2824	0.3476	4.0783	0.3417	21.3083	0.5745	10.4862	0.2740	1.14E-07
sp-20-E-06	0	70	5.16E-05	3.00	11	0.4925	0.011	2.3450	0.3586	4.0021	0.3362	22.9843	0.6224	10.8361	0.2845	1.33E-07
sp-20-E-08	0	70	5.22E-05	4.00	11	0.4886	0.011	2.3092	0.3594	4.0164	0.3435	22.2008	0.6118	10.7471	0.2872	1.27E-07
sp-20-E-10	0	70	5.20E-05	5.00	11	0.4849	0.011	2.2569	0.3515	4.0337	0.3454	22.5448	0.6219	10.4791	0.2801	1.36E-07
sp-20-E-12	0	70	5.24E-05	6.00	11	0.4811	0.010	2.2686	0.3582	4.0680	0.3533	22.2719	0.6227	10.5545	0.2860	1.33E-07
sp-20-E-14	0	70	5.04E-05	7.00	11	0.4774	0.010	2.2778	0.3477	4.1064	0.3450	21.9999	0.5946	10.5622	0.2767	1.24E-07
sp-20-E-16	0	70	4.93E-05	8.00	11	0.4739	0.010	2.2429	0.3367	3.9958	0.3295	21.6194	0.5748	10.4519	0.2693	1.20E-07
sp-20-E-18	0	70	5.16E-05	9.00	11	0.4703	0.010	2.2846	**0.3609**	4.1288	0.3592	22.5258	0.6301	10.5856	0.2870	1.35E-07
sp-20-E-19	0	70	5.33E-05	9.50	11	0.4674	0.010	2.3219	**0.3804**	4.1293	0.3725	22.2318	0.6449	10.7785	0.3031	1.33E-07
sp-20-E-23	0	70	5.41E-05	11.50	11	0.4626	0.010	2.2601	**0.3783**	3.9923	0.3670	21.4936	0.6371	10.4969	0.3016	1.30E-07
Exp. 18																
sp-21-F-BLK1	0	70			12			<DL		<DL		0.92		0.03		
sp-21-F-BLK2	0	70			12			<DL		0.35		0.84		0.18		
sp-21-F-BLK3	0	70			12			<DL		0.35		0.84		0.21		
sp-21-F-02	0	70	5.10E-05	1.00	12	0.4975	0.011	3.8254	0.5764	7.7650	0.6762	38.1413	0.9951	19.6488	0.5085	2.11E-07
sp-21-F-04	0	70	4.91E-05	2.00	12	0.4904	0.011	5.1762	0.7592	10.6307	0.9077	48.3031	1.2314	26.1309	0.6603	2.38E-07
sp-21-F-06	0	70	4.91E-05	3.00	12	0.4820	0.011	5.6195	0.8336	10.2424	0.8836	52.0447	1.3435	28.3948	0.7263	2.57E-07
sp-21-F-08	0	70	5.07E-05	4.00	12	0.4730	0.010	5.6517	0.8758	10.1931	0.9185	52.3912	1.4129	27.4967	0.7344	2.70E-07
sp-21-F-10	0	70	5.13E-05	5.00	12	0.4640	0.010	5.5419	0.8801	10.0596	0.9287	51.1913	1.4143	27.1518	0.7431	2.69E-07

Table A2. SPFT Results from Dissolution of Glass IDF21-EC14 at 70°C (cont.)

Sample ID	Inf [Si] ppm	T °C	Flow Rate, m^3/d	Time, days	pH 23°C	Glass Mass g	SA m^2	[B] ppm	B Rate $g\ m^{-2}\ d^{-1}$	[Al] ppm	Al Rate $g\ m^{-2}\ d^{-1}$	[Na] ppm	Na Rate $g\ m^{-2}\ d^{-1}$	[Si] ppm	Si Rate $g\ m^{-2}\ d^{-1}$	r_{IEX} $mol\ m^{-2}\ s^{-1}$
sp-21-F-12	0	70	4.93E-05	6.00	12	0.4550	0.010	5.6715	0.8773	10.1958	0.9171	52.9222	1.4248	27.4286	0.7312	2.76E-07
sp-21-F-14	0	70	4.91E-05	7.00	12	0.4460	0.010	5.8909	0.9201	10.5529	0.9591	53.7865	1.4624	28.7094	0.7732	2.73E-07
sp-21-F-16	0	70	5.04E-05	8.00	12	0.4365	0.010	6.1732	**1.0037**	10.8284	1.0250	55.3730	1.5679	29.3705	0.8235	2.84E-07
sp-21-F-17	0	70	4.61E-05	8.50	12	0.4293	0.010	6.1858	0.9314	10.9301	0.9582	55.7178	1.4611	29.5484	0.7673	2.67E-07
sp-21-F-20	0	70	4.77E-05	10.00	12	0.4197	0.010	6.4714	**1.0237**	11.3180	1.0432	58.6053	1.6157	30.8789	0.8427	2.98E-07
sp-21-F-23	0	70	5.17E-05	11.50	12	0.4047	0.009	6.1473	**1.0797**	10.7341	1.0973	55.2140	1.6887	29.2515	0.8859	3.06E-07
Exp. 19																
sp-21-G-BLK1	1	70			9			<DL		<DL		0.04		1.04		
sp-21-G-BLK2	1	70			9			<DL		<DL		0.02		1.01		
sp-21-G-BLK3	1	70			9			<DL		<DL		<DL		1.07		
sp-21-G-03	1	70	6.27E-05	1.50	9	0.5013	0.011	0.4440	0.0795	0.7262	0.0786	4.7921	0.1555	3.5038	0.0793	3.83E-08
sp-21-G-04	1	70	6.25E-05	2.00	9	0.5004	0.011	0.4760	0.0852	0.8384	0.0907	4.7580	0.1540	3.7188	0.0860	3.46E-08
sp-21-G-06	1	70	5.90E-05	3.00	9	0.4997	0.011	0.4894	0.0828	0.9082	0.0929	4.3020	0.1314	3.8749	0.0860	2.45E-08
sp-21-G-09	1	70	6.27E-05	4.50	9	0.4986	0.011	0.4586	0.0824	0.8245	0.0896	3.3302	0.1081	3.7708	0.0881	1.29E-08
sp-21-G-10	1	70	6.30E-05	5.00	9	0.4977	0.011	0.4614	0.0834	0.7819	0.0855	3.1491	0.1028	3.7280	0.0873	9.74E-09
sp-21-G-11	1	70	6.27E-05	5.50	9	0.4973	0.011	0.4663	0.0840	0.7758	0.0845	3.0688	0.0998	3.7677	0.0883	7.92E-09
sp-21-G-14	1	70	6.32E-05	7.00	9	0.4964	0.011	0.4511	0.0819	0.7811	0.0858	2.9744	0.0976	3.6431	0.0850	7.86E-09
sp-21-G-16	1	70	6.06E-05	8.00	9	0.4953	0.011	0.4524	**0.0789**	0.7917	0.0835	2.8129	0.0885	3.6477	0.0817	4.84E-09
sp-21-G-18	1	70	6.08E-05	9.00	9	0.4945	0.011	0.4479	**0.0784**	0.7926	0.0840	2.7335	0.0864	3.6791	0.0831	4.00E-09
sp-21-G-20	1	70	5.94E-05	10.00	9	0.4936	0.011	0.4513	**0.0774**	0.8010	0.0831	2.7337	0.0845	3.6901	0.0817	3.61E-09
sp-21-G-23	1	70	6.21E-05	11.50	9	0.4926	0.011	0.4510	0.0809	0.5714	0.0618	2.5822	0.0836	3.7767	0.0883	1.32E-09
Exp. 20																
sp-21-H-BLK1	5	70			9			<DL		<DL		0.07		4.84		
sp-21-H-BLK2	5	70			9			<DL		<DL		0.03		4.76		
sp-21-H-BLK3	5	70			9			<DL		<DL		<DL		4.70		
sp-21-H-02	5	70	6.44E-05	1.00	9	0.5034	0.011	0.3394	0.0615	0.4306	0.0472	4.9680	0.1645	6.0064	0.0408	5.18E-08
sp-21-H-04	5	70	6.43E-05	2.00	9	0.5027	0.011	0.3762	0.0684	0.6524	0.0721	4.3950	0.1454	6.6300	0.0613	3.87E-08
sp-21-H-06	5	70	6.36E-05	3.00	9	0.5019	0.011	0.3983	0.0718	0.6750	0.0738	3.6628	0.1197	6.8541	0.0679	2.41E-08
sp-21-H-08	5	70	6.43E-05	4.00	9	0.5012	0.011	0.3675	0.0669	0.4310	0.0473	2.9629	0.0978	6.8338	0.0681	1.55E-08
sp-21-H-10	5	70	6.46E-05	5.00	9	0.5004	0.011	0.3797	0.0696	0.5906	0.0656	2.6359	0.0873	6.8401	0.0687	8.91E-09
sp-21-H-12	5	70	6.41E-05	6.00	9	0.4997	0.011	0.3835	0.0699	0.4131	0.0453	2.4500	0.0805	6.8757	0.0694	5.37E-09
sp-21-H-14	5	70	6.47E-05	7.00	9	0.4989	0.011	0.3795	0.0698	0.6158	0.0687	2.3398	0.0776	6.8833	0.0703	3.94E-09
sp-21-H-16	5	70	6.09E-05	8.00	9	0.4982	0.011	0.3809	0.0660	0.4477	0.0467	2.2749	0.0710	6.8641	0.0657	2.54E-09
sp-21-H-18	5	70	6.46E-05	9.00	9	0.4974	0.011	0.3847	**0.0708**	0.6225	0.0695	2.2352	0.0741	6.9809	0.0737	1.66E-09
sp-21-H-19	5	70	6.17E-05	9.50	9	0.4969	0.011	0.3783	**0.0665**	0.6716	0.0717	2.4008	0.0762	6.9403	0.0691	4.86E-09
sp-21-H-23	5	70	6.01E-05	11.50	9	0.4960	0.011	0.3661	**0.0627**	0.6872	0.0717	2.3640	0.0732	6.9413	0.0675	5.26E-09
Exp. 21																
sp-21-I-BLK1	10	70			9			<DL		<DL		0.05		9.52		
sp-21-I-BLK2	10	70			9			<DL		<DL		0.05		9.38		
sp-21-I-BLK3	10	70			9			<DL		<DL		<DL		9.17		
sp-21-I-02	10	70	6.44E-05	1.00	9	1.0000	0.022	0.7930	0.0741	0.0299	0.0011	8.8146	0.1473	10.7177	0.0225	3.69E-08
sp-21-I-04	10	70	6.38E-05	2.00	9	0.9986	0.022	0.5639	0.0518	0.0335	0.0013	6.9958	0.1157	10.936	0.0259	3.22E-08

Table A2. SPFT Results from Dissolution of Glass IDF21-EC14 at 70°C (cont.)

Sample ID	Inf [Si] ppm	T °C	Flow Rate, m^3/d	Time, days	pH 23°C	Glass Mass g	SA m^2	[B] ppm	B Rate $g\ m^{-2}\ d^{-1}$	[Al] ppm	Al Rate $g\ m^{-2}\ d^{-1}$	[Na] ppm	Na Rate $g\ m^{-2}\ d^{-1}$	[Si] ppm	Si Rate $g\ m^{-2}\ d^{-1}$	r_{IEX} $mol\ m^{-2}\ s^{-1}$
sp-21-I-06	10	70	6.30E-05	3.00	9	0.9977	0.022	0.4029	0.0362	0.0309	0.0011	5.5266	0.0902	11.0997	0.0282	2.72E-08
sp-21-I-08	10	70	6.03E-05	4.00	9	0.9970	0.021	0.3248	0.0277	0.0173	0.0004	4.2717	0.0666	11.0044	0.0256	1.96E-08
sp-21-I-10	10	70	6.37E-05	5.00	9	0.9964	0.021	0.2999	0.0269	0.0300	0.0011	3.5867	0.0591	10.9284	0.0258	1.62E-08
sp-21-I-12	10	70	6.34E-05	6.00	9	0.9958	0.021	0.3044	0.0273	0.0201	0.0006	3.3342	0.0546	10.9197	0.0255	1.38E-08
sp-21-I-13	10	70	6.35E-05	6.50	9	0.9954	0.021	0.3175	0.0285	0.0349	0.0014	3.3867	0.0556	11.0755	0.0281	1.36E-08
sp-21-I-16	10	70	6.03E-05	8.00	9	0.9947	0.021	0.3646	0.0313	0.0165	0.0003	3.0707	0.0478	11.1023	0.0271	8.30E-09
sp-21-I-18	10	70	6.31E-05	9.00	9	0.9939	0.021	0.3697	**0.0333**	0.0346	0.0014	2.9078	0.0474	11.2228	0.0304	7.10E-09
sp-21-I-19	10	70	6.20E-05	9.50	9	0.9933	0.021	0.3758	**0.0332**	0.0334	0.0013	2.8558	0.0457	11.2421	0.0301	6.26E-09
sp-21-I-23	10	70	6.11E-05	11.50	9	0.9925	0.021	0.3743	**0.0327**	0.0180	0.0004	2.7173	0.0429	11.1593	0.0285	5.14E-09
Exp. 22																
sp-21-J-BLK1	20	70			9			<DL		0.02		0.05		19.33		
sp-21-J-BLK2	20	70			9			<DL		<DL		0.03		19.15		
sp-21-J-BLK3	20	70			9			<DL		0.01		<DL		19.89		
sp-21-J-02	20	70	6.41E-05	1.00	9	1.0003	0.022	0.9192	0.0858	0.4151	0.0226	9.4110	0.1569	22.1187	0.0439	3.58E-08
sp-21-J-04	20	70	6.02E-05	2.00	9	0.9985	0.021	0.8971	0.0787	0.5066	0.0261	7.7874	0.1220	22.1187	0.0413	2.18E-08
sp-21-J-06	20	70	6.42E-05	3.00	9	0.9969	0.021	0.7813	0.0729	0.2099	0.0111	6.5234	0.1089	22.4185	0.0490	1.81E-08
sp-21-J-08	20	70	6.06E-05	4.00	9	0.9955	0.021	0.6015	0.0528	0.2626	0.0133	5.1474	0.0811	22.0015	0.0398	1.43E-08
sp-21-J-10	20	70	6.42E-05	5.00	9	0.9944	0.021	0.5584	0.0519	0.4403	0.0241	4.9366	0.0825	21.1260	0.0277	1.54E-08
sp-21-J-12	20	70	6.12E-05	6.00	9	0.9934	0.021	0.4967	0.0439	0.4047	0.0211	4.4520	0.0709	21.4700	0.0318	1.36E-08
sp-21-J-14	20	70	6.48E-05	7.00	9	0.9925	0.021	0.4415	0.0411	0.4161	0.0230	4.1649	0.0702	21.2684	0.0303	1.46E-08
sp-21-J-16	20	70	6.43E-05	8.00	9	0.9916	0.021	0.3945	**0.0364**	0.4060	0.0223	3.8294	0.0641	21.4081	0.0324	1.39E-08
sp-21-J-18	20	70	6.42E-05	9.00	9	0.9909	0.021	0.3486	**0.0319**	0.4029	0.0221	3.6703	0.0613	21.3548	0.0315	1.48E-08
sp-21-J-20	20	70	6.29E-05	10.00	9	0.9903	0.021	0.3172	**0.0283**	0.4028	0.0216	3.3783	0.0552	21.8601	0.0391	1.35E-08
sp-21-J-23	20	70	5.91E-05	11.50	9	0.9896	0.021	0.2832	0.0237	0.3678	0.0185	2.9118	0.0447	21.9437	0.0381	1.06E-08
Exp. 23																
sp-21-K-BLK1	40	70			9			<DL		0.03		0.10		40.74		
sp-21-K-BLK2	40	70			9			<DL		0.02		0.09		40.60		
sp-21-K-BLK3	40	70			9			<DL		0.02		0.08		40.70		
sp-21-K-02	40	70	6.63E-05	1.00	9	1.0001	0.027	1.1085	0.0851	0.3288	0.0141	9.8736	0.1343	42.1807	0.0203	2.48E-08
sp-21-K-04	40	70	6.54E-05	2.00	9	0.9977	0.027	1.2566	0.0955	0.3528	0.0150	8.9274	0.1199	42.9630	0.0305	1.23E-08
sp-21-K-06	40	70	6.14E-05	3.00	9	0.9952	0.027	1.2292	0.0878	0.3429	0.0137	7.7660	0.0979	42.2765	0.0201	5.10E-09
sp-21-K-08	40	70	6.43E-05	4.00	9	0.9929	0.027	1.1547	0.0865	0.3148	0.0131	6.9513	0.0918	43.0811	0.0317	2.70E-09
sp-21-K-09	40	70	6.29E-05	4.50	9	0.9912	0.027	1.0706	0.0784	0.3198	0.0130	6.4937	0.0839	43.9669	0.0424	2.77E-09
sp-21-K-12	40	70	6.47E-05	6.00	9	0.9891	0.027	1.0177	0.0766	0.2999	0.0125	5.9280	0.0787	43.7344	0.0406	1.05E-09
sp-21-K-14	40	70	6.28E-05	7.00	9	0.9866	0.027	0.9624	0.0705	0.2926	0.0118	5.9053	0.0763	42.7308	0.0265	2.94E-09
sp-21-K-16	40	70	6.25E-05	8.00	9	0.9847	0.027	0.9263	**0.0675**	0.2694	0.0108	5.8935	0.0758	42.0918	0.0182	4.19E-09
sp-21-K-18	40	70	6.21E-05	9.00	9	0.9830	0.027	0.8954	**0.0649**	0.2662	0.0106	5.8569	0.0750	43.7850	0.0398	5.08E-09
sp-21-K-20	40	70	6.17E-05	10.00	9	0.9813	0.027	0.8656	**0.0624**	0.2660	0.0105	5.7373	0.0731	43.7179	0.0388	5.37E-09
sp-21-K-22	40	70	5.71E-05	11.50	9	0.9793	0.027	0.8496	0.0568	0.2690	0.0099	5.7021	0.0673	43.9423	0.0386	5.31E-09
Exp. 24																
sp-21-L-BLK1	80	70			9			<DL		0.08		0.11		79.57		
sp-21-L-BLK2	80	70			9			<DL		0.04		0.11		80.87		

Table A2. SPFT Results from Dissolution of Glass IDF21-EC14 at 70°C (cont.)

Sample ID	**Inf [Si]** ppm	**T** °C	**Flow Rate,** m^3/d	**Time,** days	**pH** 23°C	**Glass Mass** g	**SA** m^2	**[B]** ppm	**B Rate** $g\ m^{-2}\ d^{-1}$	**[Al]** ppm	**Al Rate** $g\ m^{-2}\ d^{-1}$	**[Na]** ppm	**Na Rate** $g\ m^{-2}\ d^{-1}$	**[Si]** ppm	**Si Rate** $g\ m^{-2}\ d^{-1}$	r_{IEX} $mol\ m^{-2}\ s^{-1}$
sp-21-L-BLK3	80	70			9			<DL		0.04		0.09		81.43		
sp-21-L-02	80	70	6.92E-05	1.00	9	1.9992	0.043	2.2687	0.1153	0.2606	0.0064	17.4517	0.1567	86.2840	0.0504	2.08E-08
sp-21-L-04	80	70	6.96E-05	2.00	9	1.9939	0.043	2.5813	0.1322	0.2460	0.0060	17.5847	0.1589	89.3382	0.0781	1.34E-08
sp-21-L-06	80	70	6.88E-05	3.00	9	1.9884	0.043	2.4618	0.1250	0.2430	0.0058	15.6122	0.1398	84.4876	0.0343	7.46E-09
sp-21-L-08	80	70	7.06E-05	4.00	9	1.9831	0.043	2.2872	0.1192	0.2388	0.0058	13.4055	0.1231	84.9578	0.0395	1.99E-09
sp-21-L-09	80	70	6.78E-05	4.50	9	1.9794	0.043	2.1942	0.1099	0.2316	0.0054	12.6592	0.1118	87.4487	0.0599	9.27E-10
sp-21-L-12	80	70	7.11E-05	6.00	9	1.9749	0.043	1.9817	0.1042	0.2154	0.0052	11.3728	0.1054	85.7849	0.0476	5.86E-10
sp-21-L-14	80	70	7.19E-05	7.00	9	1.9695	0.043	1.8525	0.0986	0.2055	0.0049	11.0369	0.1036	85.6962	0.0474	2.48E-09
sp-21-L-15	80	70	6.91E-05	7.50	9	1.9664	0.043	1.8317	0.0938	0.2147	0.0050	10.2565	0.0925	87.1449	0.0586	-6.50E-10
sp-21-L-17	80	70	6.93E-05	8.50	9	1.9634	0.043	1.7450	0.0897	0.2134	0.0050	10.1637	0.0920	85.8718	0.0473	1.18E-09
sp-21-L-20	80	70	6.99E-05	10.00	9	1.9587	0.042	1.7046	0.0885	0.2000	0.0046	10.0863	0.0922	86.2490	0.0512	1.90E-09
sp-21-L-23	80	70	6.71E-05	11.50	9	1.9533	0.042	1.6223	0.0810	0.2045	0.0046	9.5334	0.0839	85.9992	0.0471	1.44E-09

***In bold: Samples used to calculate steady state dissolution rates.**

**** The r_{IEX} values listed are calculated based on the previous conventional formula without any correction. To obtain the corrected values, the listed values have to be multiplied by the correction factor of 0.24x46/62 = 0.178.**

Table A3. SPFT Results from Dissolution of Glass IDF21-EC14 at 40°C.

Sample ID	Inf [Si] ppm	T °C	Flow Rate, m^3/d	Time, days	pH 23°C	Glass Mass g	SA m^2	[B] ppm	B Rate g m^{-2} d^{-1}	[Al] ppm	Al Rate g m^{-2} d^{-1}	[Na] ppm	Na Rate g m^{-2} d^{-1}	[Si] ppm	Si Rate g m^{-2} d^{-1}	r_{IEX} mol m^{-2} s^{-1}
Exp. 25																
sp-22-A-BLK1	0	40			7			<DL		<DL		<DL		0.2957		
sp-22-A-BLK2	0	40			7			< DL		<DL		<DL		0.2797		
sp-22-A-BLK3	0	40			7			< DL		<DL		<DL		0.2780		
sp-22-A-02	0	40	4.13E-05	2.00	7	1.0035	0.022	0.5903	0.0350	0.0155	0.00019	5.6368	0.0603	0.5284	0.0026	1.27E-08
sp-22-A-04	0	40	3.90E-05	4.00	7	1.0021	0.022	0.5844	0.0328	0.0149	0.00016	4.4291	0.0448	0.4898	0.0021	6.03E-09
sp-22-A-06	0	40	4.35E-05	6.00	7	1.0007	0.022	0.5022	0.0314	0.0168	0.00026	3.3354	0.0376	0.4504	0.0019	3.15E-09
sp-22-A-08	0	40	4.11E-05	8.00	7	0.9995	0.022	0.4373	0.0257	0.0224	0.00044	2.8011	0.0298	0.4220	0.0015	2.07E-09
sp-22-A-10	0	40	3.88E-05	10.00	7	0.9985	0.022	0.3548	0.0195	0.0175	0.00025	2.3232	0.0233	0.4022	0.0012	1.91E-09
sp-22-A-12	0	40	3.97E-05	12.00	7	0.9977	0.022	0.3348	0.0188	0.0166	0.00023	2.0863	0.0214	0.3994	0.0012	1.31E-09
sp-22-A-14	0	40	3.98E-05	14.00	7	0.9969	0.022	0.3225	0.0181	0.0164	0.00022	1.9251	0.0198	0.3989	0.0012	8.33E-10
sp-22-A-16	0	40	4.11E-05	16.00	7	0.9961	0.021	0.3136	0.0182	0.0167	0.00024	1.8433	0.0196	0.4159	0.0014	6.90E-10
sp-22-A-17	0	40	4.12E-05	17.00	7	0.9955	0.021	0.3017	**0.0175**	0.0163	0.00022	1.7982	0.0191	0.4220	0.0015	8.14E-10
sp-22-A-20	0	40	4.02E-05	20.00	7	0.9948	0.021	0.3033	**0.0172**	0.0115	0.00005	1.7916	0.0186	0.2384	-0.0005	7.11E-10
sp-22-A-21	0	40	4.02E-05	21.00	7	0.9940	0.021	0.3033	**0.0172**	0.0134	0.00012	1.8832	0.0196	0.1926	-0.0010	1.20E-09
Exp. 26																
sp-22-B-BLK1	0	40			8			<DL		<DL		<DL		<DL		
sp-22-B-BLK2	0	40			8			<DL		<DL		<DL		<DL		
sp-22-B-BLK3	0	40			8			<DL		<DL		<DL		<DL		
sp-22-B-02	0	40	4.14E-05	2.00	8	1.0031	0.022	0.2233	0.0127	0.0593	0.0018	3.4462	0.0369	0.2960	0.0030	1.21E-08
sp-22-B-03	0	40	3.97E-05	4.00	8	1.0026	0.022	0.1859	0.0101	0.0630	0.0018	2.2860	0.0234	0.2614	0.0026	6.73E-09
sp-22-B-06	0	40	4.34E-05	6.00	8	1.0022	0.022	0.1522	0.0088	0.0593	0.0019	1.6107	0.0180	0.2233	0.0024	4.60E-09
sp-22-B-08	0	40	4.11E-05	8.00	8	1.0018	0.022	0.1367	0.0074	0.0550	0.0016	1.3785	0.0145	0.2019	0.0020	3.58E-09
sp-22-B-09	0	40	3.89E-05	10.00	8	1.0016	0.022	0.1053	0.0052	0.0437	0.0011	1.0906	0.0109	0.1709	0.0016	2.83E-09
sp-22-B-12	0	40	3.98E-05	12.00	8	1.0013	0.022	0.0986	0.0050	0.0428	0.0011	0.9403	0.0095	0.1615	0.0016	2.31E-09
sp-22-B-13	0	40	3.98E-05	14.00	8	1.0011	0.022	0.0939	0.0047	0.0401	0.0010	0.8303	0.0084	0.1540	0.0015	1.88E-09
sp-22-B-16	0	40	4.13E-05	16.00	8	1.0009	0.022	0.0923	0.0048	0.0391	0.0010	0.8963	0.0094	0.1503	0.0015	2.35E-09
sp-22-B-18	0	40	4.14E-05	17.00	8	1.0008	0.022	0.0904	**0.0047**	0.0372	0.0010	0.7766	0.0082	0.1477	0.0015	1.77E-09
sp-22-B-20	0	40	4.03E-05	20.00	8	1.0006	0.022	0.0986	**0.0050**	0.0386	0.0010	0.7976	0.0082	0.1597	0.0016	1.59E-09
sp-22-B-23	0	40	4.02E-05	21.00	8	1.0004	0.022	0.0917	**0.0046**	0.0368	0.0009	0.7669	0.0078	0.1556	0.0015	1.63E-09
Exp. 27																
sp-22-C-BLK1	0	40						<DL		<DL		<DL		0.04		
sp-22-C-BLK2	0	40			9			<DL		<DL		<DL		0.01		
sp-22-C-BLK3	0	40			9			<DL		<DL		0.02		0.05		
sp-22-C-02	0	40	3.92E-05	2.00	9	1.0032	0.022	0.1568	0.0082	0.1497	0.0048	2.4663	0.0250	0.5291	0.0050	8.41E-09
sp-22-C-04	0	40	3.84E-05	4.00	9	1.0029	0.022	0.1519	0.0078	0.2177	0.0070	1.6703	0.0165	0.7900	0.0075	4.38E-09
sp-22-C-06	0	40	4.13E-05	6.00	9	1.0025	0.022	0.1593	0.0088	0.0359	0.0009	1.3464	0.0142	0.8947	0.0091	2.72E-09
sp-22-C-08	0	40	4.11E-05	8.00	9	1.0021	0.022	0.1668	0.0092	0.3970	0.0139	1.1788	0.0124	0.9765	0.0099	1.58E-09
sp-22-C-10	0	40	3.86E-05	10.00	9	1.0017	0.022	0.1552	0.0080	0.3002	0.0098	0.9834	0.0097	0.9263	0.0088	8.30E-10
sp-22-C-11	0	40	3.93E-05	12.00	9	1.0014	0.022	0.1578	0.0083	0.0396	0.0010	0.9195	0.0092	0.8984	0.0087	4.41E-10
sp-22-C-14	0	40	3.91E-05	14.00	9	1.0011	0.022	0.1481	0.0077	0.0749	0.0022	0.8218	0.0082	0.8913	0.0086	2.20E-10
sp-22-C-15	0	40	4.04E-05	16.00	9	1.0007	0.022	0.1484	0.0080	0.1219	0.0040	0.8923	0.0092	0.9025	0.0090	5.90E-10

Table A3. SPFT Results from Dissolution of Glass IDF21-EC14 at 40°C (cont.)

Sample ID	Inf [Si] ppm	T °C	Flow Rate, m^3/d	Time, days	pH 23°C	Glass Mass g	SA m^2	[B] ppm	B Rate $g\ m^{-2}\ d^{-1}$	[Al] ppm	Al Rate $g\ m^{-2}\ d^{-1}$	[Na] ppm	Na Rate $g\ m^{-2}\ d^{-1}$	[Si] ppm	Si Rate $g\ m^{-2}\ d^{-1}$	r_{IEX} $mol\ m^{-2}\ s^{-1}$
sp-22-C-18	0	40	4.04E-05	18.00	9	1.0004	0.022	0.1443	**0.0078**	0.1491	0.0049	0.7837	0.0080	0.8760	0.0087	1.39E-10
sp-22-C-20	0	40	3.94E-05	20.00	9	1.0000	0.022	0.1445	**0.0076**	0.2962	0.0099	0.8576	0.0086	0.8565	0.0083	5.11E-10
sp-22-C-21	0	40	3.93E-05	21.00	9	0.9998	0.022	0.1453	**0.0076**	0.1423	0.0046	0.7752	0.0077	0.8697	0.0085	6.22E-11
Exp. 28																
sp-22-D-BLK1	0	40						<DL		<DL		<DL		<DL		
sp-22-D-BLK2	0	40						<DL		<DL		<DL		<DL		
sp-22-D-BLK3	0	40	-	-	10	-	-	<DL		<DL		<DL		0.02		
sp-22-D-02	0	40	3.95E-05	2.00	10	0.5045	0.011	0.1840	0.0197	0.0638	0.0037	1.3824	0.0279	0.9964	0.0198	4.13E-09
sp-22-D-04	0	40	3.97E-05	4.00	10	0.5039	0.011	0.2794	0.0308	0.2072	0.0136	1.5746	0.0319	1.5093	0.0303	5.47E-10
sp-22-D-06	0	40	4.30E-05	6.00	10	0.5033	0.011	0.2683	0.0320	0.1851	0.0131	1.4976	0.0329	1.4681	0.0319	4.35E-10
sp-22-D-08	0	40	3.91E-05	8.00	10	0.5026	0.011	0.2909	0.0318	0.1542	0.0098	1.4848	0.0297	1.5419	0.0305	-1.04E-09
sp-22-D-09	0	40	3.83E-05	9.00	10	0.5021	0.011	0.2797	0.0299	0.2138	0.0136	1.4922	0.0292	1.5128	0.0293	-3.11E-10
sp-22-D-12	0	40	3.76E-05	12.00	10	0.5014	0.011	0.2786	0.0292	0.1706	0.0105	1.4538	0.0280	1.4905	0.0284	-6.21E-10
sp-22-D-14	0	40	3.74E-05	14.00	10	0.5006	0.011	0.2739	0.0286	0.4534	0.0290	1.4428	0.0277	1.5495	0.0295	-4.67E-10
sp-22-D-16	0	40	3.87E-05	16.00	10	0.5000	0.011	0.2542	0.0274	0.2370	0.0154	1.4333	0.0285	1.5338	0.0302	5.52E-10
sp-22-D-18	0	40	3.88E-05	18.00	10	0.4994	0.011	0.2516	**0.0272**	0.1706	0.0109	1.4309	0.0285	1.4918	0.0294	6.79E-10
sp-22-D-20	0	40	3.80E-05	20.00	10	0.4989	0.011	0.2485	**0.0263**	0.4048	0.0263	1.3043	0.0254	1.4222	0.0275	-4.21E-10
sp-22-D-21	0	40	3.79E-05	21.00	10	0.4984	0.011	0.2446	**0.0258**	0.3607	0.0233	1.3769	0.0269	1.4649	0.0283	5.22E-10
Exp. 29																
sp-22-E-BLK1	0	40			11			<DL		<DL		0.05		<DL		
sp-22-E-BLK2	0	40			11			<DL		0.43		0.05		0.34		
sp-22-E-BLK3	0	40			11			<DL		0.43		0.05		0.34		
sp-22-E-02	0	40	4.09E-05	2.00	11	0.4999	0.011	0.5909	0.0698	1.2965	0.0723	7.2826	0.1545	3.1096	0.0606	4.26E-08
sp-22-E-04	0	40	4.00E-05	4.00	11	0.4980	0.011	0.7300	0.0848	1.5378	0.0878	7.9962	0.1663	3.7686	0.0730	4.10E-08
sp-22-E-07	0	40	4.06E-05	7.00	11	0.4962	0.011	0.6027	0.0710	1.2696	0.0702	6.3502	0.1342	3.0715	0.0597	3.18E-08
sp-22-E-08	0	40	4.07E-05	8.00	11	0.4947	0.011	0.6475	0.0767	1.4176	0.0811	6.6299	0.1407	3.4188	0.0672	3.22E-08
sp-22-E-09	0	40	4.01E-05	9.00	11	0.4939	0.011	0.6469	0.0756	1.4441	0.0818	6.8643	0.1437	3.4257	0.0664	3.43E-08
sp-22-E-12	0	40	3.96E-05	12.00	11	0.4923	0.011	0.6396	0.0740	1.4291	0.0800	6.6643	0.1382	3.3752	0.0648	3.23E-08
sp-22-E-14	0	40	3.97E-05	14.00	11	0.4903	0.011	0.6297	0.0732	1.4197	0.0797	6.6120	0.1377	3.3754	0.0651	3.25E-08
sp-22-E-16	0	40	4.12E-05	16.00	11	0.4887	0.011	0.6382	0.0771	1.4594	0.0857	6.8368	0.1480	3.4453	0.0691	3.57E-08
sp-22-E-17	0	40	4.13E-05	17.00	11	0.4875	0.011	0.6574	**0.0798**	1.5036	0.0894	7.4070	0.1613	3.5655	0.0721	4.10E-08
sp-22-E-20	0	40	4.07E-05	20.00	11	0.4859	0.011	0.6276	**0.0752**	1.4067	0.0813	6.9926	0.1504	3.2908	0.0654	3.78E-08
sp-22-E-21	0	40	4.08E-05	21.00	11	0.4843	0.011	0.5888	**0.0707**	1.3186	0.0752	6.4725	0.1396	3.1555	0.0627	3.47E-08
Exp. 30																
sp-22-F-BLK1	0	40			12			<DL		0.01		0.86		0.05		
sp-22-F-BLK2	0	40			12			<DL		0.32		0.79		0.27		
sp-22-F-BLK3	0	40			12			<DL		0.31		0.75		0.27		
sp-22-F-02	0	40	4.10E-05	2.00	12	0.5034	0.011	0.9977	0.1183	2.4062	0.1565	13.6144	0.2720	5.1481	0.1035	7.74E-08
sp-22-F-03	0	40	3.74E-05	3.00	12	0.5014	0.011	1.2793	0.1392	3.0031	0.1822	14.8633	0.2732	6.5439	0.1215	6.74E-08
sp-22-F-06	0	40	3.76E-05	6.00	12	0.4982	0.011	1.3623	0.1499	3.1756	0.1955	15.4862	0.2882	6.9625	0.1308	6.96E-08
sp-22-F-08	0	40	4.04E-05	8.00	12	0.4939	0.011	1.5058	0.1793	3.5768	0.2399	16.2400	0.3276	7.8121	0.1592	7.46E-08
sp-22-F-10	0	40	3.82E-05	10.00	12	0.4903	0.011	1.3926	0.1571	3.3059	0.2091	15.1764	0.2892	7.2078	0.1389	6.65E-08

Table A3. SPFT Results from Dissolution of Glass IDF21-EC14 at 40°C (cont.)

Sample ID	Inf [Si] ppm	T °C	Flow Rate, m^3/d	Time, days	pH 23°C	Glass Mass g	SA m^2	[B] ppm	B Rate $g\ m^{-2}\ d^{-1}$	[Al] ppm	Al Rate $g\ m^{-2}\ d^{-1}$	[Na] ppm	Na Rate $g\ m^{-2}\ d^{-1}$	[Si] ppm	Si Rate $g\ m^{-2}\ d^{-1}$	r_{IEX} mol $m^{-2}\ s^{-1}$
sp-22-F-12	0	40	3.90E-05	12.00	12	0.4869	0.011	1.3922	0.1613	3.2969	0.2142	15.7108	0.3081	7.2442	0.1435	7.39E-08
sp-22-F-14	0	40	3.90E-05	14.00	12	0.4834	0.011	1.4228	0.1657	3.3053	0.2159	16.3489	0.3229	7.3890	0.1472	7.91E-08
sp-22-F-16	0	40	4.03E-05	16.00	12	0.4800	0.011	1.3522	0.1634	3.1957	0.2161	15.5180	0.3172	7.0284	0.1451	7.74E-08
sp-22-F-18	0	40	3.98E-05	18.00	12	0.4765	0.010	1.3795	**0.1655**	3.2955	0.2217	15.6278	0.3172	7.1980	0.1476	7.64E-08
sp-22-F-20	0	40	3.95E-05	20.00	12	0.4732	0.010	1.2929	**0.1545**	3.1017	0.2072	15.5986	0.3157	6.6987	0.1367	8.11E-08
sp-22-F-21	0	40	3.95E-05	21.00	12	0.4708	0.010	1.3071	**0.1565**	3.1143	0.2085	15.8425	0.3215	6.7683	0.1384	8.30E-08
Exp. 31																
SP-22-G-BLK1	1	40			9			< -0.0009		< -0.0006		< 0.0016		0.98		
SP-22-G-BLK2	1	40			9			< -0.0004		< 0.0004		< 0.0048		0.96		
SP-22-G-BLK3	1	40			9			< -0.0005		< -0.0011		0.0104		0.98		
SP-22-G-02	1	40	1.93E-05	3.00	9	0.5015	0.011	0.1358	0.0069	0.1178	0.0036	2.3997	0.0239	1.4547	0.0047	8.54E-09
SP-22-G-04	1	40	1.94E-05	5.00	9	0.5013	0.011	0.1855	0.0098	0.2641	0.0086	2.5234	0.0253	1.8159	0.0084	7.80E-09
SP-22-G-06	1	40	1.93E-05	7.00	9	0.5010	0.011	0.2274	0.0121	0.0282	0.0006	2.4348	0.0242	1.9874	0.0100	6.10E-09
SP-22-G-08	1	40	1.92E-05	9.00	9	0.5008	0.011	0.2390	0.0128	0.3841	0.0126	2.5378	0.0252	2.2500	0.0126	6.28E-09
SP-22-G-10	1	40	1.92E-05	11.00	9	0.5005	0.011	0.2445	0.0131	0.3942	0.0129	2.2377	0.0222	2.2457	0.0125	4.60E-09
SP-22-G-12	1	40	1.92E-05	13.00	9	0.5002	0.011	0.2344	0.0125	0.3946	0.0129	1.9828	0.0196	2.2716	0.0128	3.60E-09
SP-22-G-14	1	40	1.91E-05	15.00	9	0.4999	0.011	0.2426	0.0129	0.4095	0.0134	2.1051	0.0208	2.3050	0.0130	3.97E-09
SP-22-G-16	1	40	1.98E-05	17.00	9	0.4997	0.011	0.2335	0.0128	0.1150	0.0036	1.8173	0.0185	2.1706	0.0121	2.88E-09
SP-22-G-18	1	40	2.01E-05	19.00	9	0.4994	0.011	0.2304	**0.0129**	0.1982	0.0066	1.7422	0.0181	2.2677	0.0134	2.63E-09
SP-22-G-20	1	40	1.98E-05	21.00	9	0.4991	0.011	0.2270	**0.0125**	0.3953	0.0134	1.6909	0.0173	2.3240	0.0137	2.43E-09
SP-22-G-22	1	40	2.00E-05	23.00	9	0.4988	0.011	0.2243	**0.0124**	0.1753	0.0058	1.5687	0.0162	2.2390	0.0130	1.89E-09
Exp. 32																
sp-22-H-BLK1	5	40			9			< -0.0009		< 0.0018		0.0191		4.84		
sp-22-H-BLK2	5	40			9			< -0.0006		< 0.0012		0.02		4.76		
sp-22-H-BLK3	5	40			9			< -0.0003		0.00		0.02		4.70		
SP-22-H-02	5	40	1.97E-05	3.00	9	0.4997	0.011	0.1719	0.0092	0.1271	0.0040	2.2642	0.0231	5.7843	0.0113	6.99E-09
SP-22-H-04	5	40	1.98E-05	5.00	9	0.4994	0.011	0.1901	0.0103	0.1035	0.0032	2.3762	0.0243	5.6131	0.0096	7.07E-09
SP-22-H-06	5	40	1.96E-05	7.00	9	0.4992	0.011	0.2197	0.0119	0.2715	0.0090	2.2979	0.0233	5.8719	0.0121	5.73E-09
SP-22-H-08	5	40	1.86E-05	9.00	9	0.4989	0.011	0.2415	0.0125	0.3028	0.0096	1.9679	0.0189	6.3524	0.0162	3.23E-09
SP-22-H-10	5	40	1.94E-05	11.00	9	0.4986	0.011	0.2272	0.0123	0.0264	0.0006	1.8648	0.0187	6.0448	0.0138	3.26E-09
SP-22-H-12	5	40	1.94E-05	13.00	9	0.4984	0.011	0.2245	0.0121	0.0639	0.0018	1.6591	0.0166	6.0018	0.0133	2.29E-09
SP-22-H-14	5	40	1.93E-05	15.00	9	0.4981	0.011	0.2202	0.0118	0.3061	0.0101	1.6729	0.0167	5.9834	0.0131	2.47E-09
SP-22-H-16	5	40	2.01E-05	17.00	9	0.4978	0.011	0.2208	0.0123	0.2640	0.0090	1.5105	0.0157	6.0277	0.0141	1.69E-09
SP-22-H-18	5	40	2.02E-05	19.00	9	0.4976	0.011	0.2094	**0.0117**	0.1327	0.0044	1.5630	0.0164	5.9396	0.0133	2.33E-09
SP-22-H-20	5	40	2.01E-05	21.00	9	0.4973	0.011	0.2068	**0.0115**	0.3137	0.0108	1.4472	0.0150	5.8629	0.0124	1.78E-09
SP-22-H-22	5	40	2.00E-05	23.00	9	0.4971	0.011	0.2101	**0.0116**	0.1256	0.0041	1.4311	0.0148	6.0834	0.0147	1.59E-09
Exp. 33																
sp-22-I-BLK1	15				9			< 0.0003		0.01		0.04		14.92		
sp-22-I-BLK2	15				9			0.00		0.01		0.04		14.43		
sp-22-I-BLK3	15				9			0.00		0.00		0.04		14.82		
SP-22-I-02	15	40	1.90E-05	3.00	9	0.9983	0.022	0.2577	0.0068	0.13	0.0021	4.4346	0.0218	15.4856	0.0037	7.51E-09
SP-22-I-04	15	40	1.91E-05	5.00	9	0.9979	0.022	0.2623	0.0070	0.05	0.0006	4.6919	0.0232	15.0725	0.0017	8.15E-09

Table A3. SPFT Results from Dissolution of Glass IDF21-EC14 at 40°C (cont.)

Sample ID	Inf [Si] ppm	T °C	Flow Rate, m^3/d	Time, days	pH 23°C	Glass Mass g	SA m^2	[B] ppm	B Rate $g\ m^{-2}\ d^{-1}$	[Al] ppm	Al Rate $g\ m^{-2}\ d^{-1}$	[Na] ppm	Na Rate $g\ m^{-2}\ d^{-1}$	[Si] ppm	Si Rate $g\ m^{-2}\ d^{-1}$	r_{IEX} $mol\ m^{-2}\ s^{-1}$
SP-22-I-06	15	40	1.91E-05	7.00	9	0.9976	0.022	0.2552	0.0068	0.22	0.0035	4.1286	0.0204	14.5998	-0.0006	6.82E-09
SP-22-I-08	15	40	1.67E-05	9.00	9	0.9973	0.022	0.2559	0.0060	0.23	0.0032	4.1036	0.0177	16.0051	0.0055	5.91E-09
SP-22-I-10	15	40	1.92E-05	11.00	9	0.9971	0.022	0.2164	0.0057	0.19	0.0030	3.5047	0.0174	22.686	0.0394	5.85E-09
SP-22-I-12	15	40	1.92E-05	13.00	9	0.9968	0.021	0.2063	0.0055	0.22	0.0036	3.2428	0.0161	15.3837	0.0033	5.34E-09
SP-22-I-14	15	40	1.92E-05	15.00	9	0.9966	0.021	0.1938	0.0051	0.22	0.0035	2.6627	0.0131	14.914	0.0009	4.04E-09
SP-22-I-16	15	40	2.00E-05	17.00	9	0.9964	0.021	0.1965	0.0054	0.22	0.0037	2.6740	0.0138	16.5211	0.0093	4.21E-09
SP-22-I-18	15	40	2.02E-05	19.00	9	0.9962	0.021	0.1862	**0.0051**	0.21	0.0036	2.3073	0.0119	16.0053	0.0067	3.42E-09
SP-22-I-20	15	40	2.01E-05	21.00	9	0.9959	0.021	0.1792	**0.0049**	0.23	0.0038	2.0797	0.0107	15.5629	0.0043	2.92E-09
SP-22-I-22	15	40	2.00E-05	23.00	9	0.9957	0.021	0.1849	**0.0051**	0.18	0.0030	2.0457	0.0105	16.361	0.0085	2.74E-09
Exp. 34																
sp-22-J-BLK1	30	40			9			0.00		0.01		0.07		19.33		
sp-22-J-BLK2	30	40			9			0.00		0.01		0.09		19.15		
sp-22-J-BLK3	30	40			9			0.00		0.01		0.11		19.89		
SP-22-J-02	30	40	1.91E-05	3.00	9	1.0028	0.022	0.2335	0.0062	0.1179	0.0017	4.9415	0.0242	34.4714	0.0180	9.05E-09
SP-22-J-04	30	40	1.92E-05	5.00	9	1.0025	0.022	0.2378	0.0063	0.1292	0.0019	4.7763	0.0235	33.1691	0.0116	8.61E-09
SP-22-J-06	30	40	1.91E-05	7.00	9	1.0022	0.022	0.2348	0.0062	0.1553	0.0024	4.5677	0.0223	32.3651	0.0076	8.08E-09
SP-22-J-08	30	40	1.90E-05	9.00	9	1.0019	0.022	0.2213	0.0058	0.1296	0.0019	4.2149	0.0205	34.5290	0.0182	7.37E-09
SP-22-J-10	30	40	1.90E-05	11.00	9	1.0017	0.022	0.1938	0.0050	0.1469	0.0022	3.6280	0.0175	32.5331	0.0084	6.28E-09
SP-22-J-12	30	40	1.90E-05	13.00	9	1.0015	0.022	0.1738	0.0045	0.1372	0.0021	3.4321	0.0165	33.4052	0.0127	6.07E-09
SP-22-J-14	30	40	1.90E-05	15.00	9	1.0013	0.022	0.1626	0.0042	0.1178	0.0017	2.9200	0.0140	34.8226	0.0196	4.95E-09
SP-22-J-16	30	40	1.97E-05	17.00	9	1.0011	0.022	0.1491	0.0039	0.1172	0.0018	2.7557	0.0137	35.2877	0.0227	4.92E-09
SP-22-J-18	30	40	1.99E-05	19.00	9	1.0010	0.022	0.1375	**0.0036**	0.1152	0.0018	2.3327	0.0116	34.0279	0.0164	4.02E-09
SP-22-J-20	30	40	1.97E-05	21.00	9	1.0008	0.022	0.1251	**0.0032**	0.1261	0.0019	2.3392	0.0116	33.6198	0.0143	4.19E-09
SP-22-J-22	30	40	1.94E-05	23.00	9	1.0007	0.022	0.1216	**0.0031**	0.0957	0.0014	2.0997	0.0101	34.1391	0.0166	3.56E-09
Exp. 35																
sp-22-K-BLK1	45	40			9			0.00		0.02		0.09		40.74		
sp-22-K-BLK2	45	40			9			0.01		0.02		0.09		40.60		
sp-22-K-BLK3	45	40			9			0.01		0.02		0.10		40.70		
SP-22-K-02	45	40	1.92E-05	3.00	9	1.9999	0.043	0.4485	0.0062	0.1078	0.0007	9.0197	0.0223	54.4886	0.0217	8.14E-09
SP-22-K-04	45	40	1.92E-05	5.00	9	1.9992	0.043	0.5368	0.0074	0.1779	0.0013	9.4270	0.0234	51.8155	0.0152	8.04E-09
SP-22-K-06	45	40	1.91E-05	7.00	9	1.9985	0.043	0.6861	0.0095	0.2020	0.0015	8.7036	0.0215	49.7328	0.0100	6.03E-09
SP-22-K-08	45	40	1.91E-05	9.00	9	1.9978	0.043	0.4663	0.0064	0.1948	0.0015	8.3329	0.0205	53.0716	0.0182	7.12E-09
SP-22-K-10	45	40	1.90E-05	11.00	9	1.9973	0.043	0.4202	0.0057	0.1476	0.0011	6.8696	0.0168	50.8811	0.0127	5.58E-09
SP-22-K-12	45	40	1.89E-05	13.00	9	1.9968	0.043	0.3715	0.0050	0.1610	0.0012	6.5078	0.0159	51.8029	0.0149	5.46E-09
SP-22-K-14	45	40	1.89E-05	15.00	9	1.9964	0.043	0.3714	0.0050	0.1483	0.0011	5.8872	0.0143	51.6744	0.0146	4.69E-09
SP-22-K-16	45	40	1.97E-05	17.00	9	1.9959	0.043	0.3404	0.0048	0.1160	0.0008	5.3197	0.0135	51.9746	0.0160	4.38E-09
SP-22-K-18	45	40	1.99E-05	19.00	9	1.9955	0.043	0.3155	**0.0044**	0.1369	0.0010	5.0198	0.0128	49.7572	0.0105	4.21E-09
SP-22-K-20	45	40	1.94E-05	21.00	9	1.9952	0.043	0.2981	**0.0041**	0.1320	0.0010	4.4678	0.0111	49.5064	0.0096	3.53E-09
SP-22-K-22	45	40	1.93E-05	23.00	9	1.9948	0.043	0.2968	**0.0040**	0.1219	0.0009	4.3690	0.0108	51.8582	0.0154	3.40E-09
Exp. 36																
sp-22-L-BLK1	60	40	-	-	9	-	-	0.01	-	0.02	-	0.10	-	60.86	-	-
sp-22-L-BLK2	60	40	-	-	9	-	-	0.01	-	0.02	-	0.10	-	60.07	-	-

Table A3. SPFT Results from Dissolution of Glass IDF21-EC14 at 40°C (cont.)

Sample ID	Inf [Si] ppm	T °C	Flow Rate, m^3/d	Time, days	pH 23°C	Glass Mass g	SA m^2	[B] ppm	B Rate $g\ m^{-2}\ d^{-1}$	[Al] ppm	Al Rate $g\ m^{-2}\ d^{-1}$	[Na] ppm	Na Rate $g\ m^{-2}\ d^{-1}$	[Si] ppm	Si Rate $g\ m^{-2}\ d^{-1}$	r_{IEX} $mol\ m^{-2}\ s^{-1}$
sp-22-L-BLK3	60	40			9			0.01		0.03		0.11		61.46		
SP-22-L-02	60	40	2.11E-05	3.00	9	2.0039	0.043	0.5030	0.0076	0.1570	0.0012	8.5976	0.0233	64.6486	0.0104	7.91E-09
SP-22-L-04	60	40	2.09E-05	5.00	9	2.0031	0.043	0.5299	0.0080	0.1576	0.0012	8.8750	0.0239	68.4699	0.0206	8.02E-09
SP-22-L-06	60	40	2.07E-05	7.00	9	2.0024	0.043	0.5248	0.0078	0.1400	0.0010	8.9156	0.0238	70.5814	0.0260	8.03E-09
SP-22-L-08	60	40	2.06E-05	9.00	9	2.0017	0.043	0.4858	0.0072	0.1543	0.0012	8.6972	0.0231	66.9911	0.0164	8.01E-09
SP-22-L-10	60	40	2.05E-05	11.00	9	2.0012	0.043	0.4396	0.0064	0.1324	0.0010	6.4726	0.0170	64.6375	0.0101	5.32E-09
SP-22-L-12	60	40	2.05E-05	13.00	9	2.0006	0.043	0.4239	0.0062	0.1230	0.0009	6.4429	0.0170	67.6323	0.0180	5.41E-09
SP-22-L-14	60	40	2.02E-05	15.00	9	2.0001	0.043	0.4191	0.0060	0.0990	0.0007	5.7031	0.0148	67.9521	0.0186	4.39E-09
SP-22-L-16	60	40	2.12E-05	17.00	9	1.9996	0.043	0.3717	0.0056	0.0878	0.0006	5.3490	0.0145	66.1602	0.0146	4.49E-09
SP-22-L-18	60	40	2.12E-05	19.00	9	1.9991	0.043	0.3512	**0.0053**	0.0825	0.0005	4.6640	0.0126	68.4232	0.0208	3.69E-09
SP-22-L-20	60	40	2.11E-05	21.00	9	1.9987	0.043	0.3337	**0.0050**	0.0910	0.0006	4.7425	0.0128	68.7584	0.0216	3.93E-09
SP-22-L-22	60	40	2.12E-05	23.00	9	1.9982	0.043	0.3346	**0.0050**	0.0899	0.0006	4.2310	0.0114	69.3338	0.0232	3.21E-09

***In bold: Samples used to calculate steady state dissolution rates.**

**** The r_{IEX} values listed are calculated based on the previous conventional formula without any correction. To obtain the corrected values, the listed values have to be multiplied by the correction factor of 0.24x46/62 = 0.178.**

Table A4. SPFT Results from Dissolution of Glass IDF21-EC14 at 23°C.

Sample ID	Inf [Si] ppm	T °C	Flow Rate, m^3/d	Time, days	pH 23°C	Glass Mass g	SA m^2	[B] ppm	B Rate $g\ m^{-2}\ d^{-1}$	[Al] ppm	Al Rate $g\ m^{-2}\ d^{-1}$	[Na] ppm	Na Rate $g\ m^{-2}\ d^{-1}$	[Si] ppm	Si Rate $g\ m^{-2}\ d^{-1}$	r_{IEX} $mol\ m^{-2}\ s^{-1}$
Exp. 37																
SP-23-A-BLK1	0	23			7			< -0.0027		< -0.0002		< -0.0282		< -0.0001		
SP-23-A-BLK2	0	23			7			< -0.0027		< -0.0013		< -0.0165		0.0092		
SP-23-A-BLK3	0	23			7			< -0.0026		< -0.0008		< -0.0333		< 0.0004		
SP-23-A-01	0	23	2.22E-05	2.00	7	1.0042	0.022	0.1749	0.0053	0.0095	0.0000680	2.5982	0.0149	0.1286	0.0007	4.85E-09
SP-23-A-02	0	23	1.05E-05	5.00	7	1.0040	0.022	0.1781	0.0025	0.0062	0.0000018	2.4734	0.0067	0.1178	0.0003	2.09E-09
SP-23-A-03	0	23	1.02E-05	8.00	7	1.0038	0.022	0.1988	0.0028	0.0087	0.0000242	2.6099	0.0069	0.1350	0.0003	2.07E-09
SP-23-A-04	0	23	1.04E-05	11.00	7	1.0036	0.022	0.1909	0.0027	0.0096	0.0000327	1.9716	0.0053	0.1266	0.0003	1.29E-09
SP-23-A-05	0	23	1.03E-05	14.00	7	1.0035	0.022	0.1837	0.0026	0.0099	0.0000353	1.9482	0.0052	0.1227	0.0003	1.31E-09
SP-23-A-06	0	23	1.03E-05	17.00	7	1.0033	0.022	0.1726	0.0024	0.0108	0.0000434	1.5538	0.0041	0.1196	0.0003	8.62E-10
SP-23-A-07	0	23	1.04E-05	20.00	7	1.0032	0.022	0.1598	0.0022	0.0104	0.0000398	1.4888	0.0040	0.1029	0.0002	8.73E-10
SP-23-A-08	0	23	1.04E-05	23.00	7	1.0030	0.022	0.1475	0.0020	0.0127	0.0000610	1.3686	0.0037	0.0979	0.0002	8.10E-10
SP-23-A-09	0	23	1.04E-05	26.00	7	1.0029	0.022	0.1383	0.0019	0.0120	0.0000548	1.1415	0.0030	0.0923	0.0002	5.73E-10
SP-23-A-10	0	23	1.05E-05	29.00	7	1.0028	0.022	0.1328	0.0018	0.0115	0.0000504	1.1914	0.0032	0.0900	0.0002	6.86E-10
SP-23-A-11	0	23	1.05E-05	32.00	7	1.0027	0.022	0.1269	**0.0017**	0.0110	0.0000458	0.9425	0.0025	0.0818	0.0002	3.91E-10
SP-23-A-12	0	23	1.05E-05	35.00	7	1.0025	0.022	0.1203	**0.0016**	0.0122	0.0000570	0.9778	0.0026	0.0810	0.0002	4.92E-10
SP-23-A-13	0	23	1.05E-05	38.00	7	1.0022	0.022	0.1156	**0.0016**	0.0129	0.0000633	0.9804	0.0026	0.0746	0.0002	5.31E-10
Exp. 38																
SP-23-B-BLK1	0	23			8			< -0.0018		< 0.0000		< -0.0218		< -0.0046		
SP-23-B-BLK2	0	23			8			< -0.0028		< -0.0004		< -0.0218		< 0.0055		
SP-23-B-BLK3	0	23			8			< -0.0041		< -0.0012		< -0.0293		< -0.0017		
SP-23-B-01	0	23	2.30E-05	2.00	8	1.0014	0.022	0.0999	0.0029	0.0315	0.0004	2.4386	0.0145	0.1105	0.0006	5.83E-09
SP-23-B-02	0	23	1.05E-05	5.00	8	1.0013	0.022	0.0944	0.0012	0.0389	0.0003	2.2444	0.0061	0.1384	0.0004	2.45E-09
SP-23-B-03	0	23	1.03E-05	8.00	8	1.0012	0.022	0.0958	0.0012	0.0500	0.0004	1.7117	0.0045	0.1748	0.0004	1.66E-09
SP-23-B-04	0	23	1.05E-05	11.00	8	1.0012	0.022	0.0861	0.0011	0.0503	0.0004	1.6633	0.0045	0.1786	0.0005	1.70E-09
SP-23-B-05	0	23	1.04E-05	14.00	8	1.0011	0.022	0.0786	0.0010	0.0513	0.0004	1.5374	0.0041	0.1800	0.0005	1.57E-09
SP-23-B-06	0	23	1.04E-05	17.00	8	1.0010	0.022	0.0689	0.0008	0.0504	0.0004	1.1264	0.0030	0.1789	0.0005	1.08E-09
SP-23-B-07	0	23	1.04E-05	20.00	8	1.0010	0.022	0.0604	0.0007	0.0502	0.0004	1.1280	0.0030	0.1677	0.0004	1.16E-09
SP-23-B-08	0	23	1.05E-05	23.00	8	1.0009	0.022	0.0556	0.0006	0.0483	0.0004	0.9223	0.0025	0.1589	0.0004	9.20E-10
SP-23-B-09	0	23	1.05E-05	26.00	8	1.0009	0.022	0.0514	0.0006	0.0467	0.0003	0.8425	0.0023	0.1586	0.0004	8.44E-10
SP-23-B-10	0	23	1.05E-05	29.00	8	1.0009	0.022	0.0471	0.0005	0.0465	0.0003	0.8426	0.0023	0.1535	0.0004	8.78E-10
SP-23-B-11	0	23	1.05E-05	32.00	8	1.0008	0.022	0.0433	**0.0005**	0.0448	0.0003	0.6700	0.0018	0.1489	0.0004	6.72E-10
SP-23-B-12	0	23	1.06E-05	35.00	8	1.0008	0.022	0.0417	**0.0004**	0.0438	0.0003	0.6763	0.0018	0.1462	0.0004	6.97E-10
SP-23-B-13	0	23	1.06E-05	38.00	8	1.0008	0.022	0.0378	**0.0004**	0.0434	0.0003	0.6928	0.0019	0.1433	0.0004	7.51E-10
Exp. 39																
SP-23-C-BLK1	0	23						< -0.0034		< -0.0015		< -0.0251		0.02		
SP-23-C-BLK2	0	23			9			< -0.0042		< -0.0010		< -0.0393		0.01		
SP-23-C-BLK3	0	23			9			< -0.0052		0.0194		< -0.0382		0.02		
SP-23-C-01	0	23	2.25E-05	2.00	9	1.0011	0.022	0.0809	0.0022	0.0460	0.0006	1.7278	0.0100	0.1658	0.0009	3.92E-09
SP-23-C-02	0	23	1.04E-05	5.00	9	1.0009	0.022	0.0658	0.0008	0.0725	0.0005	1.5572	0.0042	0.2356	0.0006	1.70E-09
SP-23-C-03	0	23	1.01E-05	8.00	9	1.0009	0.022	0.0768	0.0009	0.1119	0.0009	1.4188	0.0037	0.3595	0.0009	1.39E-09
SP-23-C-04	0	23	1.03E-05	11.00	9	1.0009	0.022	0.0739	0.0009	0.1159	0.0009	1.1753	0.0031	0.4020	0.0010	1.10E-09

Table A4. SPFT Results from Dissolution of Glass IDF21-EC14 at 23°C (cont.)

Sample ID	**Inf [Si]** ppm	**T °C**	**Flow Rate,** m^3/d	**Time,** days	**pH** 23°C	**Glass Mass** g	**SA** m^2	**[B]** ppm	**B Rate** $g\ m^{-2}\ d^{-1}$	**[Al]** ppm	**Al Rate** $g\ m^{-2}\ d^{-1}$	**[Na]** ppm	**Na Rate** $g\ m^{-2}\ d^{-1}$	**[Si]** ppm	**Si Rate** $g\ m^{-2}\ d^{-1}$	r_{IEX} $mol\ m^{-2}\ s^{-1}$
SP-23-C-05	0	23	1.03E-05	14.00	9	1.0008	0.022	0.0805	0.0010	0.1290	0.0010	1.0966	0.0029	0.4694	0.0012	9.44E-10
SP-23-C-06	0	23	1.02E-05	17.00	9	1.0007	0.022	0.0849	0.0011	0.1404	0.0011	0.9199	0.0024	0.5144	0.0013	6.70E-10
SP-23-C-07	0	23	1.02E-05	20.00	9	1.0007	0.022	0.0827	0.0010	0.1496	0.0012	0.8848	0.0023	0.5383	0.0014	6.41E-10
SP-23-C-08	0	23	1.03E-05	23.00	9	1.0006	0.022	0.0868	0.0011	0.1580	0.0013	0.8907	0.0023	0.5735	0.0015	6.24E-10
SP-23-C-09	0	23	1.04E-05	26.00	9	1.0005	0.022	0.0906	0.0012	0.1647	0.0014	0.7394	0.0019	0.6002	0.0016	3.91E-10
SP-23-C-10	0	23	1.04E-05	29.00	9	1.0004	0.022	0.0954	0.0012	0.1705	0.0014	0.7516	0.0020	0.6176	0.0016	3.71E-10
SP-23-C-11	0	23	1.04E-05	32.00	9	1.0004	0.022	0.0992	**0.0013**	0.1743	0.0015	0.7629	0.0020	0.6463	0.0017	3.58E-10
SP-23-C-12	0	23	1.05E-05	35.00	9	1.0003	0.022	0.0986	**0.0013**	0.0999	0.0008	0.6289	0.0017	0.6545	0.0017	1.81E-10
sp-22-C-23	0	23	1.05E-05	38.00	9	1.0003	0.022	0.0983	**0.0013**	0.1850	0.0016	0.7184	0.0019	0.6711	0.0018	3.06E-10
Exp. 40																
SP-23-D-BLK1	0	23						< -0.0050		< -0.0020		< -0.0436		< 0.0000		
SP-23-D-BLK2	0	23						< -0.0048		< -0.0018		< -0.0391		< 0.0003		
SP-23-D-BLK3	0	23			10			< -0.0050		< -0.0021		< -0.0340		< 0.0062		
SP-23-D-01	0	23	2.15E-05	2.00	10	0.5002	0.011	0.0443	0.0019	0.0367	0.0010	0.7971	0.0087	0.1215	0.0012	3.43E-09
SP-23-D-02	0	23	9.96E-06	5.00	10	0.5001	0.011	0.0481	0.0010	0.0788	0.0012	0.6236	0.0031	0.2529	0.0013	1.08E-09
SP-23-D-03	0	23	9.73E-06	8.00	10	0.5001	0.011	0.1090	0.0027	0.2054	0.0033	0.8770	0.0044	0.6711	0.0033	8.19E-10
SP-23-D-04	0	23	9.90E-06	11.00	10	0.5000	0.011	0.1681	0.0045	0.3043	0.0051	0.9047	0.0046	1.0299	0.0052	3.55E-11
SP-23-D-05	0	23	9.86E-06	14.00	10	0.4998	0.011	0.2048	0.0056	0.3624	0.0061	1.1492	0.0058	1.2347	0.0062	1.30E-10
SP-23-D-06	0	23	9.80E-06	17.00	10	0.4996	0.011	0.2259	0.0061	0.0414	0.0005	1.1156	0.0056	1.2707	0.0064	-2.65E-10
SP-23-D-07	0	23	9.85E-06	20.00	10	0.4994	0.011	0.2321	0.0064	0.4070	0.0069	1.2819	0.0065	1.3792	0.0070	7.31E-11
SP-23-D-08	0	23	9.98E-06	23.00	10	0.4992	0.011	0.2367	0.0066	0.4092	0.0070	1.1593	0.0059	1.3986	0.0071	-3.16E-10
SP-23-D-09	0	23	1.00E-05	26.00	10	0.4990	0.011	0.2356	0.0066	0.1359	0.0022	1.2641	0.0065	1.3288	0.0068	-2.47E-11
SP-23-D-10	0	23	1.00E-05	29.00	10	0.4988	0.011	0.2367	0.0066	0.4382	0.0075	1.2258	0.0063	1.3931	0.0071	-1.42E-10
SP-23-D-11	0	23	1.01E-05	32.00	10	0.4986	0.011	0.2366	**0.0066**	0.4039	0.0070	1.2081	0.0063	1.4002	0.0072	-1.88E-10
SP-23-D-12	0	23	1.01E-05	35.00	10	0.4984	0.011	0.2377	**0.0067**	0.1539	0.0025	1.2680	0.0066	1.3245	0.0068	-4.61E-11
SP-23-D-13	0	23	1.01E-05	38.00	10	0.4983	0.011	0.2390	**0.0067**	0.1644	0.0027	1.1978	0.0062	1.3439	0.0070	-2.53E-10
Exp. 41																
SP-23-E-BLK1	0	23			11			< -0.0015		0.0012		0.05		0.0291		
SP-23-E-BLK2	0	23			11			< -0.0022		0.16		0.03		0.18		
SP-23-E-BLK3	0	23			11			< -0.0013		0.00		0.05		0.03		
SP-23-E-01	0	23	2.31E-05	2.00	11	0.5025	0.011	0.1517	0.0094	0.4628	0.0163	3.3206	0.0393	0.9671	0.0105	1.51E-08
SP-23-E-02	0	23	1.07E-05	5.00	11	0.5022	0.011	0.3707	0.0112	0.9290	0.0163	4.9683	0.0274	2.0691	0.0109	8.14E-09
SP-23-E-03	0	23	1.05E-05	8.00	11	0.5018	0.011	0.5640	0.0169	1.3140	0.0230	6.7249	0.0363	2.9881	0.0156	9.75E-09
SP-23-E-04	0	23	1.07E-05	11.00	11	0.5012	0.011	0.6252	0.0192	1.4360	0.0257	7.8131	0.0431	3.2418	0.0173	1.20E-08
SP-23-E-05	0	23	1.06E-05	14.00	11	0.5005	0.011	0.6556	0.0200	1.5010	0.0267	7.0401	0.0386	3.3566	0.0178	9.33E-09
SP-23-E-06	0	23	1.05E-05	17.00	11	0.4999	0.011	0.6715	0.0204	1.6109	0.0286	8.1205	0.0442	3.4391	0.0181	1.20E-08
SP-23-E-07	0	23	1.06E-05	20.00	11	0.4992	0.011	0.6672	0.0204	1.5382	0.0275	7.0291	0.0386	3.3945	0.0180	9.13E-09
SP-23-E-08	0	23	1.07E-05	23.00	11	0.4986	0.011	0.6490	0.0200	1.5184	0.0274	7.8679	0.0436	3.3156	0.0178	1.19E-08
SP-23-E-09	0	23	1.06E-05	26.00	11	0.4979	0.011	0.6367	0.0196	1.5070	0.0270	7.0128	0.0387	3.2706	0.0175	9.61E-09
SP-23-E-10	0	23	1.06E-05	29.00	11	0.4973	0.011	0.6377	0.0196	1.5160	0.0272	7.3064	0.0403	3.2302	0.0172	1.04E-08
SP-23-E-11	0	23	1.07E-05	32.00	11	0.4967	0.011	0.6421	**0.0199**	1.5530	0.0281	7.9433	0.0442	3.3127	0.0178	1.22E-08
SP-23-E-12	0	23	1.07E-05	35.00	11	0.4960	0.011	0.6417	**0.0199**	1.5521	0.0281	7.1349	0.0396	3.3131	0.0178	9.95E-09

Table A4. SPFT Results from Dissolution of Glass IDF21-EC14 at 23°C (cont.)

Sample ID	**Inf [Si]** ppm	**T °C**	**Flow Rate,** m^3/d	**Time,** days	**pH** 23°C	**Glass Mass** g	**SA** m^2	**[B]** ppm	**B Rate** $g\ m^{-2}\ d^{-1}$	**[Al]** ppm	**Al Rate** $g\ m^{-2}\ d^{-1}$	**[Na]** ppm	**Na Rate** $g\ m^{-2}\ d^{-1}$	**[Si]** ppm	**Si Rate** $g\ m^{-2}\ d^{-1}$	r_{IEX} $mol\ m^{-2}\ s^{-1}$
SP-23-E-13	0	23	1.07E-05	38.00	11	0.4954	0.011	0.6212	**0.0194**	1.5296	0.0278	7.8559	0.0440	3.1975	0.0173	1.24E-08
Exp. 42																
SP-23-F-BLK1	0	23			12			< 0.0010		0.00		0.95		0.04		
SP-23-F-BLK2	0	23			12			< 0.0010		0.08		0.85		0.12		
SP-23-F-BLK3	0	23			12			< 0.0016		0.00		0.96		0.04		
SP-23-F-01	0	23	2.23E-05	2.00	12	0.5002	0.011	0.4811	0.0308	1.3454	0.0513	8.3318	0.0862	2.7336	0.0306	2.79E-08
SP-23-F-02	0	23	1.05E-05	5.00	12	0.4994	0.011	0.9273	0.0284	2.3930	0.0435	12.0659	0.0611	4.9857	0.0266	1.65E-08
SP-23-F-03	0	23	1.02E-05	8.00	12	0.4983	0.011	1.3726	0.0409	3.4674	0.0614	18.7284	0.0947	7.1713	0.0373	2.71E-08
SP-23-F-04	0	23	1.03E-05	11.00	12	0.4969	0.011	1.4905	0.0452	3.7455	0.0675	17.7412	0.0909	7.8498	0.0415	2.30E-08
SP-23-F-05	0	23	1.03E-05	14.00	12	0.4954	0.011	1.5406	0.0466	3.8671	0.0694	20.2249	0.1040	8.0106	0.0422	2.89E-08
SP-23-F-06	0	23	1.02E-05	17.00	12	0.4939	0.011	1.5626	0.0470	3.8975	0.0696	19.4418	0.0992	8.1416	0.0426	2.63E-08
SP-23-F-07	0	23	1.02E-05	20.00	12	0.4924	0.011	1.5554	0.0469	3.8896	0.0696	19.3039	0.0986	8.0790	0.0424	2.61E-08
SP-23-F-08	0	23	1.02E-05	23.00	12	0.4909	0.011	1.5332	0.0464	3.8305	0.0689	21.2257	0.1096	7.8884	0.0416	3.18E-08
SP-23-F-09	0	23	1.02E-05	26.00	12	0.4894	0.011	1.5343	0.0466	3.8305	0.0691	18.3787	0.0945	7.9127	0.0419	2.41E-08
SP-23-F-10	0	23	1.02E-05	29.00	12	0.4879	0.011	1.5255	0.0463	3.8296	0.0691	20.1818	0.1042	7.9500	0.0421	2.91E-08
SP-23-F-11	0	23	1.02E-05	32.00	12	0.4865	0.011	1.5184	**0.0461**	3.8299	0.0691	18.3247	0.0942	7.9219	0.0419	2.42E-08
SP-23-F-12	0	23	1.02E-05	35.00	12	0.4850	0.011	1.5031	**0.0458**	3.7675	0.0682	19.9843	0.1035	7.7969	0.0414	2.90E-08
SP-23-F-13	0	23	1.02E-05	38.00	12	0.4850	0.011	1.5060	**0.0458**	3.7598	0.0678	17.8132	0.0914	7.8124	0.0413	2.30E-08
Exp. 43																
SP-23-G-BLK1	1	23			9			<DL		<DL		<DL		1.05		
SP-23-G-BLK2	1	23			9			<DL		<DL		<DL		1.06		
SP-23-G-BLK3	1	23			9			<DL		<DL		<DL		1.07		
SP-23-G-01	1	23	2.16E-05	2.00	9	4.0032	0.086	0.3596	2.7549E-03	0.1115	0.0005	6.4960	0.0091	1.6406	0.0008	3.20E-09
SP-23-G-02	1	23	1.06E-05	5.00	9	4.0028	0.086	0.2669	9.8498E-04	0.0425	0.0001	4.7868	0.0033	1.7060	0.0004	1.15E-09
SP-23-G-03	1	23	9.88E-06	8.00	9	4.0026	0.086	0.2584	8.9085E-04	0.2297	0.0005	4.9814	0.0032	1.9143	0.0005	1.16E-09
SP-23-G-04	1	23	9.99E-06	11.00	9	4.0023	0.086	0.2380	8.2598E-04	0.0112	0.0000	3.8542	0.0025	1.9340	0.0006	8.42E-10
SP-23-G-05	1	23	9.98E-06	14.00	9	4.0021	0.086	0.2184	7.5258E-04	0.2506	0.0005	3.3308	0.0022	2.0800	0.0007	7.05E-10
SP-23-G-06	1	23	9.95E-06	17.00	9	4.0019	0.086	0.1977	6.7436E-04	0.2526	0.0005	3.1533	0.0020	2.0956	0.0007	6.84E-10
SP-23-G-07	1	23	9.92E-06	20.00	9	4.0018	0.086	0.1813	6.1233E-04	0.2581	0.0005	2.6766	0.0017	2.0318	0.0006	5.57E-10
SP-23-G-08	1	23	9.98E-06	23.00	9	4.0016	0.086	0.1730	5.8531E-04	0.2525	0.0005	2.2966	0.0015	2.0566	0.0006	4.51E-10
SP-23-G-09	1	23	1.00E-05	26.00	9	4.0015	0.086	0.1691	5.7260E-04	0.0297	0.0000	2.3380	0.0015	2.0385	0.0006	4.73E-10
SP-23-G-10	1	23	9.98E-06	29.00	9	4.0013	0.086	0.1717	5.8055E-04	0.2665	0.0006	1.9700	0.0013	2.1332	0.0007	3.47E-10
SP-23-G-11	1	23	9.99E-06	32.00	9	4.0012	0.086	0.1716	**5.8103E-04**	0.2649	0.0006	2.0552	0.0013	2.1626	0.0007	3.75E-10
SP-23-G-12	1	23	1.00E-05	35.00	9	4.0010	0.086	0.1755	**5.9716E-04**	0.1021	0.0002	1.8372	0.0012	2.1745	0.0007	2.97E-10
SP-23-G-13	1	23	9.99E-06	38.00	9	4.0009	0.086	0.1775	**6.0284E-04**	0.2757	0.0006	1.7400	0.0011	2.2513	0.0008	2.61E-10
Exp. 44																
sp-23-H-BLK1	15	23			9			< DL		< DL		< DL		4.84		
sp-23-H-BLK2	15	23			9			< DL		< DL		< DL		4.76		
sp-23-H-BLK3	15	23			9			< DL		< DL		< DL		4.70		
SP-23-H-01	15	23	2.13E-05	2.00	9	4.0005	0.086	0.3132	2.3514E-03	0.0686	0.000273	7.5775	0.0105	16.8539	0.0031	4.09E-09
SP-23-H-02	15	23	1.04E-05	5.00	9	4.0002	0.086	0.2603	9.4810E-04	0.1102	0.000229	5.7180	0.0039	16.8756	0.0016	1.47E-09
SP-23-H-03	15	23	9.73E-06	8.00	9	3.9999	0.086	0.2481	8.4139E-04	0.1279	0.000252	5.4021	0.0034	17.6111	0.0019	1.29E-09

Table A4. SPFT Results from Dissolution of Glass IDF21-EC14 at 23°C (cont.)

Sample ID	Inf [Si] ppm	T °C	Flow Rate, m^3/d	Time, days	pH 23°C	Glass Mass g	SA m^2	[B] ppm	B Rate $g\ m^{-2}\ d^{-1}$	[Al] ppm	Al Rate $g\ m^{-2}\ d^{-1}$	[Na] ppm	Na Rate $g\ m^{-2}\ d^{-1}$	[Si] ppm	Si Rate $g\ m^{-2}\ d^{-1}$	r_{IEX} mol $m^{-2}\ s^{-1}$
SP-23-H-04	15	23	9.84E-06	11.00	9	3.9997	0.086	0.2213	7.5272E-04	0.1228	0.000243	4.6583	0.0030	17.0479	0.0016	1.12E-09
SP-23-H-05	15	23	9.85E-06	14.00	9	3.9996	0.086	0.1947	6.5702E-04	0.1178	0.000233	4.4428	0.0028	17.4704	0.0018	1.10E-09
SP-23-H-06	15	23	9.84E-06	17.00	9	3.9994	0.086	0.1734	5.7866E-04	0.1141	0.000224	3.3715	0.0021	17.6038	0.0019	7.89E-10
SP-23-H-07	15	23	9.76E-06	20.00	9	3.9993	0.086	0.1528	5.0011E-04	0.0054	-0.000010	3.3247	0.0021	17.2105	0.0017	8.06E-10
SP-23-H-08	15	23	9.79E-06	23.00	9	3.9991	0.086	0.1423	4.6359E-04	0.1104	0.000215	3.0670	0.0019	17.5590	0.0019	7.44E-10
SP-23-H-09	15	23	9.81E-06	26.00	9	3.9990	0.086	0.1250	4.0158E-04	0.1072	0.000209	2.3224	0.0015	17.4866	0.0018	5.37E-10
SP-23-H-10	15	23	9.81E-06	29.00	9	3.9989	0.086	0.1171	**3.7296E-04**	0.0514	0.000089	2.4544	0.0016	17.1789	0.0017	5.94E-10
SP-23-H-11	15	23	9.78E-06	32.00	9	3.9988	0.086	0.1071	**3.3573E-04**	0.1035	0.000200	2.0306	0.0013	17.1718	0.0016	4.75E-10
SP-23-H-12	15	23	9.81E-06	35.00	10	3.9987	0.086	0.1001	**3.1135E-04**	0.0095	-0.000001	2.2054	0.0014	17.3478	0.0018	5.45E-10
SP-23-H-13	15	23	9.78E-06	38.00	11	3.9987	0.086	0.0956	2.9418E-04	0.0991	0.000191	1.8133	0.0011	17.7103	0.0020	4.26E-10
Exp. 45																
sp-23-I-BLK1	22.5				9			< DL		< DL		0.03		24.27		
sp-23-I-BLK2	22.5				9			< DL		< DL		0.05		24.27		
sp-23-I-BLK3	22.5				9			< DL		< DL		0.04		24.27		
SP-23-I-01	22.5	23	2.16E-05	2.00	9	4.0001	0.054	0.3238	0.0039	0.08	0.0005	6.8674	0.0153	24.4729	0.0004	5.72E-09
SP-23-I-02	22.5	23	1.06E-05	5.00	9	3.9998	0.054	0.2543	0.0015	0.11	0.0004	5.7757	0.0063	24.8201	0.0006	2.43E-09
SP-23-I-03	22.5	23	9.99E-06	8.00	9	3.9995	0.054	0.2461	0.0014	0.12	0.0004	5.0036	0.0051	25.2187	0.0010	1.90E-09
SP-23-I-04	22.5	23	1.01E-05	11.00	9	3.9993	0.054	0.2151	0.0012	0.09	0.0003	4.7638	0.0050	24.8374	0.0006	1.89E-09
SP-23-I-05	22.5	23	1.01E-05	14.00	9	3.9991	0.054	0.1849	0.0010	0.05	0.0001	3.7689	0.0039	24.7378	0.0005	1.46E-09
SP-23-I-06	22.5	23	1.01E-05	17.00	9	3.9990	0.054	0.1605	0.0009	0.04	0.0001	3.5649	0.0037	25.0788	0.0008	1.42E-09
SP-23-I-07	22.5	23	1.01E-05	20.00	9	3.9988	0.054	0.1442	0.0008	0.10	0.0003	2.7284	0.0028	24.8786	0.0006	1.02E-09
SP-23-I-08	22.5	23	1.01E-05	23.00	9	3.9987	0.054	0.1247	0.0007	0.10	0.0003	2.6695	0.0028	24.8283	0.0006	1.06E-09
SP-23-I-09	22.5	23	1.01E-05	26.00	9	3.9986	0.054	0.1145	0.0006	0.09	0.0003	2.1877	0.0023	24.9419	0.0007	8.35E-10
SP-23-I-10	22.5	23	1.01E-05	29.00	9	3.9985	0.054	0.1064	0.0005	0.09	0.0003	2.1435	0.0022	25.178	0.0009	8.35E-10
SP-23-I-11	22.5	23	1.01E-05	32.00	9	3.9984	0.054	0.0992	**0.0005**	0.08	0.0003	1.8599	0.0019	24.8772	0.0006	7.07E-10
SP-23-I-12	22.5	23	1.02E-05	35.00	9	3.9984	0.054	0.0904	**0.0005**	0.03	0.0001	1.9522	0.0020	24.7136	0.0005	7.84E-10
SP-23-I-13	22.5	23	1.01E-05	38.00	9	3.9983	0.054	0.0870	**0.0004**	0.08	0.0003	1.6227	0.0017	25.1391	0.0009	6.18E-10
Exp. 46																
sp-23-J-BLK1	30	23			9			< DL		< DL		0.07		19.33		
sp-23-J-BLK2	30	23			9			< DL		< DL		0.09		19.15		
sp-23-J-BLK3	30	23			9			< DL		< DL		0.11		19.89		
SP-23-J-01	30	23	2.12E-05	2.00	9	3.9989	0.054	0.3132	0.0037	0.0964	0.0006	7.0915	0.0155	34.6997	0.0032	5.91E-09
SP-23-J-02	30	23	1.04E-05	5.00	9	3.9985	0.054	0.2454	0.0014	0.1076	0.0004	5.4329	0.0058	33.9069	0.0007	2.21E-09
SP-23-J-03	30	23	9.73E-06	8.00	9	3.9984	0.054	0.2268	0.0012	0.1098	0.0003	5.5335	0.0055	34.3391	0.0011	2.17E-09
SP-23-J-04	30	23	9.89E-06	11.00	9	3.9982	0.054	0.1949	0.0010	0.1021	0.0003	4.4038	0.0045	34.1336	0.0009	1.72E-09
SP-23-J-05	30	23	9.84E-06	14.00	9	3.9980	0.054	0.1719	0.0009	0.0560	0.0002	3.8319	0.0039	34.7243	0.0015	1.48E-09
SP-23-J-06	30	23	9.79E-06	17.00	9	3.9979	0.054	0.1511	0.0008	0.0260	0.0001	3.4255	0.0034	34.7993	0.0016	1.33E-09
SP-23-J-07	30	23	9.79E-06	20.00	9	3.9978	0.054	0.1289	0.0007	0.0843	0.0003	2.8887	0.0029	34.8232	0.0016	1.12E-09
SP-23-J-08	30	23	9.81E-06	23.00	9	3.9977	0.054	0.1140	0.0006	0.0737	0.0002	2.7651	0.0028	34.9520	0.0018	1.10E-09
SP-23-J-09	30	23	9.81E-06	26.00	9	3.9976	0.054	0.1018	**0.0005**	0.0714	0.0002	2.5184	0.0025	34.8378	0.0016	1.01E-09
SP-23-J-10	30	23	9.79E-06	29.00	9	3.9975	0.054	0.0942	**0.0005**	0.0685	0.0002	2.3577	0.0023	34.5477	0.0013	9.45E-10
SP-23-J-11	30	23	9.75E-06	32.00	9	3.9974	0.054	0.0870	**0.0004**	0.0647	0.0002	1.9228	0.0019	34.9117	0.0017	7.41E-10

Table A4. SPFT Results from Dissolution of Glass IDF21-EC14 at 23°C (cont.)

Sample ID	Inf [Si] ppm	T °C	Flow Rate, m^3/d	Time, days	pH 23°C	Glass Mass g	SA m^2	[B] ppm	B Rate $g\ m^{-2}\ d^{-1}$	[Al] ppm	Al Rate $g\ m^{-2}\ d^{-1}$	[Na] ppm	Na Rate $g\ m^{-2}\ d^{-1}$	[Si] ppm	Si Rate $g\ m^{-2}\ d^{-1}$	r_{IEX} $mol\ m^{-2}\ s^{-1}$
SP-23-J-12	30	23	9.79E-06	35.00	9	3.9974	0.054	0.0815	0.0004	0.0258	0.0001	2.0308	0.0020	34.9491	0.0017	8.15E-10
SP-23-J-13	30	23	9.76E-06	38.00	9	3.9973	0.054	0.0753	0.0004	0.0654	0.0002	1.6774	0.0016	35.3358	0.0021	6.51E-10
Exp. 47																
sp-23-K-BLK1	45	23			9			< DL		0.02		0.06		50.58		
sp-23-K-BLK2	45	23			9			< DL		0.02		0.06		45.21		
sp-23-K-BLK3	45	23			9			< DL		0.02		0.07		52.52		
SP-23-K-01	45	23	2.11E-05	2.00	9	3.9995	0.068	0.3448	0.0032	0.0962	0.0005	6.5042	0.0112	51.6834	0.0038	3.98E-09
SP-23-K-02	45	23	1.04E-05	5.00	9	3.9991	0.068	0.2648	0.0012	0.1087	0.0003	5.5513	0.0047	50.2932	0.0007	1.74E-09
SP-23-K-03	45	23	9.66E-06	8.00	9	3.9989	0.068	0.2455	0.0010	0.0989	0.0002	5.1335	0.0040	51.8023	0.0018	1.50E-09
SP-23-K-04	45	23	9.73E-06	11.00	9	3.9987	0.068	0.2105	0.0009	0.0884	0.0002	4.7408	0.0037	50.6403	0.0009	1.43E-09
SP-23-K-05	45	23	9.69E-06	14.00	9	3.9985	0.068	0.1888	0.0008	0.0748	0.0002	3.8176	0.0030	50.5256	0.0009	1.11E-09
SP-23-K-07	45	23	9.72E-06	20.00	9	3.9983	0.068	0.1442	0.0006	0.0736	0.0002	3.0938	0.0024	50.1624	0.0006	9.21E-10
SP-23-K-08	45	23	9.66E-06	23.00	9	3.9982	0.068	0.1245	0.0005	0.0621	0.0001	2.7030	0.0021	50.2879	0.0007	8.04E-10
SP-23-K-09	45	23	9.71E-06	26.00	9	3.9981	0.068	0.1137	0.0004	0.0565	0.0001	2.3636	0.0018	50.9296	0.0012	6.96E-10
SP-23-K-10	45	23	9.71E-06	29.00	9	3.9980	0.068	0.1062	0.0004	0.0536	0.0001	2.3595	0.0018	50.5077	0.0008	7.12E-10
SP-23-K-11	45	23	9.68E-06	32.00	9	3.9979	0.068	0.1003	**0.0004**	0.0520	0.0001	1.9900	0.0015	50.7538	0.0010	5.75E-10
SP-23-K-12	45	23	9.66E-06	35.00	9	3.9978	0.068	0.0928	**0.0004**	0.0504	0.0001	1.9910	0.0015	50.2099	0.0006	5.92E-10
SP-23-K-13	45	23	9.71E-06	38.00	9	3.9977	0.068	0.0869	**0.0003**	0.0490	0.0001	1.7342	0.0013	50.6986	0.0010	5.05E-10
Exp. 48																
sp-23-L-BLK1	52.5	23			9			< DL		0.03		0.08		55.10		
sp-23-L-BLK2	52.5	23			9			< DL		0.02		0.07		55.10		
sp-23-L-BLK3	52.5	23			9			< DL		0.02		0.09		55.10		
SP-23-L-01	52.5	23	2.21E-05	2.00	9	4.0016	0.068	0.3422	0.0034	0.0995	0.0005	6.4432	0.0115	56.0618	0.0017	4.11E-09
SP-23-L-02	52.5	23	1.12E-05	5.00	9	4.0012	0.068	0.2338	0.0011	0.0916	0.0002	5.4161	0.0049	56.4305	0.0012	1.89E-09
SP-23-L-03	52.5	23	1.04E-05	8.00	9	4.0010	0.068	0.2213	0.0010	0.0689	0.0001	4.6518	0.0039	55.4664	0.0003	1.47E-09
SP-23-L-04	52.5	23	1.06E-05	11.00	9	4.0008	0.068	0.1889	0.0009	0.0628	0.0001	4.0656	0.0035	55.4225	0.0003	1.31E-09
SP-23-L-05	52.5	23	1.06E-05	14.00	9	4.0006	0.068	0.1656	0.0007	0.0505	0.0001	3.3111	0.0028	56.1251	0.0009	1.04E-09
SP-23-L-06	52.5	23	1.05E-05	17.00	9	4.0005	0.068	0.1434	0.0006	0.0576	0.0001	2.9430	0.0025	56.8365	0.0015	9.29E-10
SP-23-L-07	52.5	23	1.05E-05	20.00	9	4.0004	0.068	0.1281	0.0006	0.0645	0.0001	2.4318	0.0020	56.0622	0.0008	7.39E-10
SP-23-L-08	52.5	23	1.06E-05	23.00	9	4.0003	0.068	0.1145	0.0005	0.0376	0.0000	2.3291	0.0020	56.5825	0.0013	7.34E-10
SP-23-L-09	52.5	23	1.06E-05	26.00	9	4.0002	0.068	0.1039	0.0004	0.0409	0.0001	2.1559	0.0018	56.9652	0.0016	6.87E-10
SP-23-L-10	52.5	23	1.06E-05	29.00	9	4.0001	0.068	0.0974	0.0004	0.0387	0.0001	1.9109	0.0016	56.9121	0.0016	5.94E-10
SP-23-L-11	52.5	23	1.06E-05	32.00	9	4.0000	0.068	0.0905	**0.0004**	0.0368	0.0000	1.7985	0.0015	56.9689	0.0016	5.62E-10
SP-23-L-12	52.5	23	1.06E-05	35.00	9	3.9999	0.068	0.0849	**0.0003**	0.0348	0.0000	1.7180	0.0014	57.4039	0.0020	5.43E-10
SP-23-L-13	52.5	23	1.06E-05	38.00	9	3.9999	0.068	0.0809	**0.0003**	0.0346	0.0000	1.4649	0.0012	57.4053	0.0020	4.43E-10

***In bold: Samples used to calculate steady state dissolution rates.**

**** The r_{IEX} values listed are calculated based on the previous conventional formula without any correction. To obtain the corrected values, the listed values have to be multiplied by the correction factor of 0.24x46/62 = 0.178.**

Table A5. Additional Analysis of Select SPFT Samples-All Temperatures.

Sample ID	Inf [Si] ppm	T °C	Flow Rate, m^3/d	Time, days	pH 23°C	Glass Mass g	SA m^2	[Re] ppm	Re Rate $g\ m^{-2}\ d^{-1}$	$r_{IEX\ [Re]}$ * mol $m^{-2}\ s^{-1}$
Exp. 7										
sp-20-G-BLK1	1	90	-	-	9	-	-	<DL	-	-
sp-20-G-BLK2	1	90	-	-	9	-	-	<DL	-	-
sp-20-G-BLK3	1	90	-	-	9	-	-	<DL	-	-
sp-20-G-02	1	90	6.75E-05	1.00	9	0.5000	0.011	0.0267	0.2863	1.20E-07
sp-20-G-04	1	90	6.62E-05	2.00	9	0.4957	0.011	0.0230	0.2400	9.63E-08
sp-20-G-06	1	90	6.54E-05	3.00	9	0.4934	0.011	0.0210	0.2149	5.73E-08
sp-20-G-08	1	90	6.78E-05	4.00	9	0.4915	0.011	0.0206	0.2188	2.89E-08
sp-20-G-10	1	90	6.85E-05	5.00	9	0.4903	0.011	0.0212	0.2285	-1.56E-09
sp-20-G-12	1	90	6.83E-05	6.00	9	0.4893	0.011	0.0136	0.1375	3.25E-08
sp-20-G-15	1	90	6.72E-05	7.00	9	0.4884	0.011	0.0135	0.1343	2.52E-08
sp-20-G-16	1	90	6.80E-05	8.00	9	0.4874	0.011	0.0137	0.1384	2.03E-08
sp-20-G-18	1	90	6.86E-05	9.00	9	0.4864	0.011	0.0130	0.1313	2.15E-08
sp-20-G-20	1	90	6.56E-05	10.00	9	0.4854	0.011	0.0133	0.1293	1.44E-08
sp-20-G-22	1	90	6.71E-05	11.00	9	0.4843	0.011	0.0120	0.1170	3.19E-08
Exp. 8										
sp-20-H-BLK1	5	90	-	-	9	-	-	<DL	-	-
sp-20-H-BLK2	5	90	-	-	9	-	-	<DL	-	-
sp-20-H-BLK3	5	90	-	-	9	-	-	<DL	-	-
sp-20-H-02	5	90	6.92E-05	1.00	9	0.4994	0.011	0.0233	0.2534	1.78E-07
sp-20-H-04	5	90	7.09E-05	2.00	9	0.4942	0.011	0.0195	0.2143	1.83E-07
sp-20-H-06	5	90	7.06E-05	3.00	9	0.4895	0.011	0.0173	0.1876	1.43E-07
sp-20-H-08	5	90	6.89E-05	4.00	9	0.4857	0.011	0.0152	0.1588	1.08E-07
sp-20-H-10	5	90	7.04E-05	5.00	9	0.4825	0.011	0.0166	0.1803	8.01E-08
sp-20-H-12	5	90	7.18E-05	6.00	9	0.4798	0.010	0.0051	0.0382	1.36E-07
sp-20-H-14	5	90	6.81E-05	7.00	9	0.4775	0.010	0.0046	0.0303	1.13E-07
sp-20-H-16	5	90	6.73E-05	8.00	9	0.4757	0.010	0.0044	0.0276	9.69E-08
sp-20-H-18	5	90	6.78E-05	9.00	9	0.4741	0.010	0.0049	0.0339	8.79E-08
sp-20-H-20	5	90	6.86E-05	10.00	9	0.4727	0.010	0.0040	0.0233	8.33E-08
sp-20-H-22	5	90	7.13E-05	11.00	9	0.4715	0.010	0.0031	0.0128	9.11E-08
Exp. 9										
sp-20-I-BLK1	10	90	-	-	9	-	-	<DL	-	-
sp-20-I-BLK2	10	90	-	-	9	-	-	<DL	-	-
sp-20-I-BLK3	10	90	-	-	9	-	-	<DL	-	-
sp-20-I-02	10	90	6.83E-05	1.00	9	0.9976	0.022	0.0379	0.2112	1.54E-07
sp-20-I-04	10	90	7.10E-05	2.00	9	0.9879	0.021	0.0268	0.1525	1.75E-07
sp-20-I-06	10	90	7.19E-05	3.00	9	0.9788	0.021	0.0214	0.1214	1.46E-07
sp-20-I-08	10	90	7.10E-05	4.00	9	0.9708	0.021	0.0196	0.1093	1.34E-07
sp-20-I-10	10	90	6.97E-05	5.00	9	0.9640	0.021	0.0199	0.1096	1.13E-07
sp-20-I-12	10	90	7.13E-05	6.00	9	0.9580	0.021	0.0183	0.1025	9.92E-08
sp-20-I-14	10	90	7.16E-05	7.00	9	0.9525	0.021	0.0170	0.0951	9.11E-08
sp-20-I-16	10	90	7.09E-05	8.00	9	0.9475	0.021	0.0180	0.1008	8.58E-08
sp-20-I-18	10	90	7.06E-05	9.00	9	0.9430	0.021	0.0168	0.0931	7.41E-08
sp-20-I-20	10	90	7.20E-05	10.00	9	0.9388	0.021	0.0167	0.0945	6.86E-08
sp-20-I-22	10	90	7.27E-05	11.00	9	0.9349	0.021	0.0148	0.0834	7.57E-08
Exp. 10										
sp-20-J-BLK1	20	90	-	-	9	-	-	<DL	-	-
sp-20-J-BLK2	20	90	-	-	9	-	-	<DL	-	-
sp-20-J-BLK3	20	90	-	-	9	-	-	<DL	-	-
sp-20-J-02	20	90	7.35E-05	1.00	9	0.9942	0.021	0.0339	0.2162	-
sp-20-J-04	20	90	7.43E-05	2.00	9	0.9835	0.021	0.0223	0.1447	1.81E-07
sp-20-J-06	20	90	7.64E-05	3.00	9	0.9737	0.021	0.0181	0.1215	1.75E-07

Table A5. Additional Analysis of Select SPFT Samples (cont.)

Sample ID	Inf [Si] ppm	T °C	Flow Rate, m^3/d	Time, days	pH 23°C	Glass Mass g	SA m^2	[Re] ppm	Re Rate $g\ m^{-2}\ d^{-1}$	$r_{IEX\ [Re]}$ * $mol\ m^{-2}\ s^{-1}$
sp-20-J-08	20	90	7.41E-05	4.00	9	0.9650	0.021	0.0158	0.1035	1.45E-07
sp-20-J-10	20	90	7.19E-05	5.00	9	0.9577	0.021	0.0160	0.1022	1.29E-07
sp-20-J-12	20	90	6.98E-05	6.00	9	0.9513	0.021	0.0118	0.0736	1.12E-07
sp-20-J-14	20	90	7.25E-05	7.00	9	0.9456	0.021	0.0123	0.0799	1.04E-07
sp-20-J-16	20	90	7.42E-05	8.00	9	0.9403	0.021	0.0127	0.0848	1.00E-07
sp-20-J-18	20	90	6.97E-05	9.00	9	0.9354	0.021	0.0130	0.0818	9.24E-08
sp-20-J-20	20	90	7.15E-05	10.00	9	0.9308	0.021	0.0126	0.0816	8.73E-08
sp-20-J-22	20	90	7.44E-05	11.00	9	0.9265	0.020	0.0104	0.0703	1.07E-07
Exp. 11										
sp-20-K-BLK1	80	90	-	-	9	-	-	0.01	-	-
sp-20-K-BLK2	80	90	-	-	9	-	-	0.00	-	-
sp-20-K-BLK3	80	90	-	-	9	-	-	0.01	-	-
sp-20-K-02	80	90	7.37E-05	1.00	9	1.9888	0.043	0.0442	0.1244	1.92E-07
sp-20-K-04	80	90	7.17E-05	2.00	9	1.9664	0.043	0.0244	0.0599	1.94E-07
sp-20-K-06	80	90	7.43E-05	3.00	9	1.9458	0.042	0.0176	0.0404	1.88E-07
sp-20-K-08	80	90	7.49E-05	4.00	9	1.9272	0.042	0.0141	0.0294	1.74E-07
sp-20-K-10	80	90	7.34E-05	5.00	9	1.9107	0.042	0.0131	0.0257	1.62E-07
sp-20-K-12	80	90	7.57E-05	6.00	9	1.8967	0.042	0.0095	0.0144	1.46E-07
sp-20-K-14	80	90	7.55E-05	7.00	9	1.8845	0.041	0.0085	0.0111	1.36E-07
sp-20-K-16	80	90	7.33E-05	8.00	9	1.8735	0.041	0.0086	0.0111	1.30E-07
sp-20-K-18	80	90	7.37E-05	9.00	9	1.8635	0.041	0.0082	0.0099	1.18E-07
sp-20-K-20	80	90	7.52E-05	10.00	9	1.8539	0.041	0.0075	0.0077	1.11E-07
sp-20-K-22	80	90	7.40E-05	11.00	9	1.8447	0.041	0.0076	0.0080	1.25E-07
Exp. 12										
sp-20-L-BLK1	120	90	-	-	9	-	-	0.01	-	-
sp-20-L-BLK2	120	90	-	-	9	-	-	0.01	-	-
sp-20-L-BLK3	120	90	-	-	9	-	-	0.01	-	-
sp-20-L-02	120	90	7.24E-05	1.00	9	1.9924	0.043	0.0372	0.0908	1.71E-07
sp-20-L-04	120	90	7.10E-05	2.00	9	1.9717	0.043	0.0258	0.0544	1.91E-07
sp-20-L-06	120	90	6.95E-05	3.00	9	1.9519	0.042	0.0176	0.0287	1.85E-07
sp-20-L-08	120	90	7.20E-05	4.00	9	1.9335	0.042	0.0159	0.0245	1.82E-07
sp-20-L-10	120	90	7.54E-05	5.00	9	1.9157	0.042	0.0137	0.0184	1.95E-07
sp-20-L-13	120	90	7.30E-05	6.50	9	1.8983	0.042	0.0100	0.0059	1.43E-07
sp-20-L-15	120	90	7.51E-05	7.50	9	1.8844	0.041	0.0095	0.0044	1.39E-07
sp-20-L-16	120	90	7.71E-05	8.00	9	1.8765	0.041	0.0096	0.0049	1.29E-07
sp-20-L-18	120	90	8.09E-05	9.00	9	1.8687	0.041	0.0100	0.0066	1.29E-07
sp-20-L-20	120	90	7.82E-05	10.00	9	1.8588	0.041	0.0100	0.0064	1.26E-07
sp-20-L-21	120	90	7.59E-05	10.50	9	1.8518	0.041	0.0103	0.0072	1.23E-07
sp-20-L-22	120	90	7.55E-05	11.00	9	1.8474	0.041	0.0098	0.0055	1.24E-07
Exp. 19										
sp-21-G-BLK1	1	70	-	-	9	-	-	<DL	-	-
sp-21-G-BLK2	1	70	-	-	9	-	-	<DL	-	-
sp-21-G-BLK3	1	70	-	-	9	-	-	<DL	-	-
sp-21-G-03	1	70	6.27E-05	1.50	9	0.5013	0.011	0.0109	0.0950	3.04E-08
sp-21-G-04	1	70	6.25E-05	2.00	9	0.5004	0.011	0.0107	0.0927	3.09E-08
sp-21-G-06	1	70	5.90E-05	3.00	9	0.4997	0.011	0.0130	0.1109	1.03E-08
sp-21-G-09	1	70	6.27E-05	4.50	9	0.4986	0.011	0.0129	0.1169	-4.46E-09
sp-21-G-10	1	70	6.30E-05	5.00	9	0.4977	0.011	0.0133	0.1220	-9.68E-09
sp-21-G-11	1	70	6.27E-05	5.50	9	0.4973	0.011	0.0134	0.1226	-1.15E-08
sp-21-G-14	1	70	6.32E-05	7.00	9	0.4964	0.011	0.0126	0.1150	-8.78E-09
sp-21-G-16	1	70	6.06E-05	8.00	9	0.4953	0.011	0.0124	0.1083	-9.95E-09
sp-21-G-18	1	70	6.08E-05	9.00	9	0.4945	0.011	0.0122	0.1067	-1.02E-08

Table A5. Additional Analysis of Select SPFT Samples (cont.)

Sample ID	Inf [Si] ppm	T °C	Flow Rate, m^3/d	Time, days	pH 23°C	Glass Mass g	SA m^2	[Re] ppm	Re Rate g m^{-2} d^{-1}	$r_{IEX\,[Re]}$* mol m^{-2} s^{-1}
sp-21-G-20	1	70	5.94E-05	10.00	9	0.4936	0.011	0.0126	0.1085	-1.21E-08
sp-21-G-23	1	70	6.21E-05	11.50	9	0.4926	0.011	0.0135	0.1234	-2.00E-08
Exp. 20										
sp-21-H-BLK1	5	70	-	-	9	-	-	<DL	-	-
sp-21-H-BLK2	5	70	-	-	9	-	-	<DL	-	-
sp-21-H-BLK3	5	70	-	-	9	-	-	<DL	-	-
sp-21-H-02	5	70	6.44E-05	1.00	9	0.5034	0.011	0.0064	0.0475	5.89E-08
sp-21-H-04	5	70	6.43E-05	2.00	9	0.5027	0.011	0.0082	0.0673	3.93E-08
sp-21-H-06	5	70	6.36E-05	3.00	9	0.5019	0.011	0.0100	0.0863	1.68E-08
sp-21-H-08	5	70	6.43E-05	4.00	9	0.5012	0.011	0.0109	0.0974	2.21E-10
sp-21-H-10	5	70	6.46E-05	5.00	9	0.5004	0.011	0.0107	0.0956	-4.19E-09
sp-21-H-12	5	70	6.41E-05	6.00	9	0.4997	0.011	0.0105	0.0928	-6.17E-09
sp-21-H-14	5	70	6.47E-05	7.00	9	0.4989	0.011	0.0110	0.0993	-1.09E-08
sp-21-H-16	5	70	6.09E-05	8.00	9	0.4982	0.011	0.0114	0.0977	-1.34E-08
sp-21-H-18	5	70	6.46E-05	9.00	9	0.4974	0.011	0.0112	0.1016	-1.38E-08
sp-21-H-19	5	70	6.17E-05	9.50	9	0.4969	0.011	0.0105	0.0896	-6.76E-09
sp-21-H-23	5	70	6.01E-05	11.50	9	0.4960	0.011	0.0104	0.0864	-6.66E-09
Exp. 21										
sp-21-I-BLK1	10	70	-	-	9	-	-	<DL	-	-
sp-21-I-BLK2	10	70	-	-	9	-	-	<DL	-	-
sp-21-I-BLK3	10	70	-	-	9	-	-	<DL	-	-
sp-21-I-02	10	70	6.44E-05	1.00	9	1.0000	0.022	0.0153	0.0733	3.72E-08
sp-21-I-04	10	70	6.38E-05	2.00	9	0.9986	0.022	0.0120	0.0545	3.08E-08
sp-21-I-06	10	70	6.30E-05	3.00	9	0.9977	0.022	0.0083	0.0337	2.84E-08
sp-21-I-08	10	70	6.03E-05	4.00	9	0.9970	0.021	0.0075	0.0281	1.94E-08
sp-21-I-10	10	70	6.37E-05	5.00	9	0.9964	0.021	0.0069	0.0264	1.64E-08
sp-21-I-12	10	70	6.34E-05	6.00	9	0.9958	0.021	0.0074	0.0291	1.29E-08
sp-21-I-13	10	70	6.35E-05	6.50	9	0.9954	0.021	0.0074	0.0291	1.33E-08
sp-21-I-16	10	70	6.03E-05	8.00	9	0.9947	0.021	0.0078	0.0298	9.09E-09
sp-21-I-18	10	70	6.31E-05	9.00	9	0.9939	0.021	0.0080	0.0322	7.61E-09
sp-21-I-19	10	70	6.20E-05	9.50	9	0.9933	0.021	0.0092	0.0381	3.81E-09
sp-21-I-23	10	70	6.11E-05	11.50	9	0.9925	0.021	0.0077	0.0297	6.65E-09
Exp. 22										
sp-21-J-BLK1	20	70	-	-	9	-	-	<DL	-	-
sp-21-J-BLK2	20	70	-	-	9	-	-	<DL	-	-
sp-21-J-BLK3	20	70	-	-	9	-	-	<DL	-	-
sp-21-J-02	20	70	6.41E-05	1.00	9	1.0003	0.022	0.0167	0.0808	-
sp-21-J-04	20	70	6.02E-05	2.00	9	0.9985	0.021	0.0124	0.0536	3.44E-08
sp-21-J-06	20	70	6.42E-05	3.00	9	0.9969	0.021	0.0117	0.0533	2.80E-08
sp-21-J-08	20	70	6.06E-05	4.00	9	0.9955	0.021	0.0105	0.0441	1.86E-08
sp-21-J-10	20	70	6.42E-05	5.00	9	0.9944	0.021	0.0088	0.0373	2.27E-08
sp-21-J-12	20	70	6.12E-05	6.00	9	0.9934	0.021	0.0076	0.0292	2.10E-08
sp-21-J-14	20	70	6.48E-05	7.00	9	0.9925	0.021	0.0086	0.0365	1.69E-08
sp-21-J-16	20	70	6.43E-05	8.00	9	0.9916	0.021	0.0078	0.0318	1.62E-08
sp-21-J-18	20	70	6.42E-05	9.00	9	0.9909	0.021	0.0081	0.0335	1.40E-08
sp-21-J-20	20	70	6.29E-05	10.00	9	0.9903	0.021	0.0080	0.0322	1.16E-08
sp-21-J-23	20	70	5.91E-05	11.50	9	0.9896	0.021			2.25E-08

Table A5. Additional Analysis of Select SPFT Samples-All Temperatures (cont.)

Sample ID	Inf [Si] ppm	T °C	Flow Rate, m^3/d	Time, days	pH 23°C	Glass Mass g	SA m^2	[Re] ppm	Re Rate $g\ m^{-2}\ d^{-1}$	$r_{IEX\ [Re]}$ * mol $m^{-2}\ s^{-1}$
Exp. 23										
sp-21-K-BLK1	40	70	-	-	9	-	-	0.0027	-	-
sp-21-K-BLK2	40	70	-	-	9	-	-	0.0029	-	-
sp-21-K-BLK3	40	70	-	-	9	-	-	<DL	-	-
sp-21-K-02	40	70	6.63E-05	1.00	9	1.0001	0.027	0.02	0.0642	3.53E-08
sp-21-K-04	40	70	6.54E-05	2.00	9	0.9977	0.027	0.0139	0.0508	3.47E-08
sp-21-K-06	40	70	6.14E-05	3.00	9	0.9952	0.027	0.0128	0.0432	2.75E-08
sp-21-K-08	40	70	6.43E-05	4.00	9	0.9929	0.027	0.0122	0.0426	2.47E-08
sp-21-K-09	40	70	6.29E-05	4.50	9	0.9912	0.027	0.0113	0.0378	2.32E-08
sp-21-K-12	40	70	6.47E-05	6.00	9	0.9891	0.027	0.0097	0.0318	2.36E-08
sp-21-K-14	40	70	6.28E-05	7.00	9	0.9866	0.027	0.0091	0.0284	2.41E-08
sp-21-K-16	40	70	6.25E-05	8.00	9	0.9847	0.027	0.0092	0.0287	2.37E-08
sp-21-K-18	40	70	6.21E-05	9.00	9	0.9830	0.027	0.0086	0.0259	2.47E-08
sp-21-K-20	40	70	6.17E-05	10.00	9	0.9813	0.027	0.0083	0.0245	2.44E-08
sp-21-K-22	40	70	5.71E-05	11.50	9	0.9793	0.027	0.0079	0.0212	2.32E-08
Exp. 24										
sp-21-L-BLK1	80	70	-	-	9	-	-	0.01	-	-
sp-21-L-BLK2	80	70	-	-	9	-	-	0.01	-	-
sp-21-L-BLK3	80	70	-	-	9	-	-	0.01	-	-
sp-21-L-02	80	70	6.92E-05	1.00	9	1.9992	0.043	0.0276	0.0614	4.79E-08
sp-21-L-04	80	70	6.96E-05	2.00	9	1.9939	0.043	0.0205	0.0405	5.96E-08
sp-21-L-06	80	70	6.88E-05	3.00	9	1.9884	0.043	0.0169	0.0294	5.55E-08
sp-21-L-08	80	70	7.06E-05	4.00	9	1.9831	0.043	0.0142	0.0219	5.09E-08
sp-21-L-09	80	70	6.78E-05	4.50	9	1.9794	0.043	0.0134	0.0187	4.68E-08
sp-21-L-12	80	70	7.11E-05	6.00	9	1.9749	0.043	0.0123	0.0163	4.48E-08
sp-21-L-14	80	70	7.19E-05	7.00	9	1.9695	0.043	0.0123	0.0165	4.38E-08
sp-21-L-15	80	70	6.91E-05	7.50	9	1.9664	0.043	0.0112	0.0126	4.02E-08
sp-21-L-17	80	70	6.93E-05	8.50	9	1.9634	0.043	0.0109	0.0117	4.04E-08
sp-21-L-20	80	70	6.99E-05	10.00	9	1.9587	0.042	0.0109	0.0118	4.05E-08
sp-21-L-23	80	70	6.71E-05	11.50	9	1.9533	0.042	0.0111	0.0120	3.62E-08
Exp. 31										
SP-22-G-BLK1	1	40	-	-	9	-	-	<0.000014	-	-
SP-22-G-BLK2	1	40	-	-	9	-	-	<0.000014	-	-
SP-22-G-BLK3	1	40	-	-	9	-	-	<0.000014	-	-
SP-22-G-02	1	40	1.93E-05	3.00	9	0.5015	0.011	0.0005	0.0018	1.11E-08
SP-22-G-04	1	40	1.94E-05	5.00	9	0.5013	0.011	0.0006	0.0019	1.18E-08
SP-22-G-06	1	40	1.93E-05	7.00	9	0.5010	0.011	0.0006	0.0020	1.12E-08
SP-22-G-08	1	40	1.92E-05	9.00	9	0.5008	0.011	0.0007	0.0021	1.16E-08
SP-22-G-10	1	40	1.92E-05	11.00	9	0.5005	0.011	0.0006	0.0021	1.01E-08
SP-22-G-12	1	40	1.92E-05	13.00	9	0.5002	0.011	0.0007	0.0022	8.78E-09
SP-22-G-14	1	40	1.91E-05	15.00	9	0.4999	0.011	0.0006	0.0021	9.39E-09
SP-22-G-16	1	40	1.98E-05	17.00	9	0.4997	0.011	0.0006	0.0021	8.26E-09
SP-22-G-18	1	40	2.01E-05	19.00	9	0.4994	0.011	0.0006	0.0021	8.03E-09
SP-22-G-20	1	40	1.98E-05	21.00	9	0.4991	0.011	0.0007	0.0023	7.55E-09
SP-22-G-22	1	40	2.00E-05	23.00	9	0.4988	0.011	0.0006	0.0022	7.02E-09

Table A5. Additional Analysis of Select SPFT Samples-All Temperatures (cont.)

Sample ID	Inf [Si] ppm	T °C	Flow Rate, m^3/d	Time, days	pH 23°C	Glass Mass g	SA m^2	[Re] ppm	Re Rate $g\ m^{-2}\ d^{-1}$	$r_{IEX\ [Re]}$ * $mol\ m^{-2}\ s^{-1}$
Exp. 32										
sp-22-H-BLK1	5	40	-	-	9	-	-	<0.000014	-	-
sp-22-H-BLK2	5	40	-	-	9	-	-	<0.000014	-	-
sp-22-H-BLK3	5	40	-	-	9	-	-	<0.000014	-	-
SP-22-H-02	5	40	1.97E-05	3.00	9	0.4997	0.011	0.0003	0.0011	1.11E-08
SP-22-H-04	5	40	1.98E-05	5.00	9	0.4994	0.011	0.0005	0.0016	1.15E-08
SP-22-H-06	5	40	1.96E-05	7.00	9	0.4992	0.011	0.0005	0.0018	1.08E-08
SP-22-H-08	5	40	1.86E-05	9.00	9	0.4989	0.011	0.0005	0.0016	8.72E-09
SP-22-H-10	5	40	1.94E-05	11.00	9	0.4986	0.011	0.0005	0.0018	8.52E-09
SP-22-H-12	5	40	1.94E-05	13.00	9	0.4984	0.011	0.0006	0.0019	7.40E-09
SP-22-H-14	5	40	1.93E-05	15.00	9	0.4981	0.011	0.0006	0.0018	7.48E-09
SP-22-H-16	5	40	2.01E-05	17.00	9	0.4978	0.011	0.0005	0.0018	6.97E-09
SP-22-H-18	5	40	2.02E-05	19.00	9	0.4976	0.011	0.0005	0.0018	7.31E-09
SP-22-H-20	5	40	2.01E-05	21.00	9	0.4973	0.011	0.0005	0.0019	6.63E-09
SP-22-H-22	5	40	2.00E-05	23.00	9	0.4971	0.011	0.0005	0.0017	6.62E-09
Exp. 33										
sp-22-I-BLK1	15		-	-	9	-	-	<0.000014	-	-
sp-22-I-BLK2	15		-	-	9	-	-	<0.000014	-	-
sp-22-I-BLK3	15		-	-	9	-	-	<0.000014	-	-
SP-22-I-02	15	40	1.90E-05	3.00	9	0.9983	0.022	0.0006	0.0009	1.05E-08
SP-22-I-04	15	40	1.91E-05	5.00	9	0.9979	0.022	0.0006	0.0009	1.12E-08
SP-22-I-06	15	40	1.91E-05	7.00	9	0.9976	0.022	0.0006	0.0009	9.77E-09
SP-22-I-08	15	40	1.67E-05	9.00	9	0.9973	0.022	0.0005	0.0007	8.56E-09
SP-22-I-10	15	40	1.92E-05	11.00	9	0.9971	0.022	0.0005	0.0008	8.36E-09
SP-22-I-12	15	40	1.92E-05	13.00	9	0.9968	0.021	0.0005	0.0009	7.65E-09
SP-22-I-14	15	40	1.92E-05	15.00	9	0.9966	0.021	0.0005	0.0007	6.24E-09
SP-22-I-16	15	40	2.00E-05	17.00	9	0.9964	0.021	0.0004	0.0007	6.58E-09
SP-22-I-18	15	40	2.02E-05	19.00	9	0.9962	0.021	0.0004	0.0008	5.63E-09
SP-22-I-20	15	40	2.01E-05	21.00	9	0.9959	0.021	0.0005	0.0009	4.96E-09
SP-22-I-22	15	40	2.00E-05	23.00	9	0.9957	0.021	0.0004	0.0008	4.90E-09
Exp. 34										
sp-22-J-BLK1	30	40	-	-	9	-	-	<0.000014	-	-
sp-22-J-BLK2	30	40	-	-	9	-	-	<0.000014	-	-
sp-22-J-BLK3	30	40	-	-	9	-	-	<0.000014	-	-
SP-22-J-02	30	40	1.91E-05	3.00	9	1.0028	0.022	0.0005	0.0007	-
SP-22-J-04	30	40	1.92E-05	5.00	9	1.0025	0.022	0.0005	0.0008	1.14E-08
SP-22-J-06	30	40	1.91E-05	7.00	9	1.0022	0.022	0.0005	0.0007	1.08E-08
SP-22-J-08	30	40	1.90E-05	9.00	9	1.0019	0.022	0.0004	0.0007	9.96E-09
SP-22-J-10	30	40	1.90E-05	11.00	9	1.0017	0.022	0.0004	0.0006	8.52E-09
SP-22-J-12	30	40	1.90E-05	13.00	9	1.0015	0.022	0.0003	0.0005	8.05E-09
SP-22-J-14	30	40	1.90E-05	15.00	9	1.0013	0.022	0.0003	0.0005	6.80E-09
SP-22-J-16	30	40	1.97E-05	17.00	9	1.0011	0.022	0.0003	0.0004	6.69E-09
SP-22-J-18	30	40	1.99E-05	19.00	9	1.0010	0.022	0.0002	0.0004	5.64E-09
SP-22-J-20	30	40	1.97E-05	21.00	9	1.0008	0.022	0.0002	0.0003	5.65E-09
SP-22-J-22	30	40	1.94E-05	23.00	9	1.0007	0.022	0.0002	0.0003	4.93E-09
Exp. 35										
sp-22-K-BLK1	45	40	-	-	9	-	-	<0.000014	-	-
sp-22-K-BLK2	45	40	-	-	9	-	-	<0.000014	-	-
sp-22-K-BLK3	45	40	-	-	9	-	-	<0.000014	-	-
SP-22-K-02	45	40	1.92E-05	3.00	9	1.9999	0.043	0.0008	0.0006	1.09E-08
SP-22-K-04	45	40	1.92E-05	5.00	9	1.9992	0.043	0.0008	0.0007	1.14E-08
SP-22-K-06	45	40	1.91E-05	7.00	9	1.9985	0.043	0.0007	0.0006	1.05E-08
SP-22-K-08	45	40	1.91E-05	9.00	9	1.9978	0.043	0.0006	0.0005	1.01E-08

Table A5. Additional Analysis of Select SPFT Samples-All Temperatures (cont.)

Sample ID	Inf [Si] ppm	T °C	Flow Rate, m^3/d	Time, days	pH 23°C	Glass Mass g	SA m^2	[Re] ppm	Re Rate $g\ m^{-2}\ d^{-1}$	$r_{IEX\ [Re]}$ * $mol\ m^{-2}\ s^{-1}$
SP-22-K-10	45	40	1.90E-05	11.00	9	1.9973	0.043	0.0005	0.0004	8.24E-09
SP-22-K-12	45	40	1.89E-05	13.00	9	1.9968	0.043	0.0004	0.0004	7.80E-09
SP-22-K-14	45	40	1.89E-05	15.00	9	1.9964	0.043	0.0004	0.0003	7.03E-09
SP-22-K-16	45	40	1.97E-05	17.00	9	1.9959	0.043	0.0004	0.0003	6.62E-09
SP-22-K-18	45	40	1.99E-05	19.00	9	1.9955	0.043	0.0003	0.0002	6.32E-09
SP-22-K-20	45	40	1.94E-05	21.00	9	1.9952	0.043	0.0003	0.0002	5.47E-09
SP-22-K-22	45	40	1.93E-05	23.00	9	1.9948	0.043	0.0003	0.0002	5.33E-09
Exp. 36										
sp-22-L-BLK1	60	40	-	-	9	-	-	<0.000014	-	-
sp-22-L-BLK2	60	40	-	-	9	-	-	<0.000014	-	-
sp-22-L-BLK3	60	40	-	-	9	-	-	<0.000014	-	-
SP-22-L-02	60	40	2.11E-05	3.00	9	2.0039	0.043	0.0007	0.0006	1.14E-08
SP-22-L-04	60	40	2.09E-05	5.00	9	2.0031	0.043	0.0007	0.0006	1.17E-08
SP-22-L-06	60	40	2.07E-05	7.00	9	2.0024	0.043	0.0007	0.0006	1.17E-08
SP-22-L-08	60	40	2.06E-05	9.00	9	2.0017	0.043	0.0006	0.0005	1.14E-08
SP-22-L-10	60	40	2.05E-05	11.00	9	2.0012	0.043	0.0005	0.0004	8.36E-09
SP-22-L-12	60	40	2.05E-05	13.00	9	2.0006	0.043	0.0004	0.0003	8.36E-09
SP-22-L-14	60	40	2.02E-05	15.00	9	2.0001	0.043	0.0003	0.0003	7.30E-09
SP-22-L-16	60	40	2.12E-05	17.00	9	1.9996	0.043	0.0003	0.0002	7.19E-09
SP-22-L-18	60	40	2.12E-05	19.00	9	1.9991	0.043	0.0003	0.0002	6.24E-09
SP-22-L-20	60	40	2.11E-05	21.00	9	1.9987	0.043	0.0002	0.0002	6.34E-09
SP-22-L-22	60	40	2.12E-05	23.00	9	1.9982	0.043	0.0002	0.0002	5.64E-09
Exp. 43										
SP-23-G-BLK1	1	23	-	-	9	-	-	0.0000068	-	-
SP-23-G-BLK2	1	23	-	-	9	-	-	0.0000068	-	-
SP-23-G-BLK3	1	23	-	-	9	-	-	0.0000068	-	-
SP-23-G-01	1	23	2.16E-05	2.00	9	4.0032	0.086	0.0087	0.0040	2.56E-09
SP-23-G-02	1	23	1.06E-05	5.00	9	4.0028	0.086	0.0063	0.0014	9.32E-10
SP-23-G-03	1	23	9.88E-06	8.00	9	4.0026	0.086	0.0062	0.0013	9.39E-10
SP-23-G-04	1	23	9.99E-06	11.00	9	4.0023	0.086	0.0060	0.0013	6.07E-10
SP-23-G-05	1	23	9.98E-06	14.00	9	4.0021	0.086	0.0058	0.0012	4.58E-10
SP-23-G-06	1	23	9.95E-06	17.00	9	4.0019	0.086	0.0055	0.0012	4.32E-10
SP-23-G-07	1	23	9.92E-06	20.00	9	4.0018	0.086	0.0053	0.0011	3.00E-10
SP-23-G-08	1	23	9.98E-06	23.00	9	4.0016	0.086	0.0051	0.0011	1.89E-10
SP-23-G-09	1	23	1.00E-05	26.00	9	4.0015	0.086	0.0051	0.0011	2.07E-10
SP-23-G-10	1	23	9.98E-06	29.00	9	4.0013	0.086	0.0053	0.0011	6.99E-11
SP-23-G-11	1	23	9.99E-06	32.00	9	4.0012	0.086	0.0053	0.0011	8.89E-11
SP-23-G-12	1	23	1.00E-05	35.00	9	4.0010	0.086	0.0055	0.0012	4.38E-12
SP-23-G-13	1	23	9.99E-06	38.00	9	4.0009	0.086	0.0057	0.0012	-5.06E-11
Exp. 44										
sp-23-H-BLK1	15	23	-	-	9	-	-	<0.000014	-	-
sp-23-H-BLK2	15	23	-	-	9	-	-	<0.000014	-	-
sp-23-H-BLK3	15	23	-	-	9	-	-	<0.000014	-	-
SP-23-H-01	15	23	2.13E-05	2.00	9	4.0005	0.086	0.0081	0.0037	3.41E-09
SP-23-H-02	15	23	1.04E-05	5.00	9	4.0002	0.086	0.0058	0.0013	1.29E-09
SP-23-H-03	15	23	9.73E-06	8.00	9	3.9999	0.086	0.0053	0.0011	1.16E-09
SP-23-H-04	15	23	9.84E-06	11.00	9	3.9997	0.086	0.0044	0.0009	1.02E-09
SP-23-H-05	15	23	9.85E-06	14.00	9	3.9996	0.086	0.0038	0.0008	1.02E-09
SP-23-H-06	15	23	9.84E-06	17.00	9	3.9994	0.086	0.0034	0.0007	7.20E-10
SP-23-H-07	15	23	9.76E-06	20.00	9	3.9993	0.086	0.0031	0.0007	7.28E-10
SP-23-H-08	15	23	9.79E-06	23.00	9	3.9991	0.086	0.0027	0.0006	6.87E-10
SP-23-H-09	15	23	9.81E-06	26.00	9	3.9990	0.086	0.0026	0.0005	4.66E-10
SP-23-H-10	15	23	9.81E-06	29.00	9	3.9989	0.086	0.0026	0.0005	5.09E-10
SP-23-H-11	15	23	9.78E-06	32.00	9	3.9988	0.086	0.0024	0.0005	3.91E-10
SP-23-H-12	15	23	9.81E-06	35.00	10	3.9987	0.086	0.0021	0.0004	4.77E-10

Table A5. Additional Analysis of Select SPFT Samples-All Temperatures (cont.)

Sample ID	Inf [Si] ppm	T °C	Flow Rate, m^3/d	Time, days	pH 23°C	Glass Mass g	SA m^2	[Re] ppm	Re Rate $g\ m^{-2}\ d^{-1}$	$r_{IEX\ [Re]}$ * $mol\ m^{-2}\ s^{-1}$
SP-23-H-13	15	23	9.78E-06	38.00	11	3.9987	0.086	0.0021	0.0004	3.51E-10
Exp. 45										
sp-23-I-BLK1	22.5		-	-	9	-	-	<0.000034	-	-
sp-23-I-BLK2	22.5		-	-	9	-	-	<0.000034	-	-
sp-23-I-BLK3	22.5		-	-	9	-	-	<0.000034	-	-
SP-23-I-01	22.5	23	2.16E-05	2.00	9	4.0001	0.054	0.0069	0.0051	5.14E-09
SP-23-I-02	22.5	23	1.06E-05	5.00	9	3.9998	0.054	0.0058	0.0021	2.12E-09
SP-23-I-03	22.5	23	9.99E-06	8.00	9	3.9995	0.054	0.0050	0.0017	1.72E-09
SP-23-I-04	22.5	23	1.01E-05	11.00	9	3.9993	0.054	0.0048	0.0016	1.66E-09
SP-23-I-05	22.5	23	1.01E-05	14.00	9	3.9991	0.054	0.0038	0.0013	1.31E-09
SP-23-I-06	22.5	23	1.01E-05	17.00	9	3.9990	0.054	0.0036	0.0012	1.24E-09
SP-23-I-07	22.5	23	1.01E-05	20.00	9	3.9988	0.054	0.0027	0.0009	9.39E-10
SP-23-I-08	22.5	23	1.01E-05	23.00	9	3.9987	0.054	0.0027	0.0009	9.24E-10
SP-23-I-09	22.5	23	1.01E-05	26.00	9	3.9986	0.054	0.0022	0.0008	7.54E-10
SP-23-I-10	22.5	23	1.01E-05	29.00	9	3.9985	0.054	0.0021	0.0007	7.38E-10
SP-23-I-11	22.5	23	1.01E-05	32.00	9	3.9984	0.054	0.0019	0.0006	6.38E-10
SP-23-I-12	22.5	23	1.02E-05	35.00	9	3.9984	0.054	0.0020	0.0007	6.72E-10
SP-23-I-13	22.5	23	1.01E-05	38.00	9	3.9983	0.054	0.0016	0.0006	5.54E-10
Exp. 46										
sp-23-J-BLK1	30	23	-	-	9	-	-	<0.000014	-	-
sp-23-J-BLK2	30	23	-	-	9	-	-	<0.000014	-	-
sp-23-J-BLK3	30	23	-	-	9	-	-	<0.000014	-	-
SP-23-J-01	30	23	2.12E-05	2.00	9	3.9989	0.054	0.0083	0.0060	-
SP-23-J-02	30	23	1.04E-05	5.00	9	3.9985	0.054	0.0059	0.0021	1.86E-09
SP-23-J-03	30	23	9.73E-06	8.00	9	3.9984	0.054	0.0050	0.0017	1.95E-09
SP-23-J-04	30	23	9.89E-06	11.00	9	3.9982	0.054	0.0039	0.0013	1.58E-09
SP-23-J-05	30	23	9.84E-06	14.00	9	3.9980	0.054	0.0035	0.0012	1.35E-09
SP-23-J-06	30	23	9.79E-06	17.00	9	3.9979	0.054	0.0034	0.0011	1.15E-09
SP-23-J-07	30	23	9.79E-06	20.00	9	3.9978	0.054	0.0026	0.0009	1.01E-09
SP-23-J-08	30	23	9.81E-06	23.00	9	3.9977	0.054	0.0024	0.0008	9.88E-10
SP-23-J-09	30	23	9.81E-06	26.00	9	3.9976	0.054	0.0021	0.0007	9.07E-10
SP-23-J-10	30	23	9.79E-06	29.00	9	3.9975	0.054	0.0020	0.0007	8.46E-10
SP-23-J-11	30	23	9.75E-06	32.00	9	3.9974	0.054	0.0018	0.0006	6.48E-10
SP-23-J-12	30	23	9.79E-06	35.00	9	3.9974	0.054	0.0016	0.0006	7.32E-10
SP-23-J-13	30	23	9.76E-06	38.00	9	3.9973	0.054	0.0016	0.0005	5.67E-10
Exp. 47										
sp-23-K-BLK1	45	23	-	-	9	-	-	<0.000034	-	-
sp-23-K-BLK2	45	23	-	-	9	-	-	<0.000034	-	-
sp-23-K-BLK3	45	23	-	-	9	-	-	<0.000034	-	-
SP-23-K-01	45	23	2.11E-05	2.00	9	3.9995	0.068	0.0008	0.0004	5.39E-09
SP-23-K-02	45	23	1.04E-05	5.00	9	3.9991	0.068	0.0008	0.0002	2.24E-09
SP-23-K-03	45	23	9.66E-06	8.00	9	3.9989	0.068	0.0007	0.0002	1.93E-09
SP-23-K-04	45	23	9.73E-06	11.00	9	3.9987	0.068	0.0006	0.0002	1.80E-09
SP-23-K-05	45	23	9.69E-06	14.00	9	3.9985	0.068	0.0005	0.0001	1.43E-09
SP-23-K-07	45	23	9.72E-06	20.00	9	3.9983	0.068	0.0004	0.0001	1.16E-09
SP-23-K-08	45	23	9.66E-06	23.00	9	3.9982	0.068	0.0004	0.0001	9.98E-10
SP-23-K-09	45	23	9.71E-06	26.00	9	3.9981	0.068	0.0004	0.0001	8.76E-10
SP-23-K-10	45	23	9.71E-06	29.00	9	3.9980	0.068	0.0003	0.0001	8.82E-10
SP-23-K-11	45	23	9.68E-06	32.00	9	3.9979	0.068	0.0003	0.0001	7.31E-10
SP-23-K-12	45	23	9.66E-06	35.00	9	3.9978	0.068	0.0003	0.0001	7.30E-10
SP-23-K-13	45	23	9.71E-06	38.00	9	3.9977	0.068	0.0003	0.0001	6.31E-10

Table A5. Additional Analysis of Select SPFT Samples-All Temperatures (cont.)

Sample ID	Inf [Si] ppm	T °C	Flow Rate, m^3/d	Time, days	pH 23°C	Glass Mass g	SA m^2	[Re] ppm	Re Rate $g\ m^{-2}\ d^{-1}$	$r_{IEX\ [Re]}$ * $mol\ m^{-2}\ s^{-1}$
Exp. 48										
sp-23-L-BLK1	52.5	23	-	-	9	-	-	<0.000034	-	-
sp-23-L-BLK2	52.5	23	-	-	9	-	-	<0.000034	-	-
sp-23-L-BLK3	52.5	23	-	-	9	-	-	<0.000034	-	-
SP-23-L-01	52.5	23	2.21E-05	2.00	9	4.0016	0.068	0.0064	0.0039	3.86E-09
SP-23-L-02	52.5	23	1.12E-05	5.00	9	4.0012	0.068	0.0054	0.0016	1.64E-09
SP-23-L-03	52.5	23	1.04E-05	8.00	9	4.0010	0.068	0.0047	0.0013	1.31E-09
SP-23-L-04	52.5	23	1.06E-05	11.00	9	4.0008	0.068	0.0041	0.0012	1.15E-09
SP-23-L-05	52.5	23	1.06E-05	14.00	9	4.0006	0.068	0.0033	0.0009	9.34E-10
SP-23-L-06	52.5	23	1.05E-05	17.00	9	4.0005	0.068	0.0029	0.0008	8.25E-10
SP-23-L-07	52.5	23	1.05E-05	20.00	9	4.0004	0.068	0.0024	0.0007	6.71E-10
SP-23-L-08	52.5	23	1.06E-05	23.00	9	4.0003	0.068	0.0023	0.0007	6.47E-10
SP-23-L-09	52.5	23	1.06E-05	26.00	9	4.0002	0.068	0.0022	0.0006	5.98E-10
SP-23-L-10	52.5	23	1.06E-05	29.00	9	4.0001	0.068	0.0019	0.0005	5.25E-10
SP-23-L-11	52.5	23	1.06E-05	32.00	9	4.0000	0.068	0.0018	0.0005	4.92E-10
SP-23-L-12	52.5	23	1.06E-05	35.00	9	3.9999	0.068	0.0017	0.0005	4.71E-10
SP-23-L-13	52.5	23	1.06E-05	38.00	9	3.9999	0.068	0.0015	0.0004	3.97E-10

** The r_{IEX} values listed are calculated based on the previous conventional formula without any correction. To obtain the corrected values, the listed values have to be multiplied by the correction factor of 0.24x46/62 = 0.178.

* $r_{IEX\ [Re]}$ Values obtained by replacing boron rates by Re rates in the same r_{IEX} calculation to potentially counteract the confounding effect of the diffusive release of boron

- Empty data field

Table A6. Mean and Standard Deviation Values of the Steady State Normalized B Dissolution Rates.

Line ID	Inf [Si], ppm	T in ºC	pH (23ºC)	Steady State B Rate, g m^{-2} d^{-1}	Coefficient of Variance (%)
SP-20-A	0	90	7	0.7282±0.0711	10
SP-20-B	0	90	8	0.4294±0.0464	11
SP-20-C	0	90	9	0.1512±0.0028	2
SP-20-D	0	90	10	0.2357±0.0063	3
SP-20-E	0	90	11	1.0585±0.0382	4
SP-20-F	0	90	12	2.8921±0.0693	2
SP-20-G	1	90	9	0.1015±0.0054	5
SP-20-H	5	90	9	0.1271±0.014	11
SP-20-I	10	90	9	0.1959±0.0102	5
SP-20-J	20	90	9	0.2156±0.0093	4
SP-20-K	80	90	9	0.2290±0.0096	4
SP-20-L	120	90	9	0.2220±0.0087	4
SP-21-A	0	70	7	0.3299±0.0123	4
SP-21-B	0	70	8	0.1728±0.0108	6
SP-21-C	0	70	9	0.0446±0.0014	3
SP-21-D	0	70	10	0.1239±0.0051	4
SP-21-E	0	70	11	0.3732±0.0107	3
SP-21-F	0	70	12	1.0357±0.0394	4
SP-21-G	1	70	9	0.0782±0.0008	1
SP-21-H	5	70	9	0.0667±0.004	6
SP-21-I	10	70	9	0.0331±0.0003	1
SP-21-J	20	70	9	0.0322±0.004	12
SP-21-K	40	70	9	0.0649±0.0026	4
SP-21-L	80	70	9	0.0864±0.0047	5
SP-22-A	0	40	7	0.0173±0.0002	1
SP-22-B	0	40	8	0.0048±0.0002	5
SP-22-C	0	40	9	0.0077±0.0001	1
SP-22-D	0	40	10	0.0264±0.0007	3
SP-22-E	0	40	11	0.0753±0.0046	6
SP-22-F	0	40	12	0.1588±0.0058	4
SP-22-G	1	40	9	0.0126±0.0002	2
SP-22-H	5	40	9	0.0116±0.0001	1
SP-22-I	15	40	9	0.0050±0.0001	2
SP-22-J	30	40	9	0.0033±0.0003	8
SP-22-K	45	40	9	0.0042±0.0002	5
SP-22-L	60	40	9	0.0051±0.0002	3

Table A6. Mean and Standard Deviation Values of the Steady State Normalized B Dissolution Rates (cont.)

Line ID	Inf [Si], ppm	T in ºC	pH (23ºC)	Steady State B Rate, g m^{-2} d^{-1}	Coefficient of Variance (%)
SP-23-A	0	23	7	0.0016±0.0001	5
SP-23-B	0	23	8	0.00042±0.00004	10
SP-23-C	0	23	9	0.001303±0.000004	0.3
SP-23-D	0	23	10	0.0067±0.0001	1
SP-23-E	0	23	11	0.0197±0.0003	2
SP-23-F	0	23	12	0.0459±0.0002	0.5
SP-23-G	1	23	9	0.00059±0.00001	2
SP-23-H	15	23	9	0.00034±0.00003	9
SP-23-I	22.5	23	9	0.00046±0.00004	8
SP-23-J	30	23	9	0.00038±0.00003	9
SP-23-K	45	23	9	0.00036±0.00003	8
SP-23-L	52.5	23	9	0.00035±0.00002	6

APPENDIX B

PLOTS OF SPFT DATA FOR ALL TESTS

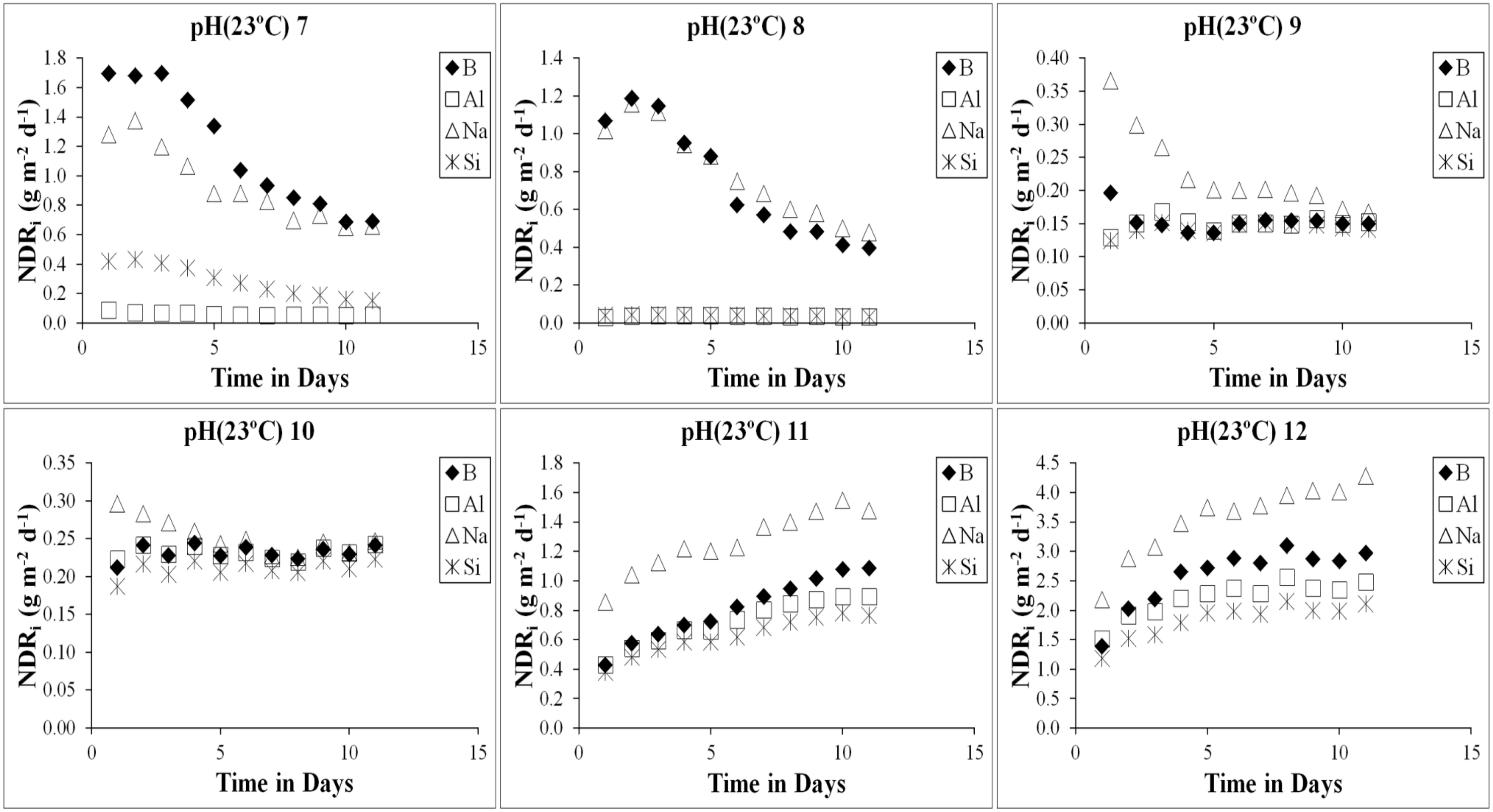

Dissolution under dilute conditions at 90 °C

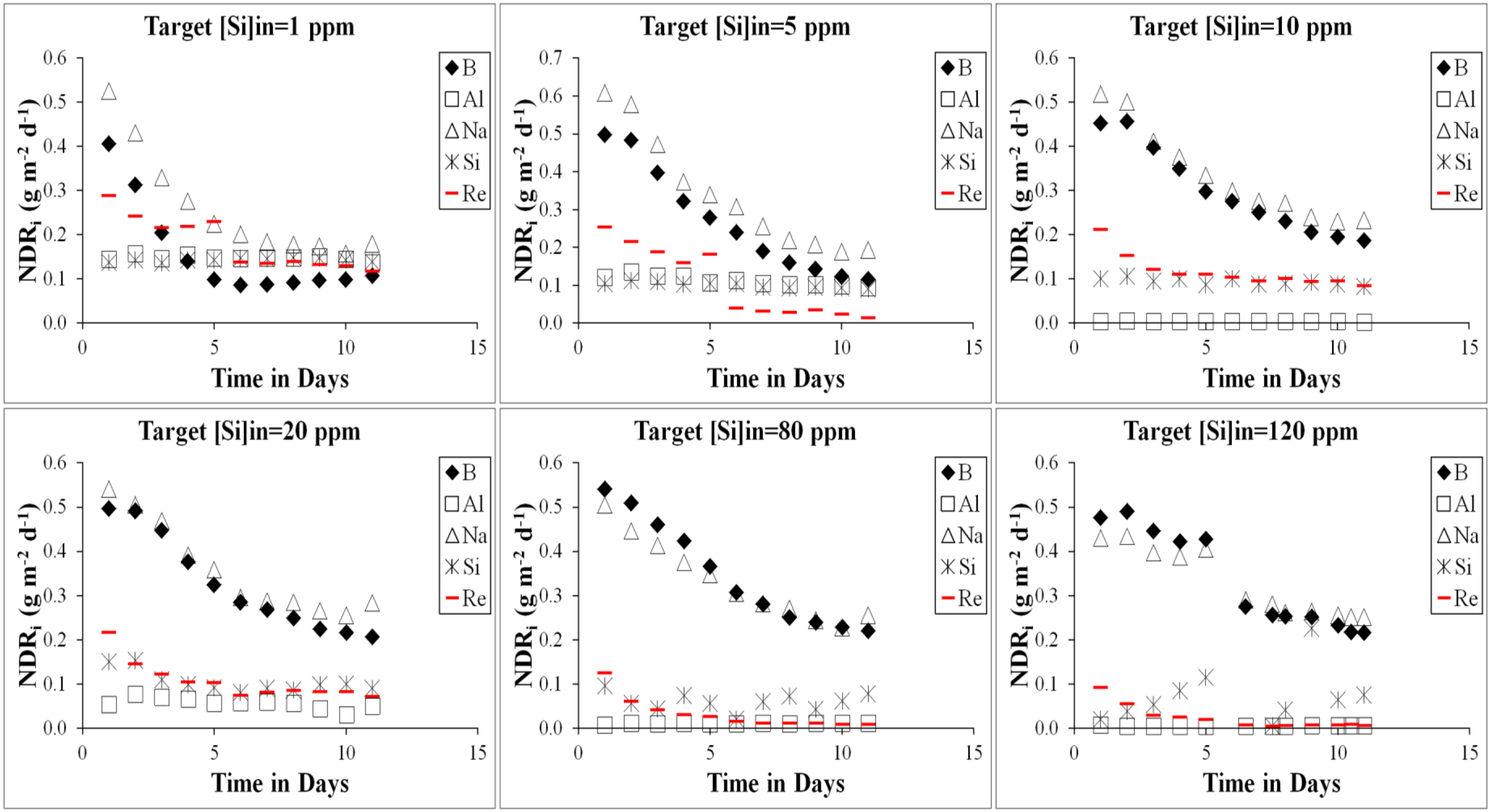

Dissolution under saturating conditions at 90 °C

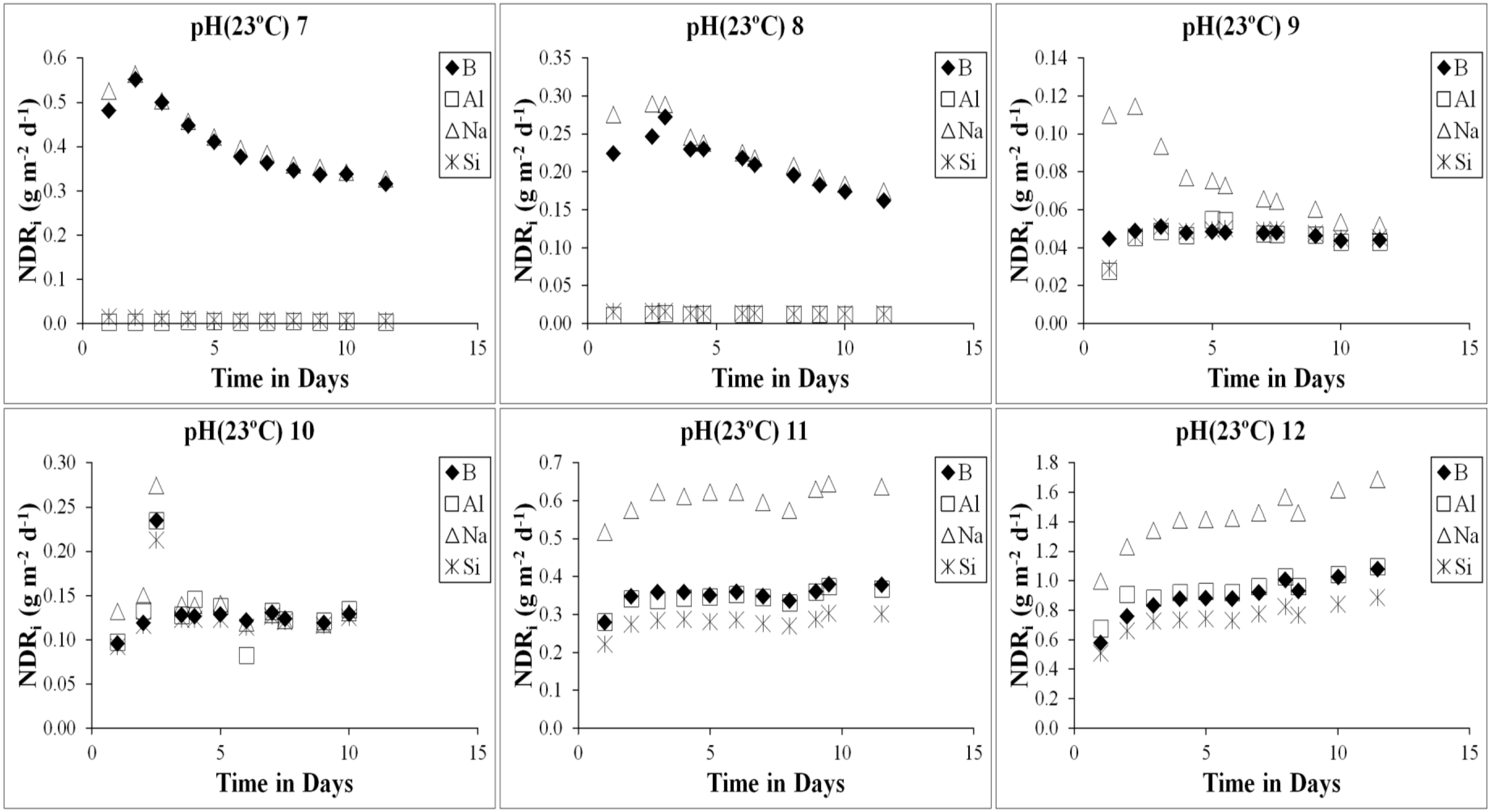

Dissolution under dilute conditions at 70 °C

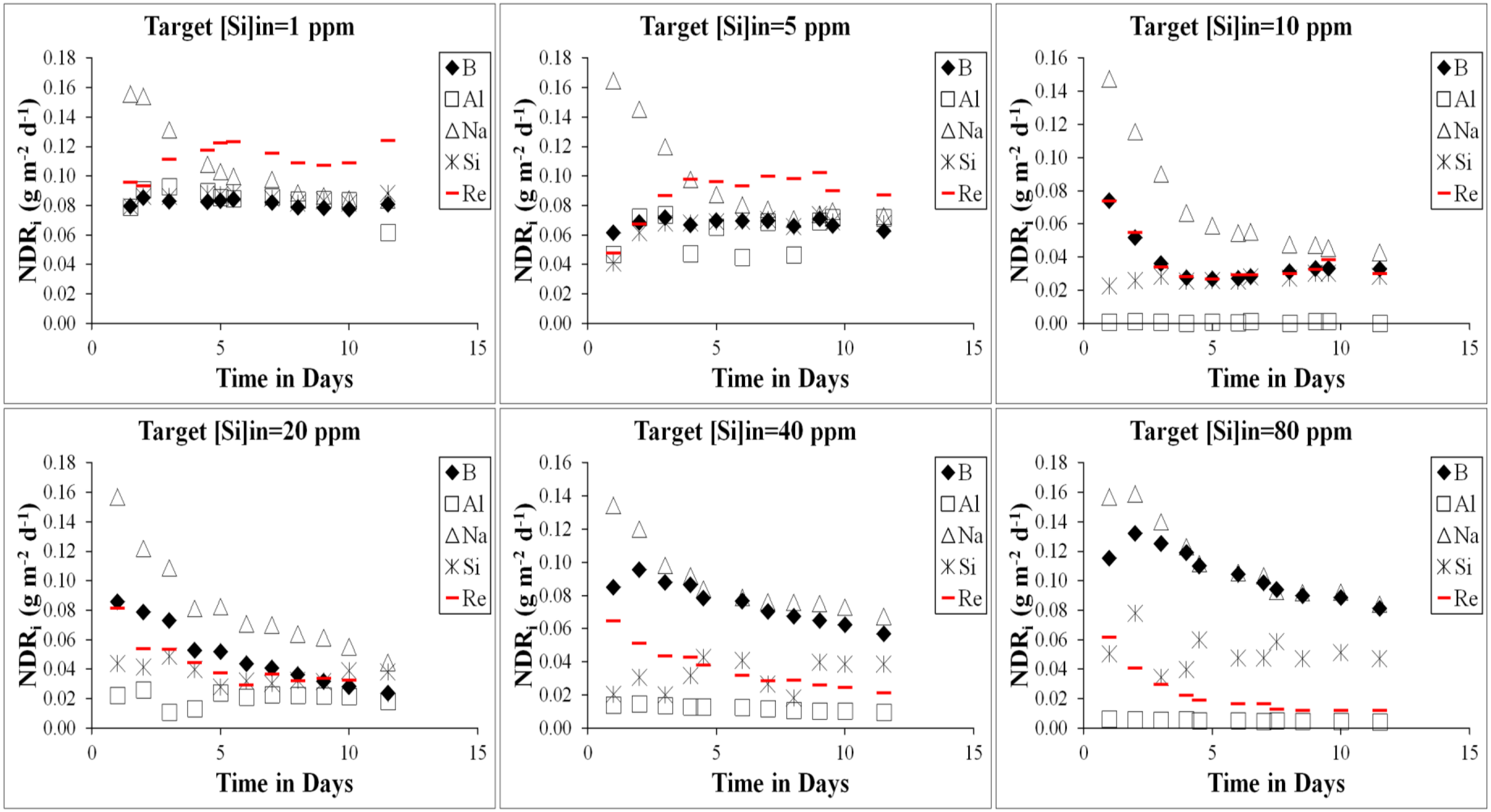

Dissolution under saturating conditions at 70 °C

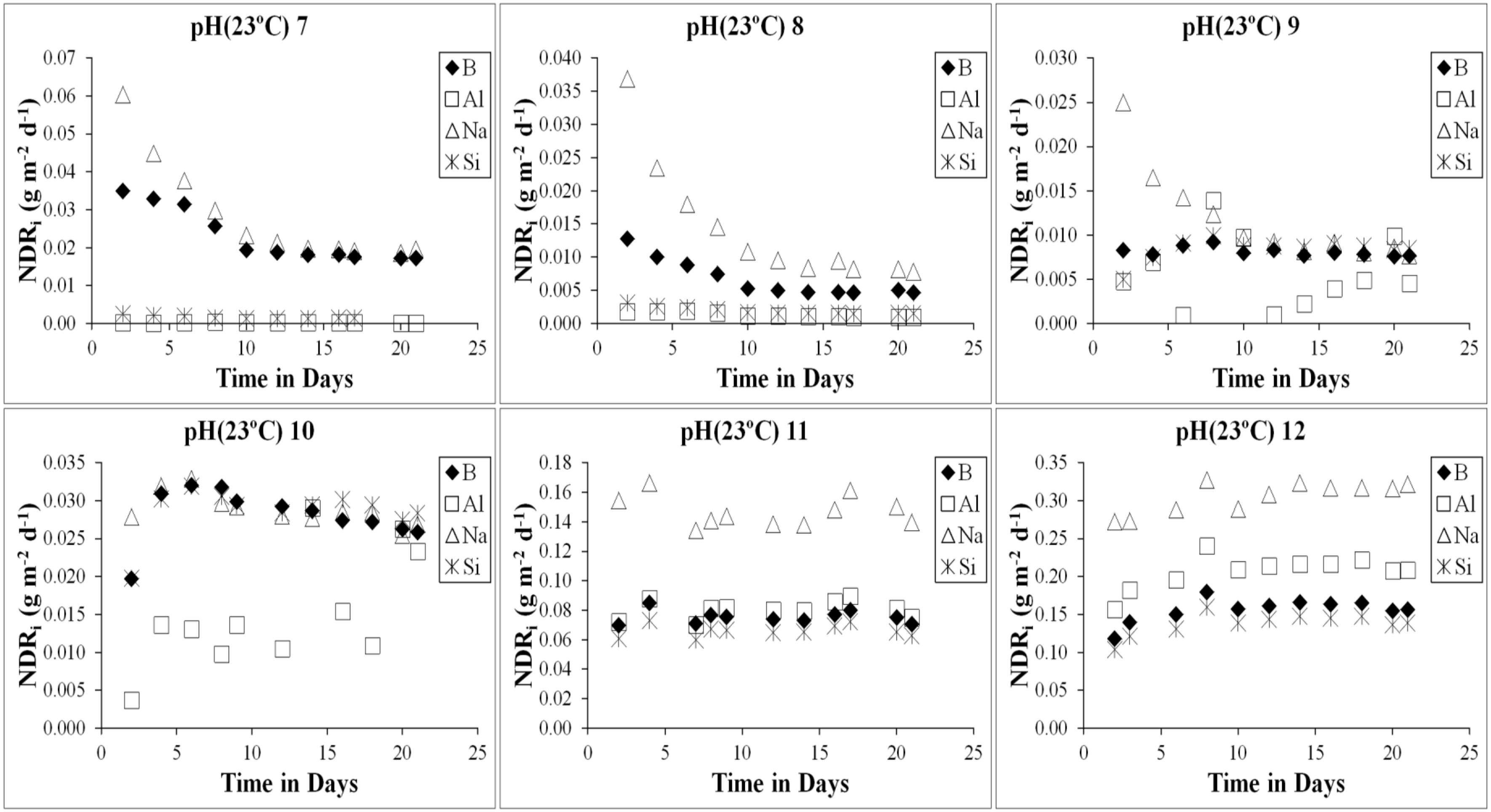

Dissolution under dilute conditions at 40 °C

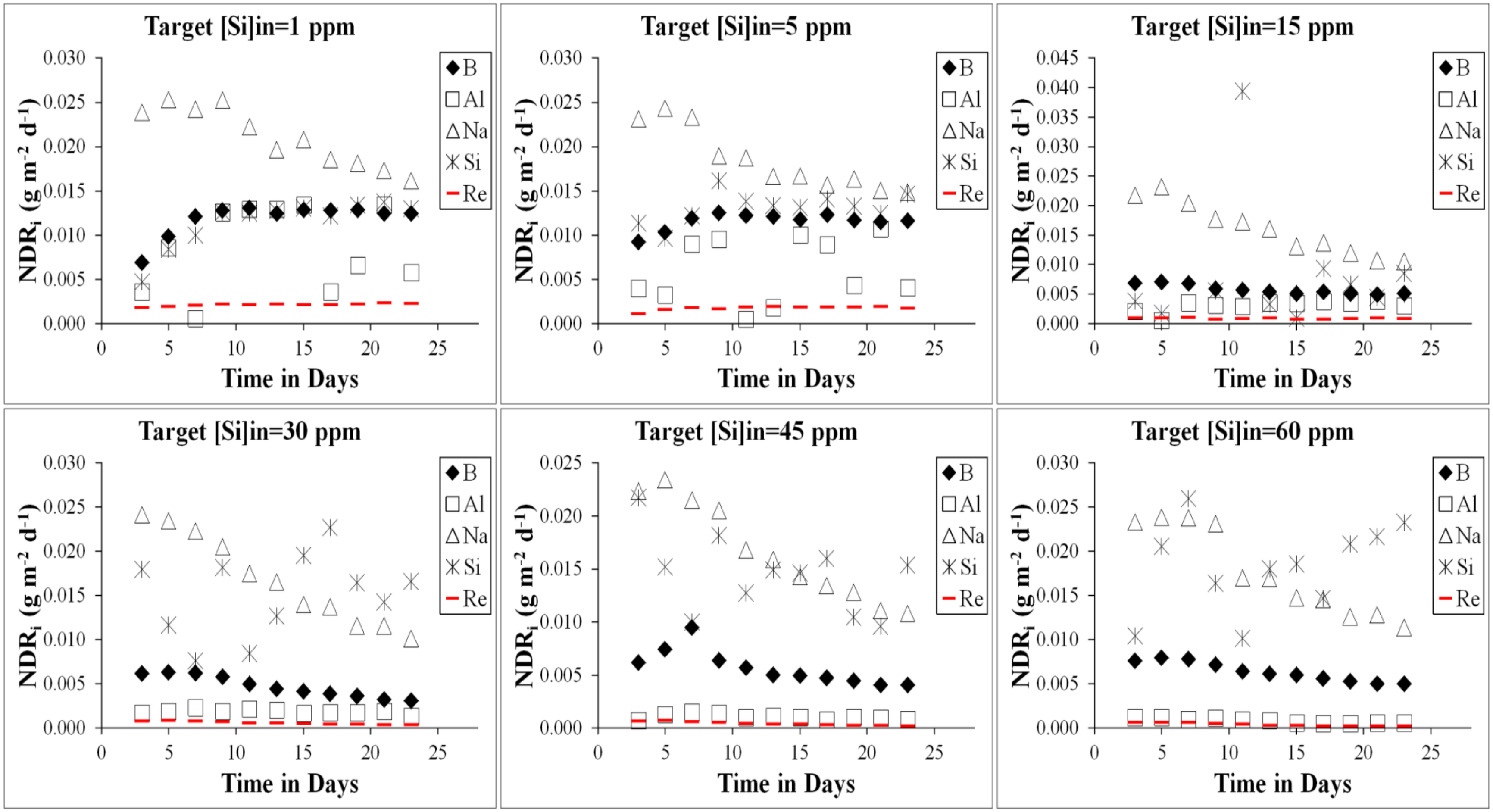

Dissolution under saturating conditions at 40 °C

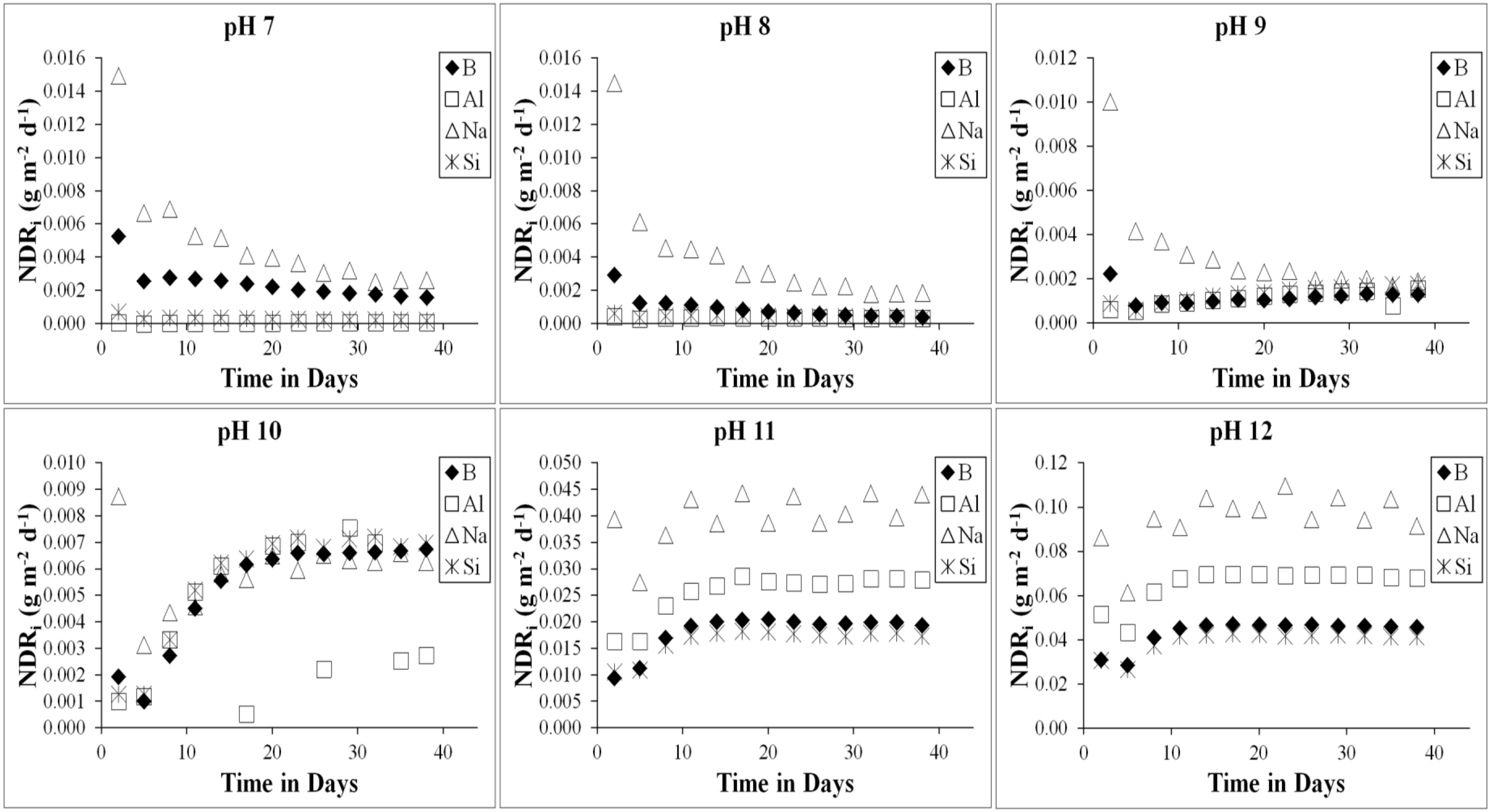

Dissolution under dilute conditions 23 °C

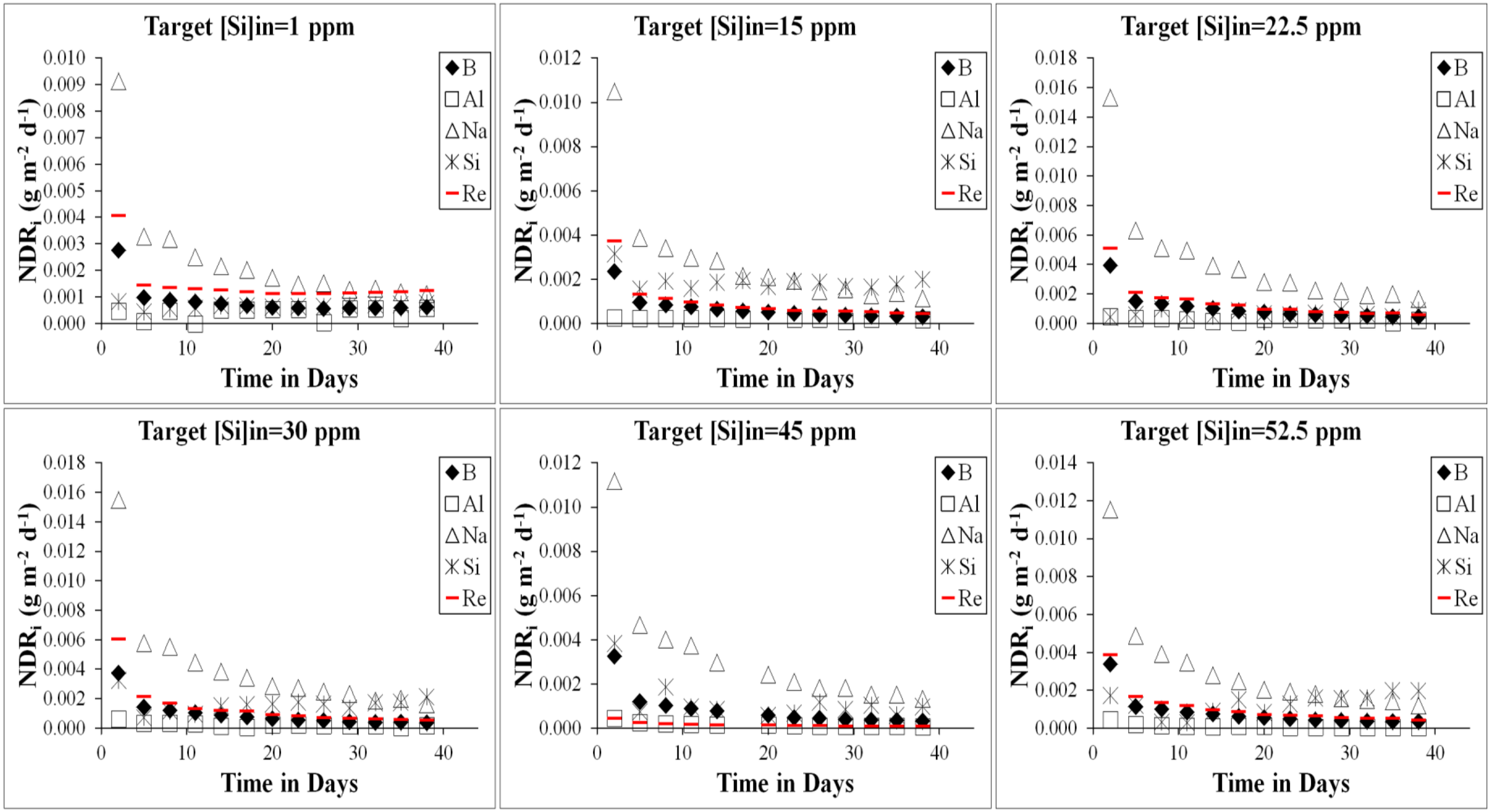

Dissolution under saturating conditions at 23 °C